GENERALIZED DIFFERENTIAL MODULATION WITH SIGNAL SPACE DIVERSITY FOR M-ARY QUADRATURE AMPLITUDE MODULATION (*M*-QAM) CONSTELLATIONS

Eulanda Masango

Submitted in fulfilment of the degree of Master of Science in Engineering (Electronic), College of Agriculture, Engineering and Science, University of KwaZulu-Natal

November 2023

Supervisor: Professor Hongjun Xu

As the candidate's supervisor, I agree to the submission of this dissertation.

Signed: ……  ……..

Professor H. Xu

29th November 2023

COLLEGE OF AGRICULTURE, ENGINEERING AND SCIENCE

DECLARATION 1 – PLAGARISM

I, Eulanda Masango, declare that

1. The research reported in this thesis, except where otherwise indicated, is my original research.
2. This thesis has not been submitted for any degree or examination at any other university.
3. This thesis does not contain other persons' data, pictures, graphs or other information, unless specifically acknowledged as being sourced from other persons.
4. This thesis does not contain other persons' writing, unless specifically acknowledged as being sourced from other researchers. Where other written sources have been quoted, then:

1. Their words have been re-written but the general information attributed to them has been referenced
2. Where their exact words have been used, then their writing has been placed in italics and inside quotation marks, and referenced.

5. This thesis does not contain text, graphics or tables copied and pasted from the Internet, unless specifically acknowledged, and the source being detailed in the thesis and in the References sections.

Signed

……

Eulanda Masango

28th November 2023

Acknowledgements

My gratitude goes to, God and my Ancestors, you made a way and walked me through it. You gave me strength, guided me even at my weakest and challenging moments. Your Grace is sufficient.

To my supervisor, Prof H Xu, I am grateful for your supervision and guidance on this journey. You offered me an opportunity to equally learn and improve on the principle of academic research and writing skills. I admire your passion, professionalism and dedication. Looking beyond your profession, you are disciplined, kind, caring and understanding. My sponsor, the Armaments Corporation of South Africa SOC Limited (ARMSCO), I am grateful for your financial assistance to pursue this journey. My friends, class and college mates, thank you for your support. I appreciate you.

To my parents, Mr S Letwaba and Ms C Letwaba, my siblings, Mr P Letwaba, Ms P Moloi and Mr K Letwaba, I will not trade your love, support and encouragement for anything in this word. I appreciate you. My daughter Ms A Masango, your presence in my life on this journey has led me to discover an admiration of my unwavering strength. You motivated me to keep going. I am honored and grateful that you were part of this journey and I got to share every moment of it with you. I appreciate you.

To my husband Mr S Masango, you have had a profound impact on this journey. Through the highs and lows, your encouragement, resilience and support helped me embrace the power of perseverance. Your believe in me has been a guiding light and an inspiration to remain steadfast in my focus on achieving my goal. I appreciate you.

I THANK YOU ALL.

Abstract

Due to an increase in wireless communication usage on several devices, the demand for high transmission rate and reliable connection has increased. In this dissertation, a generalized differential modulation with signal space diversity (GDM-SSD) for a multi-dimensional *M*-ary quadrature amplitude modulation (*M*-QAM) scheme is presented to improve the error performance of non-coherent systems in wireless communications.

Signal space diversity (SSD) comprises two fundamental stages: constellation rotation and component interleaving. The angle at which the constellation is rotated is determined based on a design criterion which maximizes the diversity order by minimizing the Euclidean square product or, alternatively, minimizes a symbol error probability (SEP) expression. In this dissertation, an angle of 31.7 degrees is used as an angle of rotation in order to achieve SSD in two dimensions.

This dissertation aims to improve the error performance of a non-coherent generalized differential modulation (GDM) wireless communication system. The proposed generalized differential scheme (GDM-SSD) is based on optimal power allocation, signal rotation and component interleaving/de-interleaving. GDM-SSD divides a frame into a reference part and normal part. The reference part is transmitted at a higher power than the normal part, and is used to encode and decode the information in the normal part. Optimal power allocation is applied to the system, and the results demonstrate that the SEP performance of the proposed GDM-SSD scheme losses about 5dB performance gap over coherent SSD scheme. It is observed that the performance of GDM-SSD detection gets better as the number of transmitted symbols in a frame increase.

Table of contents

List of figures

List of tables

List of acronyms

AWGN	- Additive white Gaussian noise
CDM	- Conventional differential modulation
CSI	- Channel state information
DM	- Differential modulation
Eq	- Equation
GDM	- Generalized differential modulation
GDM-SSD	- Generalized differential modulation with signal space diversity
i.i.d	- Independent and identically distributed
MDLB	- Minimum distance lower bound
MIMO	- Multi-Input Multi-Output
MISO	- Multi-Input-Single-Output
MRC	- Maximum ratio combining
MLD	- Maximum-likelihood detection
M-DPSK	- *M*-ary differential phase-shift keying
M-PSK	- *M*-ary phase shift keying
M-QAM	- *M*-ary quadrature amplitude modulation
NBs	- Normal blocks
NN	- Nearest neighbhour
NSs	- Normal symbols
PDF	- Probability density function
PEP	- Pairwise error probability
PEPs	- Pairwise error probabilities
QSFC	- Quasi-static fading channel
RB	- Reference blocks

RS - Reference symbol

RVs - Random variables

SSD - Signal space diversity

SIMO - Single-Input Multi-Output

SEP - Symbol error probability

SER - Signal error rate

SNR - Signal-to-noise ratio

SNRs - Signal-to-noise ratios

UB - Union bound

Symbols

x	- Scalar quantity x
$\|x\|$	- Absolute value of x
$\mathbb{C}^{N_r \times 1}$	- A set of $Q \times R$ complex-valued matrices
$(x)^*$	- Complex conjugate of x
$\boldsymbol{x}$	- Vector $\boldsymbol{x}$
$[\boldsymbol{x}]^T$	- Transpose of $\boldsymbol{x}$
$\|\|\boldsymbol{x}\|\|_F$	- Frobenius norm of $\boldsymbol{x}$
$(\boldsymbol{x})^H$	- Hermitian (conjugate transpose) of $\boldsymbol{x}$
$*$	- Convolution operator
$\approx$	- Approximately equal to
$Q(x)$	- The Gaussian Q-function of x
$Re\{x\}$	- Real part of a complex variable x
$Im\{x\}$	- Imaginary part of a complex variable x
$exp(x)$	- Exponential function of x
$argmin\{f(x)\}$	- Value of x that minimises the function (x)
$CN(\mu, \sigma^2)$	- Complex Gaussian distribution with mean μ and variance σ^2
N_t	- Number of transmit antennas
N_r	- Number of receive antennas
$\boldsymbol{\Omega}$	- *M*-QAM signal set
$\boldsymbol{\Psi}$	- *M*-PSK signal set

CHAPTER 1

INTRODUCTION

Wireless network popularity has grown at a rapid rate over the last decade, resulting in congestion of data transmission, increased interference, and other communication deficits in terms of reliability and speed [1]. As a result, there is a growing demand for higher data rates and better quality service, prompting the development of wireless communication systems that are more bandwidth efficient and reliable [1]. However, developers must tackle a number of obstacles, including limited spectrum availability and unpredictable fading conditions, in order to achieve these objectives [2]. One approach for reducing the impact of noise and fading is to use multiple receive antennas thus, the reliability of the wireless system is improved without compromising the bandwidth of the signals that are transmitted [3, 4].

Reliability can be improved in a wireless communication system by using diversity techniques [5]. Diversity techniques are employed to reduce the effect of channel fading on wireless networks and thus improve the reliability between the transmitter and receiver [5]. Some of diversity techniques are: spatial or space diversity, time diversity, receiver diversity and signal space diversity. Space diversity is achieved by implementing a multiple transmit and receive antenna technique multiple-input-multiple-output (MIMO) thus, multiple paths are established between the transmitter and the receiver [6, 5].

Time diversity is achieved by conveying multiple copies of a signal over multiple time slots with independent channel responses [5]. Specifically, time diversity can be achieved simply by repeating the same signal over a range of time slots [7, 5]. Receiver diversity referred to as antenna diversity, is a diversity technique employed in wireless communication systems which requires multiple receiver antennas such as single-input multiple-output (SIMO) to achieve diversity gain in a wireless communication system [8]. SIMO is used to meet the demand for high data rate in wireless communication systems.

Signal space diversity (SSD) incorporates diversity into a system, at no extra cost of antennas or bandwidth, this makes it an appropriate diversity technique for improving wireless communications [9, 10]. In the work presented in [9], SSD was implemented in a coherent system with *M*-ary quadrature amplitude modulation (*M*-QAM) symbol using SIMO to improve the error performance of the system however, at an expense of an increase in detection complexity.

This dissertation investigates the error performance of signal space diversity applied to a non-coherent system

1.1 Research motivation

Signal space diversity has previously been investigated and employed in coherent systems to implement diversity in wireless communication systems [9]. However, due to the detection complexity of the coherent system at the receiver, non-coherent systems were employed in wireless communication to simplify the detection complexity of coherent systems. The detection complexity of the coherent system is due to the channel state information (CSI), fading and the number of antennas amongst others [11]. Conventional differential modulation (CDM) and generalized differential modulation (GDM) are non-coherent modulations employed in wireless communication. Since CDM suffers 3dB performance loss compared to its coherent counterpart, GDM is employed to reduce the performance gap between CDM and coherent detection. The aim of this dissertation is to employ diversity in a non-coherent system to enhance the error performance of wireless communication systems by applying SSD in GDM. SSD is the ideal diversity technique to be applied to a non-coherent GDM system for its ability to achieve diversity without an additional bandwidth and transmission power as GDM uses power allocation to improve the performance of non-coherent wireless communication systems. This led to the proposed generalized differential modulation with signal space diversity (GDM-SSD) scheme for *M*-ary quadrature amplitude modulation constellations.

1.2 Research aim and objectives

This dissertation aims to improve the error performance of a non-coherent generalized differential modulation wireless communication system.

The following are the objectives of the research:

1. Investigation of error performance of SSD in a non-coherent system.
2. Investigation of power allocation in the proposed GDM-SSD.
3. Formulation of the analytical expression for the proposed GDM-SSD and validate it with simulation results.

1.3 Research contributions

This dissertation presents the following contributions, while reproducing results from existing literature to provide a benchmark:

1. In chapter 3, information bits are directly mapped onto an *M*-QAM signal set before rotation in a coherent SSD system with maximum ratio combining (MRC) reception. The received symbol combiner yields an instantaneous combined fading gain which was employed in maximum-

likelihood detection (MLD). This approach provides robust performance improvements, especially in fading environments. It also, enhances the efficiency, reliability and performance of wireless communication systems by utilizing coherent SSD techniques in conjunction with direct mapping onto an *M*-QAM signal set.

By leveraging coherent SSD techniques alongside direct mapping of the *M*-QAM signal set, demonstrates a potential for improving and advancing the effectiveness and capacity of wireless communication system in diverse environments.

2. In chapter 4, a non-coherent GDM system was presented where power allocation is based on the Lagrange multiplier method. In this system, more power is allocated to the transmitted reference symbol (RS) compared to the normal symbols (NSs). This results to a better error performance with a gain of about 2dB to that of non-coherent CDM detection.

   This improvement highlights the potential of the power allocation strategy to provide a more stable communication system without requiring channel state information at the receiver. This approach demonstrates significant potential for robust and efficient wireless communication, especially in fading environment.

3. In chapter 5, the proposed GDM-SSD scheme is presented, where SSD is applied to a non-coherent GDM system for *M*-QAM constellations. Motivated by the benefits of both the GDM and SSD techniques, the combination enhances the robustness, diversity gain and, spectral efficiency and reliability especially in challenging fading environment.

   In this scheme, *M*-QAM signals are transmitted after rotation, components interleaving and differential encoding is performed. Following the transmission of the RS, which remains constant throughout the transmission frames, the remaining encoded symbols are transmitted separately in different frames as NSs. It is assumed that fading channels experienced by the symbols during transmission remain constant thus, quasi-static fading channel (QSFC).

   Transmission power is allocation between the reference block (RB) and normal blocks (NBs) where, more power is allocated to the RB since the reference symbol provides the combine channel estimation for NBs. The received symbols are combined using MRC reception, de-interleaved and detected at the receiver.

   This approach results in an estimated 5dB performance loss of the proposed non-coherent GDM-SSD compared to the coherent SSD. Thus, the coherent SSD detection gains about 5dB over the proposed non-coherent GDM-SSD detection.

Overall, the proposed GDM-SSD scheme demonstrates significant potential in improving the performance and reliability or wireless communication systems, despite the performance gap compared to coherent SSD.

1.4 Structure of the dissertation

The remainder of this dissertation is structured as follows:

- Chapter 2 presents a literature survey of wireless communication techniques used in this research.

- Chapter 3 presents SSD in a coherent system, including the system model, error performance analysis of system, numerical and analytical results of the performance of coherent SSD system and, the chapter summary.

- Chapter 4 presents CDM and GDM, including the system models, error performance analysis of systems, numerical and analytical results of the performance of the non-coherent modulations and, the chapter summary.

- Chapter 5 presents the proposed scheme GDM-SSD literature including the system model, error performance analysis of system, numerical and analysis results of the performance of the proposed scheme and, the chapter summary.

- Chapter 6 presents the conclusion of the dissertation.

CHAPTER 2

LITERATURE SURVEY

This section presents a literature survey of wireless communication techniques involved in the investigation of the proposed generalized differential modulation with signal space diversity (GDM-SSD) scheme.

2.1 Wireless channel

During information signals transmission, each signal reaches the receiver via multiple independent paths, strength and time variations as they experience different delays and phase shift as explained in [8, 2]. This is due to the information signals going through reflection, absorption and scattering by objects (buildings, hills, ground, water, etc.) before arriving at the receiver as discussed in [2]. This phenomenon is known as multipath propagation. Multipath propagation causes constructive and destructive interference and can reduce the signal-to-noise ratio (SNR) [8]. The degradation of the signal quality is caused by fading in the multipath propagation often from a transmitter to a receiver, which is also referred to as multipath induced fading [5, 2].

Wireless communication channels are harmed by a variety of causes, but fading is the most serious one, resulting in a decrease in overall system efficiency. Fading causes the received signal power to vary and as the power varies, the quality of the received signal changes [8, 2]. Fading depends on obstacles in the signal path, which varies with time [2]. These obstacles create complex transmission effects on the transmitted signal. Fading models/channels include Rayleigh fading, Rician fading, Nakagami fading and Quasi-static fading amongst others and are referred to as fading distributions [5, 12, 2]. Each fading distribution is incorporated in the baseband data signal according to its requirements. In this research we will be using Rayleigh fading and Quasi-static fading which are discussed in Section 2.1.1 and Section 2.1.2, respectively.

2.1.1 Rayleigh fading

Rayleigh fading is the form of fading that is often experienced in an environment with a large number of reflections present. It is used to analyze the overall nature of signals scattered between the transmitter and the receiver as defined in [12, 4]. In Rayleigh fading models, it is assumed that the magnitude of a signal that has passed through a communications channel will vary randomly, or fade according to a Rayleigh distribution. The amplitude gain of the transmitted signal is characterized by a distribution where the fading coefficient is denoted as:

$$h = h^I + jh^Q = \alpha e^{j\varphi}, \tag{2.1}$$

where h^I and h^Q are the in-phase and quadrature components, respectively, distributed as complex Gaussian random variables (RVs) with distribution $CN(0,1)$ with zero mean and 1 variance $CN\ (0,1)$ as in [13] and, α is the Rayleigh fading distributed amplitude denoted as:

$$\alpha = \sqrt{(h^I)^2 + (h^Q)^2}. \tag{2.2}$$

The probability density function (PDF) of the fading amplitude α is denoted as:

$$f_\alpha(\alpha) = \frac{\alpha}{\sigma^2}\exp\left(-\frac{\alpha^2}{2\sigma^2}\right), \qquad \alpha \geq 0 \tag{2.3}$$

where σ is the scale parameter, which determines the spread of the distribution.

2.1.2 Quasi-static fading

Quasi-Static fading Channel (QSFC) is known in the literature as a channel which is frequency flat and very slow with a fading that has little variations in time over transmission frame as in [14, 15]. Meaning, the fading of QSFC is considered constant over a transmission frame. To improve the quality of the communication system over QSFC, diversity is employed in the system. This means, redundant signals are transmitted over preferably independent channels as discussed in [15]. In QSFC, the instantaneous SNR varies independently from one frame to the other. An interest in quasi-static fading channel has numerously increased due to higher demand in data rates along with capacities and more reliable connections in wireless communication systems.

Since multipath fading leads significantly to a decrease in symbol error rate (SER) and symbol error probability (SEP) efficiency in wireless communication system, reducing the effects of multipath fading can boost communication. This effect can be alleviated by the application of diversity into a wireless communication system.

2.2 Diversity

Diversity is a technique used to improve the reliability of wireless communication systems over fading channel as in [5]. In diversity techniques, instead of one signal that has passed through multiple fading channels, the receiver receives multiple copies of transmitting signals. Therefore, the employment of diversity in wireless communication systems reduces the duration and depth of fading experienced by the receiver in a case where multiple copies of the information signals are transmitted to the receiver as presented in the previous work [5]. A diversity system must have two or more transmit or receive antennas. Refer to Figure 2.1 below:

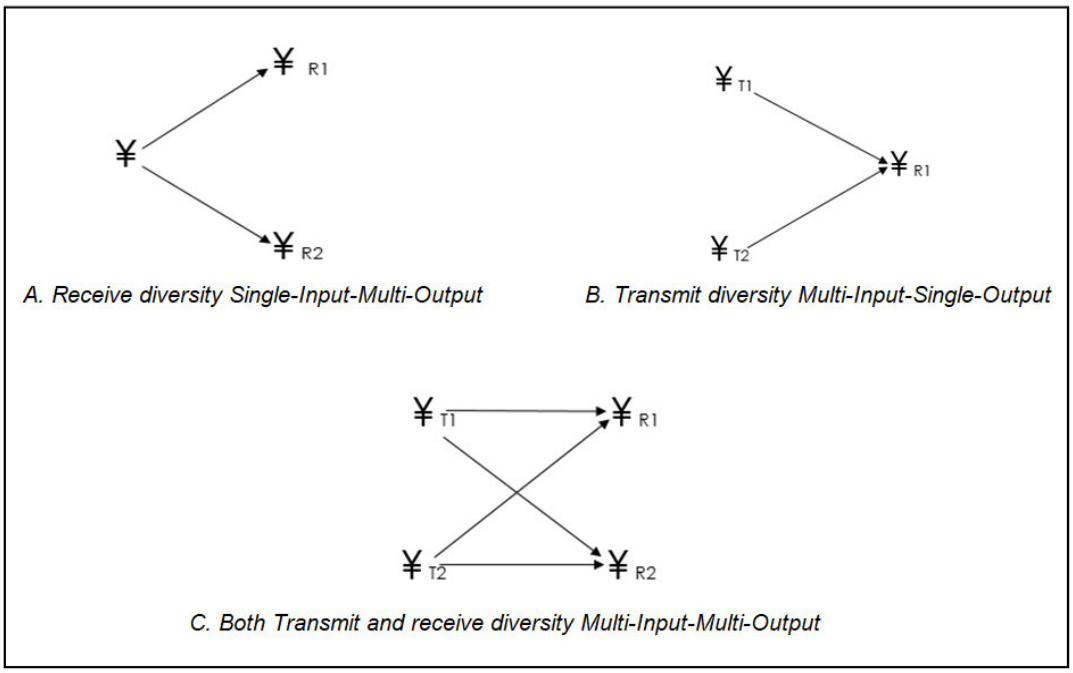

Figure 2.1: Transmit and receive diversity systems in wireless communication [16].

2.2.1 Types of diversity techniques

This section presents a brief review of some of diversity techniques used in the wireless communication systems [5].

2.2.1.1 Time diversity

Time diversity is a diversity technique employed in wireless communication systems where signals are transmitted repeatedly with time at regular intervals that exceed the coherence time of the channel such that multiple repetitions of information in the signals are received with independent fading conditions [5, 17]. The maximum ratio of variations can be used to find the optimal combination. Additionally, rotation matrix or interleaved channel code can be used to ensure different errors are associated with multiple independent channels.

2.2.1.2 Space diversity

Space diversity is a diversity technique employed in wireless communication systems with two or more transmit or receive antennas placed far apart to gain possibly independent received signals as in [5, 16]. It provides a higher system capacity without requiring any additional power or bandwidth as noted in [8, 16]. Space diversity is implemented in systems like transmit diversity multiple-input-multiple-out (MIMO) and receive diversity single-input-multiple-output (SIMO) [16].

This approach offers significant error performance improvement without compromising the vital bandwidth on the energy resources transmitted. Spatial diversity is commonly applied as it is easy to deploy and very economical. In order to prevent the correlation among the signals received from each receive antenna, the spatial positions for receive antennas are separated sufficiently [5, 17]. The usual separation between the receive antennas is a few wavelengths of the transmitted signal. Each received signal is combined to increase its overall SNR by using selection combining (SC) or maximal ratio combining (MRC), which thus mitigates the effects of fading [17, 16].

2.2.1.3 Receiver diversity

Receiver diversity referred to as antenna diversity, is a diversity technique employed in wireless communication systems which requires multiple receiver antennas such as SIMO and MIMO to achieve diversity gain in a wireless communication system [8]. This means that by using multiple receiver antennas, the channel capacity and multipath interference increases while no additional transmission bandwidth or power is needed [16]. The multiple receiver antennas must be spaced far apart from each other so that there is no correlation amongst the respective received signals [8]. The multiple transmitted signals are combined at the receiver using combining techniques such as MRC and SC as discussed in [5, 8, 16]. These combining techniques increase the SNR or the power of the received signal.

2.2.1.4 Signal space diversity

Signal space diversity (SSD) is a diversity technique used in wireless communications for its ability to improve the error performance of the system over fading channels. This is achieved by implementing diversity without the addition of bandwidth and transmission power though, at the expense of an increase in maximum-likelihood detection (MLD) complexity at the receiver as presented in [10, 9]. The increase in the detection complexity is due to the requirement of the knowledge of the channel state information (CSI) at the receiver. SSD can be considered as a conventional *M*-ary quadrature amplitude modulation (*M*-QAM) constellation that has been rotated by a certain angle. SSD is also known as a coordinate interleaving scheme, which obtains diversity by sending the components of a multidimensional signal constellation over separate fading channels [2]. The main benefit of this form of diversity is that it is only exchanged for higher demodulator complexity.

Additionally, rotation matrix or interleaved channel code can be used to ensure different errors are associated with multiple independent channels.

As the focus of this study, details of SSD are presented in chapter 3 where the diversity technique is applied in a coherent system. SSD is also presented in chapter 5 where it is applied in a non-coherent system.

2.3 Differential modulation

Differential modulation (DM) is a non-coherent system in wireless communication which simplifies the complexity of coherent detection [18]. Since the receiver of the a coherent requires full knowledge of the CSI at the receiver, it yields an increase in detection complexity. DM has been employed in wireless systems for its ability to perform detection without the knowledge of CSI at the receiver. It uses differential detection as presented in previous work [18]. This characteristic results in a reduced complexity making DM an attractive method for implementation in wireless communication systems. In order to obtain differential detection, information symbols are differently encoded at the source before transmission where the first differentially encoded symbol is referred to as a reference symbol (RS) and the other remaining symbols are referred to as normal symbols (NSs) as indicated in [18]. It is assumed that fading channels remains constant during transmission of symbols thus, QSFC. Amongst other DM schemes in wireless communication, only two are the focus of study for this dissertation namely conversional differential modulation (CDM) and generalized differential modulation (GDM) and both are presented in chapter 4, respectively.

2.3.1 Conversional differential modulation

Conversional differential modulation is a scheme used to improve the wireless communication system error performance through differential detection as presented in [19]. Though CDM is capable of performing differential detection, it suffers 3dB performance loss compared to its coherent counterparts as presented in the previous work [18, 19]. This is due to the differential encoding at the transmitter and non-coherent detection at the receiver.

2.3.2 Generalized differential modulation

Generalized differential modulation is employed in wireless communication systems as presented in [18, 19] to reduce the error performance loss suffered by CDM detection to its coherent detection counterpart. GDM uses power allocation amongst encoded blocks to reduce the error performance gap between CDM detection and coherent detection where more power is allocated to the reference block (RB) as compared to normal blocks (NBs) as the RB provides the channel estimation for the NBs [18, 19].

As the focus of this study, both CDM and GDM are further presented in chapter 4.

CHAPTER 3

SIGNAL SPACE DIVERSITY

This section presents a diversity technique, signal space diversity (SSD) as indicated in Section 2.2.1.4 and, the symbol error probability (SEP) performance analyses using union bound (UB), minimum distance lower bound (MDLB) and nearest neighbour (NN) approximation models. SSD is employed in a coherent system with maximum ratio combining (MRC) reception to implement diversity and improve the performance of the system over Rayleigh fading channel.

3.1 Introduction

Signal space diversity technique has sparked a lot of interest because it ensures that different components of a signal constellation are individually affected by independent fading without an additional bandwidth, transmit power or space. However, this is achieved at the expense of a complex maximum-likelihood detector (MLD) at the receiver [9, 2]. In a work presented in [9], SSD was applied in a coherent system with MRC reception to obtain diversity gain in fading channels. Maximum ratio combining is a diversity combining technique used to estimate the channel characteristics of a system with multiple antennas at the receiver [20, 21].

SSD employs rotation and component interleaving/de-interleaving on the multi-dimensional signal constellations such that the in–phase (real) and quadrature–phase (imaginary) components of each signal experience independent fading separately [2, 9, 21]. Signal rotation and interleaving can increase the diversity order of a multidimensional signal. The rotation of a signal constellation was implemented in [22] to achieve SSD in two dimensions. The employment of signal constellation rotation is to make the system insensitive to deep fading such that the components of the signals will not collapse at the same time [2, 10]. When non-rotated constellation signal experiences deep fading, the in-phase and quadrature components are both affected by the same fading, which makes it difficult to demodulate a symbol transmitted on components accurately [2]. To achieve rotation, constellation points are multiplied with an optimal rotation angle to increase the minimum number of distinct components between any two constellation points [23]. Figure 3.1 illustrates non-rotated and rotated conventional *M*-ary quadrature amplitude modulation (*M*-QAM) signal constellation:

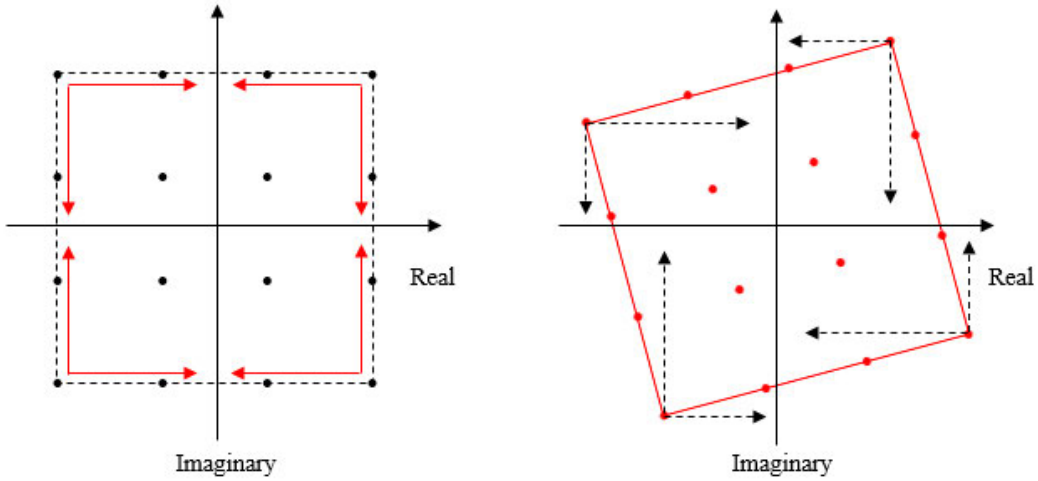

A. Original (non-rotated) constellation (u) B. Rotated Constellation(x)

Figure 3.1: Conventional non-rotated (u) and rotated (x) 16-QAM signal constellation [10].

Diversity gain is confirmed by component interleaving rotated signal constellations. The coordinate or component interleaving of the rotated signal constellation was presented in [9]. Component interleaving/de-interleaving ensures that not a single deep fade affects the components of the signal simultaneously as stipulated in [9, 2, 23]. Thus, the in-phase and quadrature components of the signal are affected by independent fading to obtain diversity. For the success of independent fading on the signals, de-interleaving is employed in an SSD system over successfully transmitted signals to reassemble the in-phase and quadrature components of the symbol pair to their original symbols [9, 2, 23].

Due to the coherent system requirement of full knowledge of the channel state information (CSI) at the receiver to perform coherent detection, received signals are combined at the receiver before detection using MRC reception. This technique is employed to achieve the diversity order of the system as defined in [9, 20]. MRC applies weights to each receive antenna in order to maximize the signal-to-noise ratio (SNR) for the summed signal [21].

Furthermore, the SEP performance of the presented coherent SSD system is analyzed by maximizing the minimum product distance of the signal constellation using the UB, MDLB and NN approximation models in a closed form.

3.2 System model

Consider a coherent SSD system containing $N_t \times N_r$ Single-Input-Multi-Output (SIMO) system with MRC reception where $N_t = 1$ is the number of transmit antennas and $N_r \geq N_t$ is the number of receive

antennas as illustrated in Figure 3.2. We assume that the receive antennas must be spaced far enough apart from each other so that there is no correlation among the respective received signals.

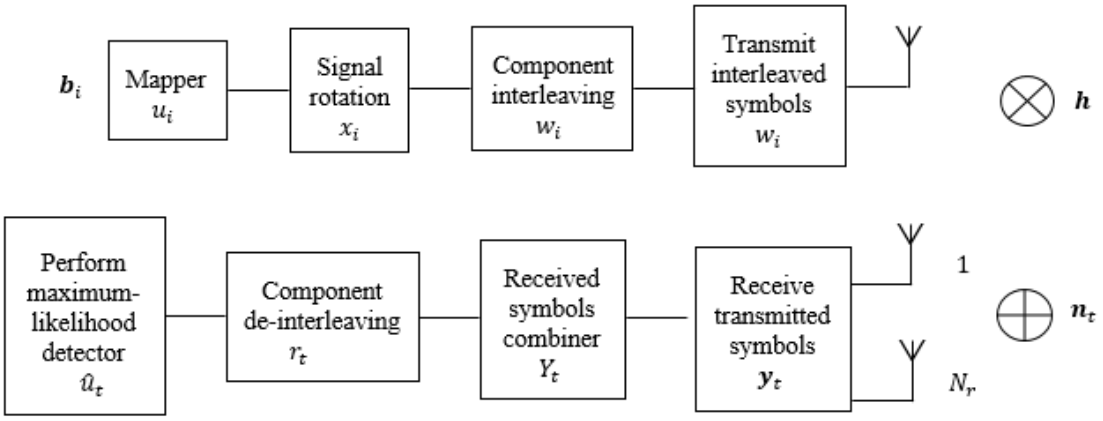

Figure 3.2: Block diagram of coherent SSD SIMO system with MRC reception.

Consider a conventional *M*-QAM signal set $\boldsymbol{\Omega}$ which yields symbol $u_i = u_i^I + ju_i^Q$, assuming $E[|u_i|^2] = E_\omega$. $(\cdot)^I$ and $(\cdot)^Q$ refer to the in-phase (real) and quadrature (imaginary) components of a signal, respectively, and $i,\ i \in [1:2]$, is the symbol index. Information bits $\boldsymbol{b}_i = [b_{i,1}\ b_{i,2}\ b_{i,3}\ \cdots b_{i,k}]$ are grouped in sequences of $k = log_2 M$ bits in size where M is the modulation order.

The grouped information bits are then directly mapped onto *M*-QAM signal set. The symbols (u_i) are then rotated at a certain angle to maximize the minimum number of distinct components between any two points in the signal constellation while retaining the same average energy as shown in Figure 3.3 of a conventional *M*-QAM signal constellation rotated at angle θ:

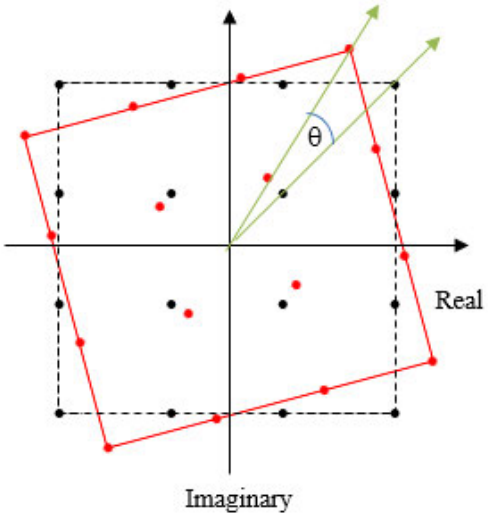

Figure 3.3: Conversional 16-QAM signal constellations rotated at angle θ.

The rotated signal $x_i = x_i^I + jx_i^Q$, is obtained by applying a rotation matrix $\boldsymbol{R}^\theta$ for a rotation angle θ to each element of the symbol u_i to form a pair of rotated symbols as shown in Eq (3.1) [9]:

$$\begin{bmatrix} x_i^I & x_i^Q \end{bmatrix} = \begin{bmatrix} u_i^I & u_i^Q \end{bmatrix} \times \boldsymbol{R}^\theta, \tag{3.1}$$

where $i \in [1:2]$ is the symbol index number, $\mathbf{R}^\theta = \begin{bmatrix} cos\,\theta & sin\,\theta \\ -\,sin\,\theta & cos\,\theta \end{bmatrix}$ is the rotation matrix with rotational angle $\theta = 31.7°$ as presented in [10].

The rotation signal sets are effectively computed as follows:

$$\begin{aligned} \begin{bmatrix} x_i^I & x_i^Q \end{bmatrix} &= \begin{bmatrix} u_i^I & u_i^Q \end{bmatrix} \begin{bmatrix} cos\,\theta & sin\,\theta \\ -\,sin\,\theta & cos\,\theta \end{bmatrix}, \\ &= \begin{bmatrix} u_i^I\,cos\,\theta - u_i^Q sin\theta & u_i^I\,sin\,\theta + u_i^Q\,cos\,\theta \end{bmatrix}, \end{aligned} \tag{3.2}$$

where $x_i^I = u_i^I\,cos\,\theta - u_i^Q\,sin\,\theta$ and $x_i^Q = u_i^I\,sin\,\theta + u_i^Q\,cos\,\theta$.

The rotated symbol pair x_i are applied to the interleaver before transmission. The symbols are interleaved by swapping their quadrature components, where a typical pair of interleaved symbols is given as w_i, $i \in [1:2]$ where the subscript i is the index of the symbol in the symbol pair denoted as:

$$w_1 = x_1^{\mathrm{I}} + jx_2^{\mathrm{Q}}, \tag{3.3a}$$

$$w_2 = x_2^{\mathrm{I}} + jx_1^{\mathrm{Q}}, \tag{3.3b}$$

The interleaved symbol pair are transmitted in two different time slots through the source. Each transmitted symbol experiences Rayleigh fading channels and additive white Gaussian noise (AWGN) as they arrive at the destination, giving received symbol vector $\boldsymbol{y}_t$:

$$\boldsymbol{y}_t = \sqrt{\frac{E_s}{E_\omega}}\boldsymbol{h}_t w_t + \boldsymbol{n}_t, \tag{3.4}$$

where $\boldsymbol{y}_t \in \mathbb{C}^{N_r \times 1}$ is the received information symbol vector, the subscript $t \in [1:2]$ is the time slot index, E_s is the transmitted power, E_ω is the average signal power, $\frac{E_s}{E_\omega}$ is the average transmit power, $\boldsymbol{h}_t$ is the independent Rayleigh fading coefficient vector with entries h_{tk} $k \in [1:N_r]$ modelled as independent and identically distributed (i.i.d.) random variables (RVs) with distribution unit variance $E[|h_{tk}|^2] = 1$ and, $\boldsymbol{n}_t$ is the AWGN vector with entries n_{tk} modelled as i.i.d. complex Gaussian RVs with distribution $n_{tk} \sim CN(0,1)$. The subscript k is the receive antenna index.

The received symbols are combined as they are received at the receiver using MRC reception on a symbol-by-symbol basis. The combined received symbols are defined as $Y_t = \boldsymbol{h}_t^H \boldsymbol{y}_t$ where the

subscript $t,\ t \in [1:2]$ is the times index and superscript H is the Hermitian transpose. The combined received symbol pair is denoted as in Eq (3.5a) and Eq (3.5b):

$$\begin{aligned} Y_1 &= \boldsymbol{h}_1^H \boldsymbol{y}_1, \\ &= \sqrt{\frac{Es}{E\omega}} \|\boldsymbol{h}_1\|_F^2 w_1 + \boldsymbol{h}_1^H \boldsymbol{n}_1, \\ &= \sqrt{\frac{E_s}{E_\omega}} \left[\|\boldsymbol{h}_1\|_F^2 \left(x_1^I + j x_2^Q\right)\right] + \boldsymbol{h}_1^H \boldsymbol{n}_1, \\ &= \sqrt{\frac{Es}{E\omega}} \left[\|\boldsymbol{h}_1\|_F^2 \left(x_1^I + j x_2^Q\right)\right] + \tilde{n}_1, \end{aligned} \tag{3.5a}$$

$$\begin{aligned} Y_2 &= \boldsymbol{h}_2^H \boldsymbol{y}_2, \\ &= \sqrt{\frac{Es}{E\omega}} \|\boldsymbol{h}_2\|_F^2 w_2 + \boldsymbol{h}_2^H \boldsymbol{n}_2, \\ &= \sqrt{\frac{E_s}{E_\omega}} \left[\|\boldsymbol{h}_2\|_F^2 \left(x_2^I + j x_1^Q\right)\right] + \boldsymbol{h}_2^H \boldsymbol{n}_2, \\ &= \sqrt{\frac{E_s}{E_\omega}} \left[\|\boldsymbol{h}_2\|_F^2 \left(x_2^I + j x_1^Q\right)\right] + \tilde{n}_2, \end{aligned} \tag{3.5b}$$

where $\|\boldsymbol{h}_t\|_F^2$ is the instantaneous combined fading gain and $\tilde{n}_t = \boldsymbol{h}_t^H \boldsymbol{n}_t$ is a noise term which has a variance of $E[|\boldsymbol{h}_t^H \boldsymbol{n}_t|^2] = \sum_{k=1}^{Nr} |h_{tk}|^2$.

De-interleaving is then performed on the combined received symbol pair in Eq (3.5a) and Eq (3.5b) to ensure that the in-phase and quadrature components of the original symbols are reassembled before detection is performed. De-interleaving is performed by swapping the in-phase and quadrature components of the combined received symbols where a typical pair of de-interleaved symbols is given as $r_t, t \in [1:2]$:

$$\begin{aligned} r_1 &= Re\left\{\left[\sqrt{\frac{E_s}{E_\omega}} \|\boldsymbol{h}_1\|_F^2 \left(x_1^I + j x_2^Q\right)\right] + \tilde{n}_1\right\} + jIm\left\{\left[\sqrt{\frac{E_s}{E_\omega}} \|\boldsymbol{h}_2\|_F^2 \left(x_2^I + j x_1^Q\right)\right] + \tilde{n}_2\right\}, \\ &= \sqrt{\frac{E_s}{E_\omega}} \|\boldsymbol{h}_1\|_F^2 \, x_1^I + j\sqrt{\frac{E_s}{E_\omega}} \|\boldsymbol{h}_2\|_F^2 \, x_1^Q + \tilde{\tilde{n}}_1, \end{aligned} \tag{3.6a}$$

$$\begin{aligned} r_2 &= Re\left\{\left[\sqrt{\frac{E_s}{E_\omega}} \|\boldsymbol{h}_2\|_F^2 \left(x_2^I + j x_1^Q\right)\right] + \tilde{n}_2\right\} + jIm\left\{\left[\sqrt{\frac{E_s}{E_\omega}} \|\boldsymbol{h}_1\|_F^2 \left(x_1^I + j x_2^Q\right)\right] + \tilde{n}_1\right\}, \\ &= \sqrt{\frac{E_s}{E_\omega}} \|\boldsymbol{h}_2\|_F^2 \, x_2^I + j\sqrt{\frac{E_s}{E_\omega}} \|\boldsymbol{h}_1\|_F^2 \, x_2^Q + \tilde{\tilde{n}}_2, \end{aligned} \tag{3.6b}$$

where the resultant noise term $\tilde{\tilde{n}}_t$ is a random variable which can be approximated as Gaussian distribution $\tilde{\tilde{n}}_t \sim CN(0,1)$ and $j = \sqrt{-1}$.

The receiver then performs MLD after the symbols are successfully de-interleaved and assuming full CSI. The MLD expressions for the symbol pair with MRC reception over Rayleigh fading for time slot $t \in [1:2]$ are then denoted as:

$$\hat{u}_1 = \underset{u_1 \in \boldsymbol{\Omega}}{argmin} \left\{ P_2 \left| r_1^I - \sqrt{\frac{E_s}{E_\omega}} \|\boldsymbol{h}_1\|_F^2 \left(u_1^I \cos\theta - u_1^Q \sin\theta\right)\right|^2 + P_1 \left| r_1^Q - j\sqrt{\frac{E_s}{E_\omega}} \|\boldsymbol{h}_2\|_F^2 \left(u_1^I \sin\theta + u_1^Q \cos\theta\right)\right|^2 \right\} \quad (3.7a)$$

$$\hat{u}_2 = \underset{u_2 \in \boldsymbol{\Omega}}{argmin} \left\{ P_1 \left| r_2^I - \sqrt{\frac{E_s}{E_\omega}} \|\boldsymbol{h}_2\|_F^2 \left(u_2^I \cos\theta - u_2^Q \sin\theta\right)\right|^2 + P_2 \left| r_2^Q - j\sqrt{\frac{E_s}{E_\omega}} \|\boldsymbol{h}_1\|_F^2 \left(u_2^I \sin\theta + u_2^Q \cos\theta\right)\right|^2 \right\} \quad (3.7b)$$

where $\hat{u}_1$ and $\hat{u}_2$ are the detected symbols for both time slots, $\boldsymbol{\Omega}$ is the *M*-QAM signal set, r_1^I, r_2^I are the real and r_1^Q, r_2^Q are the imaginary component of the de-interleaved symbols in Eq (3.6a) and Eq (3.6b), $u_1^I \cos\theta - u_1^Q \sin\theta = x_1^I, u_2^I \cos\theta - u_2^Q \sin\theta = x_2^I$ are the real and $u_1^I \sin\theta + u_1^Q \cos\theta = x_1^Q, u_2^I \sin\theta + u_2^Q \cos\theta = x_2^Q$ are the imaginary component of the rotated symbols corresponding to u_1 and u_2, respectively. P_1 and P_2 are instantaneous combined fading gain denoted as $P_t = \|\boldsymbol{h}_t\|_F^2 = \sum_{k=1}^{N_r} |h_{tk}|^2$, $t \in [1:2]$ and $k \in [1:N_r]$.

3.3 Error performance analysis of SSD

This section presents the symbol error performance analysis of the coherent SSD system with N_r-branches MRC reception for the *M*-QAM constellation presented on the system model in Section 3.2 above. In this dissertation, the symbol error performance is based on the symbol error probability (SEP) of the system in a closed form using union bound, minimum distance lower bound and nearest neighbhour approximation of the transmitted symbol u_i for each rotated constellation point and the chosen detected symbol $\hat{u}_i$.

In the high SNR region one symbol u_2 can be assumed to always be detected correct and u_1 can be considered to be a transmitted symbol and $\hat{u}_1$ as the detected symbol.

3.3.1 Union bound

Union bound (UB) as presented in [9], is an analysis method used to evaluate the error probability $P(e)$ of a signal set by summing the pairwise error probabilities (PEPs) of all possible transmitted and received symbol pair. The UB on the SEP is denoted as in [9]:

$$P_{M-QAM}^{UB}(e) \leq \frac{1}{|\boldsymbol{\Omega}|} \sum_{u_1 \in \boldsymbol{\Omega}} \sum_{\substack{\hat{u}_1 \in \boldsymbol{\Omega} \\ u_1 \neq \hat{u}_1}} P(u_1 \rightarrow \hat{u}_1), \quad (3.8)$$

where $|\boldsymbol{\Omega}|$ is the size of the *M*-QAM signal set and $P(u_1 \rightarrow \hat{u}_1)$ is the unconditional pairwise error probability (PEP) that estimated $\hat{u}_1$ at the receiver when u_1 was transmitted.

Due to the fading channel coefficient experienced by the symbol during transmission as in Eq (3.4), the unconditional PEP is conditioned as $P(u_1 \rightarrow \hat{u}_1|\boldsymbol{h}_1, \boldsymbol{h}_2)$ referred to as the conditional PEP. The unconditional PEP, $P(u_1 \rightarrow \hat{u}_1)$ is computed by averaging the conditional PEP over the independent fading distributions for MRC reception and is expressed as:

$$P(u_1 \rightarrow \hat{u}_1) = \int_0^\infty \int_0^\infty P(u_1 \rightarrow \hat{u}_1|\boldsymbol{h}_1, \boldsymbol{h}_2)\, f_{\gamma_1}(\gamma_1)\, f_{\gamma_2}(\gamma_2)\, d\gamma_1 d\gamma_2, \tag{3.9}$$

where $\boldsymbol{h}_1$ and $\boldsymbol{h}_2$ are the independent Rayleigh fading coefficient vector with entries h_{tk} for $t \in [1\colon 2]$ and $k \in [1\colon N_r]$, $h_{tk} = \alpha_{tk} e^{jQ_{tk}}$, α_{tk} is the Rayleigh fading distributed amplitude denoted as $\alpha_{tk} = \sqrt{(h_{tk}^I)^2 + \left(h_{tk}^Q\right)^2}$. γ_1 and γ_2 are combined instantaneous signal-to-noise ratio (SNR) defined as $\gamma_t = \sum_{k=1}^{N_r} \gamma_{tk}$ for $t \in [1\colon 2]$, $k \in [1\colon N_r]$ and $\gamma_{tk} = {\alpha_{tk}}^2(E_s)$ as shown in Appendix A.8. $f_{\gamma_1}(\gamma_1)$ and $f_{\gamma_2}(\gamma_2)$ are the MRC probability density function (PDF) for N_r receive antennas denoted as $f_{\gamma_t\, MRC}(\gamma_t) = \frac{1}{(N_r-1)!\,\bar{\gamma}^{N_r}} {\gamma_t}^{N_r-1} exp\left(-\frac{\gamma_t}{\bar{\gamma}}\right)$, $t \in [1\colon 2]$ and $\bar{\gamma}$ is the average SNR $\bar{\gamma} = E\{\gamma_t\}$.

The conditional PEP is defined in Eq (3.10) in a closed form as:

$$\begin{aligned} &P(u_1 \rightarrow \hat{u}_1|\boldsymbol{h}_1, \boldsymbol{h}_2) = \\ &P\left(\sum_{k=1}^{N_r} \left| r_{1k} - \sqrt{\frac{E_s}{E_\omega}}\alpha_{1k}\left(u_1^I \cos\theta - u_1^Q \sin\theta\right) - j\sqrt{\frac{E_s}{E_\omega}}\alpha_{2k}\left(u_1^I \sin\theta + u_1^Q \cos\theta\right)\right|^2 > \right. \\ &\left. \sum_{k=1}^{N_r} \left| r_{1k} - \sqrt{\frac{E_s}{E_\omega}}\alpha_{1k}\left(\hat{u}_1^I \cos\theta - \hat{u}_1^Q \sin\theta\right) - j\sqrt{\frac{E_s}{E_\omega}}\alpha_{2k}\left(\hat{u}_1^I \sin\theta + \hat{u}_1^Q \cos\theta\right)\right|^2 \right), \end{aligned} \tag{3.10}$$

where r_{1k}, $k \in [1\colon N_r]$ is the de-interleaved symbol in the first time slot as shown in Appendix A. $\frac{E_s}{E_\omega}$ is the average transmit power. $u_1^I \cos\theta - u_1^Q \sin\theta = x_1^I$ and $u_1^I \sin\theta + u_1^Q \cos\theta = x_1^Q$ are the real and imaginary components of the rotated symbol corresponding to u_1, $\hat{u}_1^I \cos\theta - \hat{u}_1^Q \sin\theta = \hat{x}_1^I$ and $\hat{u}_1^I \sin\theta + \hat{u}_1^Q \cos\theta = \hat{x}_1^Q$ are the real and imaginary components of the of the rotated symbols corresponding to $\hat{u}_1$.

The conditional PEP is effectively computed in Appendix A where the simplified conditional PEP expression is denoted as:

$$P(u_1 \rightarrow \hat{u}_1|\boldsymbol{h}_1, \boldsymbol{h}_2) = Q\left(\sqrt{\frac{1}{2E_\omega}(\gamma_1 d_1^2 + \gamma_2 d_2^2)}\right), \tag{3.11}$$

where E_ω is the average signal power, d_1 and d_2 represent the in-phase and quadrature distances between x_1 and $\hat{x}_1$, respectively.

Substituting the simplified conditional PEP in Eq (3.11) onto Eq (3.9) gives the unconditional PEP in Eq (3.12):

$$\begin{aligned} P(u_1 \to \hat{u}_1) &= \int_0^\infty \int_0^\infty Q\left(\sqrt{\frac{1}{2E_\omega}(\gamma_1 d_1^2 + \gamma_2 d_2^2)}\right) f_{\gamma_1}(\gamma_1)\, f_{\gamma_2}(\gamma_2)\, d\gamma_1\, d\gamma_2, \\ &= \frac{1}{2n} * \left[\frac{1}{2}G + \sum_{i=1}^{n-1} W\right], \\ &= \frac{1}{4n}G + \frac{1}{2n}\sum_{i=1}^{n-1} W, \end{aligned} \tag{3.12}$$

where $G = \left(\frac{2}{2+\left(\frac{d_1^2}{2E_\omega}\right)\bar{\gamma}}\right)^{N_r}\left(\frac{2}{2+\left(\frac{d_2^2}{2E_\omega}\right)\bar{\gamma}}\right)^{N_r}$ and $W = \left(\frac{S_i}{S_i+\left(\frac{d_1^2}{2E_\omega}\right)\bar{\gamma}}\right)^{N_r}\left(\frac{S_i}{S_i+\left(\frac{d_2^2}{2E_\omega}\right)\bar{\gamma}}\right)^{N_r}$.

Refer to Appendix B for the derivation of Eq (3.12). Substituting Eq (3.12) onto Eq (3.8) gives the new expression for UB on the SEP with N_r-branches MRC reception in Eq (3.13):

$$P_{M-QAM}^{UB}(e) \leq \frac{1}{|\boldsymbol{\Omega}|}\sum_{u_1 \in \boldsymbol{\Omega}} \sum_{\substack{\hat{u}_1 \in \boldsymbol{\Omega} \\ u_1 \neq \hat{u}_1}} \left\{\frac{1}{4n}G + \frac{1}{2n}\sum_{i=1}^{n-1} W\right\}. \tag{3.13}$$

3.3.2 Minimum distance lower bound

Minimum distance lower bound (MDLB) as presented in [9], is the analysis method used to derive a lower bound on the SEP using the minimum Euclidean distance of the rotated constellation. Taking into consideration the independent fading on the in-phase and quadrature components of the signal due to component interleaving/de-interleaving.

The conventional square *M*-QAM SEP is given as:

$$P_{M-QAM}(e) \geq 4\left(1-\frac{1}{\sqrt{M}}\right)Q\left(\sqrt{\frac{3E_S}{N_0(M-1)}}\right) - 4\left(1-\frac{1}{\sqrt{M}}\right)^2 Q^2\left(\sqrt{\frac{3E_S}{N_0(M-1)}}\right), \tag{3.14}$$

where M is the modulation order, $N_0 = 1$ is the power spectrum density, E_s is the transmitted power.

Let $a = \left(1-\frac{1}{\sqrt{M}}\right)$ and $b = \left(\frac{3}{M-1}\right)$. The conventional square *M*-QAM on the SEP can be rewritten as:

$$P_{M-QAM}(e) \geq 4aQ\left(\sqrt{bE_s}\right) - 4a^2Q^2\left(\sqrt{bE_s}\right), \tag{3.15}$$

Considering the fading channel coefficient experienced by the rotated symbol during transmission as in Eq (3.15), the conventional square SEP is conditioned as $P_{M-QAM}(e|\boldsymbol{h}_1, \boldsymbol{h}_2)$ referred to as the conditional SEP. The conditional SEP can be denoted as:

$$P_{M-QAM}(e|\boldsymbol{h}_1, \boldsymbol{h}_2) \geq 4aQ\left(\sqrt{b(\alpha_1^2 + \alpha_2^2)E_s}\right) - 4a^2Q^2\left(\sqrt{b(\alpha_1^2 + \alpha_2^2)E_s}\right), \tag{3.16}$$

where $\boldsymbol{h}_1$ and $\boldsymbol{h}_2$ are the independent Rayleigh fading coefficient vector with entries h_{tk} for $t \in [1:2]$ and $k \in [1:N_r]$, $h_{tk} = \alpha_{tk}e^{jQ_{tk}}$, α_{tk} is the Rayleigh fading distributed amplitude denoted as $\alpha_{tk} = \sqrt{(h_{tk}^I)^2 + \left(h_{tk}^Q\right)^2}$, $\gamma_{tk} = {\alpha_{tk}}^2(E_s)$ in the SNR as shown in Appendix A.

The conventional square *M*-QAM on the SEP may be conditioned upon instantaneous SNR and be written as:

$$P_{M-QAM}^{MDLB}(e|\gamma_1, \gamma_2) \geq 4aQ\left(\sqrt{b(\gamma_1 + \gamma_2)}\right) - 4a^2Q^2\left(\sqrt{b(\gamma_1 + \gamma_2)}\right), \tag{3.17}$$

where γ_1 and γ_2 are combined instantaneous SNR defined as $\gamma_t = \sum_{k=1}^{N_r}\gamma_{tk}$ for $t \in [1:2]$, $k \in [1:N_r]$.

Taking into consideration the minimum Euclidean distance between the rotated constellation and independent fading experienced by the in-phase and quadrature components of the signal, let $\sqrt{b\gamma_i} = \sqrt{\frac{d_i^2}{2E_\omega}}$ for i $[1:2]$. The conditional MDLB on the SEP in Eq (3.16) can be denoted as:

$$P_{M-QAM}^{MDLB}((e|\boldsymbol{h}_1, \boldsymbol{h}_2) \geq 4aQ\left(\sqrt{\frac{(d_1^2+d_2^2)}{2E_\omega}}\right) - 4a^2Q^2\left(\sqrt{\frac{(d_1^2+d_2^2)}{2E_\omega}}\right), \tag{3.18}$$

where E_ω is the average signal power, d_1 and d_2 represent the in-phase and quadrature minimum Euclidean distances between x_1 and $\hat{x}_1$, respectively [9] denoted as:

$$d_{min} = \min_{x_1, x_2 \in \boldsymbol{\Omega}}\left\{\sqrt{\|x_1 - x_2\|^2}\right\}, \tag{3.19}$$

where $\boldsymbol{\Omega}$ is the *M*-QAM signal set, x_1 and x_2 the rotated symbol corresponding to u_1 and u_2, respectively.

Due to the independent fading experienced by the in-phase (real) and quadrature (imaginary) components of the rotated signal during transmission, the minimum distance can be modified as in Eq (3.20) [9]:

$$d_{min} = \min_{x_1, x_2 \in \boldsymbol{\Omega}} \left\{ \sqrt{\boldsymbol{h}_1^2 |x_1^I - x_2^I|^2 + \boldsymbol{h}_2^2 \left|x_1^Q - x_2^Q\right|^2} \right\}, \quad (3.20)$$

where $\boldsymbol{h}_1^2$ and $\boldsymbol{h}_2^2$ are the independent Rayleigh fading vectors of the in-phase and quadrature components of the signal, x_1^I,x_2^I are the real and x_1^Q,x_2^Q are the imaginary component of the rotated symbols corresponding to u_1 and u_2, respectively.

Taking into consideration the rotation angel θ of the rotated two-dimensional constellations, the minimum distance in Eq (3.20) can be written as:

$$d_{min} = \sqrt{4\,\boldsymbol{h}_1^2 Cos^2\theta + 4\,\boldsymbol{h}_2^2 Sin^2\theta}, \quad (3.21)$$

where $\left|x_1^I - x_2^I\right| = 4\,Cos^2\theta$ and $\left|x_1^Q - x_2^Q\right| = 4\,sin^2\,\theta$.

Substitute Eq (3.21) onto Eq (3.18) and, the conditional MDLB on the SEP over instantaneous SNR in Eq (3.17) can be written as:

$$P_{M-QAM}^{MDLB}(e|\gamma_1,\gamma_2) \geq 4aQ\left(\sqrt{b(\gamma_1 \cos^2\theta + \gamma_2 \sin^2\theta)}\right) - 4a^2Q^2\left(\sqrt{b(\gamma_1 \cos^2\theta + \gamma_2 \sin^2\theta)}\right), \quad (3.22)$$

where γ_1 and γ_2 are combined instantaneous SNR defined as $\gamma_t = \sum_{k=1}^{N_r} \gamma_{tk}$ for $t \in [1\colon 2]$, $k \in [1\colon N_r]$ and $\gamma_{tk} = {\alpha_{tk}}^2(E_s)$ as shown in Appendix A.

The unconditional MDLB on the SEP is further computed by averaging the conditioned SEP in Eq (3.22) as:

$$P_{M-QAM}^{MDLB}(e) = \int_0^\infty \int_0^\infty P_{M-QAM}^{MDLB}(e|\gamma_1\gamma_2)\; f_{\gamma_1}(\gamma_1)d\gamma_1\, f_{\gamma_2}(\gamma_2)d\gamma_2, \quad (3.23)$$

where $f_{\gamma_1}(\gamma_1)$ and $f_{\gamma_2}(\gamma_2)$ are the MRC probability density function for N_r receive antennas denoted as $f_{\gamma_t\,MRC}(\gamma_t) = \frac{1}{(N_r-1)!\,\bar{\gamma}^{N_r}} {\gamma_t}^{N_r-1} exp\left(-\frac{\gamma_t}{\bar{\gamma}}\right)$, $t \in [1\colon 2]$ and $\bar{\gamma} = E\{\gamma_t\}$ is the average SNR.

Let $\zeta = \gamma_1 \cos^2\theta + \gamma_2 \sin^2\theta$. Substituting Eq (3.22) onto Eq (3.23) gives the new MDLB on the SEP as:

$$P_{M-QAM}^{MDLB}(e) = \int_0^\infty \int_0^\infty 4aQ\left(\sqrt{b\zeta}\right) - 4a^2Q^2\left(\sqrt{b\zeta}\right) f_{\gamma_1}(\gamma_1)d\gamma_1\, f_{\gamma_2}(\gamma_2)d\gamma_2,$$

$$= \frac{a}{n}\left\{\frac{1}{2} \times \left(\frac{2}{2+\alpha b\bar{\gamma}}\right)^{N_r}\left(\frac{2}{2+\delta b\bar{\gamma}}\right)^{N_r} - \frac{a}{2}\left(\frac{1}{1+\alpha b\bar{\gamma}}\right)^{N_r}\left(\frac{1}{1+\delta b\bar{\gamma}}\right)^{N_r} + (1-a)\right.$$

$$\left.\left(\sum_{i=1}^{n-1}\left(\frac{S_i}{S_i+\alpha b\bar{\gamma}}\right)^{N_r}\left(\frac{S_i}{S_i+\delta b\bar{\gamma}}\right)^{N_r}\right)\right\},$$

$$= \frac{a}{n}\left\{\frac{1}{2} \times FD - \frac{a}{2} \times AE + (1-a)\left(\sum_{i=1}^{n-1} \mathrm{CI} + \sum_{i=n}^{2n-1} OV\right)\right\}, \quad (3.24)$$

where $\alpha = \cos^2\theta$; $\delta = \sin^2\theta$, $F = \left(\frac{2}{2+\alpha b\bar{\gamma}}\right)^{N_r}$, $D = \left(\frac{2}{2+\delta b\bar{\gamma}}\right)^{N_r}$ $A = \left(\frac{1}{1+\alpha b\bar{\gamma}}\right)^{N_r}$, $E = \left(\frac{1}{1+\delta b\bar{\gamma}}\right)^{N_r}$ $C = \left(\frac{S_i}{S_i+\alpha b\bar{\gamma}}\right)^{N_r}$, $I = \left(\frac{S_i}{S_i+\delta b\bar{\gamma}}\right)^{N_r}$ and $O = \left(\frac{S_{iB}}{S_{iB}+\alpha b\bar{\gamma}}\right)^{N_r}$ and $V = \left(\frac{S_{iB}}{S_{iB}+\delta b\bar{\gamma}}\right)^{N_r}$.

Refer to Appendix B for an effective computation of the final expression of the MDLB on the SEP in Eq (3.24).

3.3.3 Nearest neighbour approximation

The nearest neighbour (NN) approximation evaluates the symbol error performance of the wireless communication system by considering the closest points in Euclidean distance to any point in a constellation. The NN approximation employed in a coherent SSD system with MRC reception in a closed form considers the nearest neighbouring points of any point of a rotated constellation. The PEPs of the rotated constellation neighbour's points has perpendicular and diagonal neighbours with different Euclidean distance. Considering u_1 was the transmitted symbol and $\hat{u}_1$ the chosen detected symbol, the NN approximation on the SEP can be written as in [9, 10]:

$$P_{M-QAM}^{NN}(e) = K_M P_{perp}(u_1 \to \hat{u}_1) + L_M P_{diag}(u_1 \to \hat{u}_1), \quad (3.25)$$

where K_M and L_M are the coefficients of the PEPs and are described in Table 3.1 as presented in [10]:

Table 3.1: Values of the PEPs coefficients K_M and L_M [10].

M-QAM Constellations	K_M	L_M
4	2	1
16	3	2.25
64	3.5	3.51
256	3.75	3.5156

$P_{\mathrm{perp}}(u_1 \to \hat{u}_1)$ and $P_{\mathrm{diag}}(u_1 \to \hat{u}_1)$ are PEPs between a rotated constellation point and its perpendicular and diagonal neighbours. The PEPs can be computed using the unconditional PEP expression in Eq (3.12) as follows:

$$P_{perp}(u_1 \to \hat{u}_1) = \int_0^\infty \int_0^\infty Q\left(\sqrt{\frac{1}{2E_\omega}\left(\gamma_1 d_{1\,perp}^2 + \gamma_2 d_{2\,perp}^2\right)}\right) f_{\gamma_1}(\gamma_1)\, f_{\gamma_2}(\gamma_2)\, d\gamma_1\, d\gamma_2 \quad (3.26a)$$

$$P_{diag}(u_1 \to \hat{u}_1) = \int_0^\infty \int_0^\infty Q\left(\sqrt{\frac{1}{2E_\omega}\left(\gamma_1 d_{1\,diag}^2 + \gamma_2 d_{2\,diag}^2\right)}\right) f_{\gamma_1}(\gamma_1)\, f_{\gamma_2}(\gamma_2)\, d\gamma_1\, d\gamma_2, \quad (3.26b)$$

where $d^2_{1\,perp}$, $d^2_{1\,diag}$ and $d^2_{2\,perp}$, $d^2_{2\,diag}$ are the Euclidean distances for the perpendicular and diagonal neighbours, respectively and are defined in Eq (3.27a) and Eq (3.27b) as:

$$d^2_{1perp} = 4\,Cos^2\theta \qquad d^2_{2perp} = 4\,sin^2\,\theta, \tag{3.27a}$$

$$d^2_{1diag} = 4(1 + sin2\theta) \qquad d^2_{2diag} = 4\,(1 - sin\,2\theta). \tag{3.27b}$$

The perpendicular and diagonal PEPs expressions are simplified in Appendix B. The perpendicular and diagonal PEPs are then denoted as:

$$P_{perp}(u_1 \to \hat{u}_1) \;= \tfrac{1}{4n}T + \tfrac{1}{2n}\textstyle\sum_{i=1}^{n-1} R, \tag{3.28a}$$

$$P_{diag}(u_1 \to \hat{u}_1) \;= \tfrac{1}{4n}T + \tfrac{1}{2n}\textstyle\sum_{i=1}^{n-1} R, \tag{3.28b}$$

where $T = \left(\frac{2}{2+\left(\frac{d^2_{1perp}}{2E_\omega}\right)\bar{\gamma}}\right)^{N_r}\left(\frac{2}{2+\left(\frac{d^2_{2perp}}{2E_\omega}\right)\bar{\gamma}}\right)^{N_r}$ and $R = \left(\frac{S_i}{S_i+\left(\frac{d^2_{1diag}}{2E_\omega}\right)\bar{\gamma}}\right)^{N_r}\left(\frac{S_i}{S_i+\left(\frac{d^2_{2diag}}{2E_\omega}\right)\bar{\gamma}}\right)^{N_r}$.

Substituting Eq (3.28a) and Eq (3.28b) into Eq (3.25) gives the final expression for NN approximation with N_r-branches MRC reception on the SEP as:

$$P^{NN}_{M\_QAM}(e) = K_M\left[\tfrac{1}{4n}T + \tfrac{1}{2n}\textstyle\sum_{i=1}^{n-1} R\;\right] + L_M\left[\tfrac{1}{4n}T + \tfrac{1}{2n}\textstyle\sum_{i=1}^{n-1} R\;\right]. \tag{3.29}$$

3.4 Numerical and analytical results

This section presents numerical and analytical results of coherent SSD maximum-likelihood detection and SEP analyses using UB, MDLB and NN approximation models of a coherent SSD SIMO system with $N_t = 1$ and $N_r = 2$, and $N_t = 1$ and $N_r = 4$ over Rayleigh fading and AWGN channel for both 16-QAM and 64-QAM modulations.

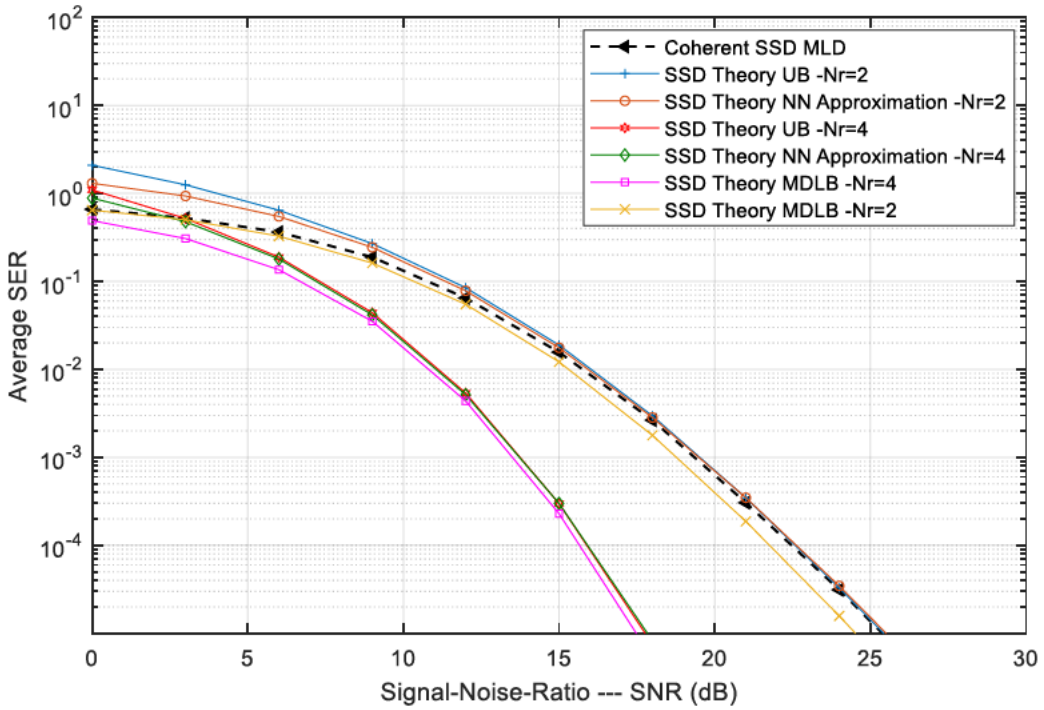

Figure 3.4: Coherent SSD maximum-likelyhood detection and SEP performance analytical results for 16-QAM with $N_r = 2$ and $N_r = 4$.

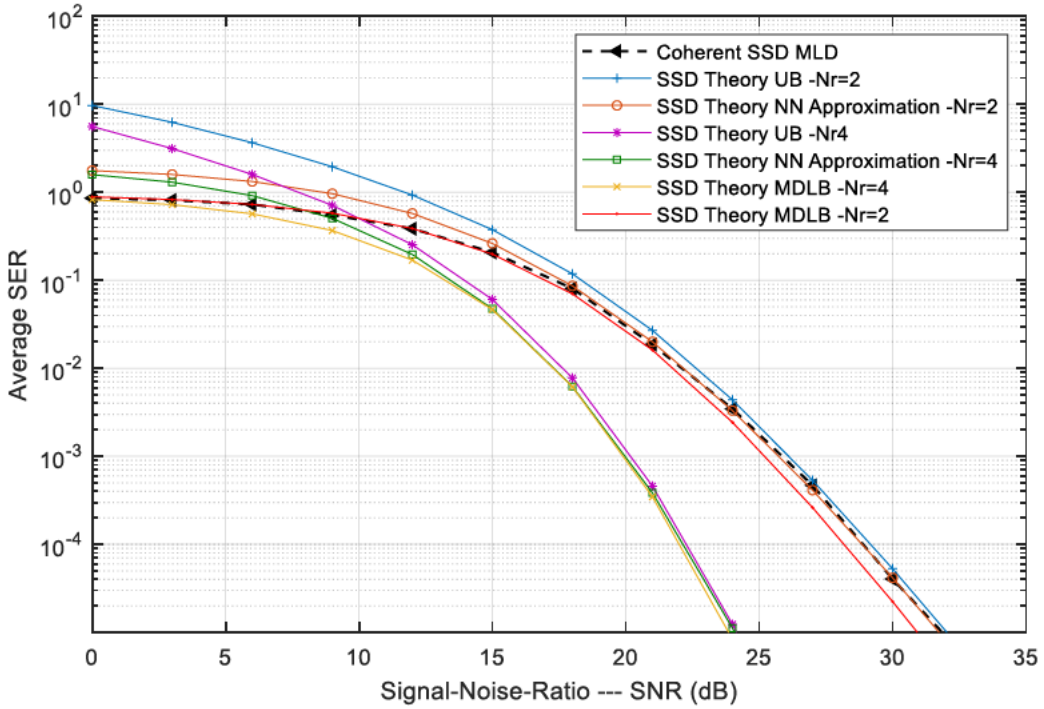

Figure 3.5: Coherent SSD maximum-likelihood detection and SEP performance analytical results for 64-QAM with $N_r = 2$ and $N_r = 4$.

For both 16-QAM and 64-QAM constellations, it is observed from Figure 3.4 and Figure 3.5 that when $N_r = 2$, the SEP performance of the coherent SSD MLD is lower and apart from that of the UB and NN approximation at a lower SNR and gradually gets closer and tight as the SNR increases. Where else, the SEP performance of the coherent SSD MLD for both 16-QAM and 64-QAM constellations is tight with that of the MDLB when the SNR is 0 and then gradually separates as the SNR increases.

For both 16-QAM and 64-QAM constellations, it is observed from Figure 3.4 and Figure 3.5 that when $N_r = 4$, the SEP performance of the coherent SSD MLD is lower and apart from that of the UB and NN approximation when the SNR is 0 and increasingly separates as the SNR increases. For 16-QAM when $N_r = 4$, the SEP performance of the coherent SSD MLD is higher and apart from that of the MDLB when the SNR is 0 and increasingly separates as the SNR increases. Where else, for 64-QAM, the SEP performance of the coherent SSD MLD is tight with that of the MDLB when the SNR is 0 and then gradually separates as the SNR increases.

3.5 Chapter summary

In this chapter, a coherent SSD system for *M*-QAM signal constellations using SIMO was successfully presented. Where, the signal rotation and components interleave/de-interleave were presented and discussed in the SSD system model to implement diversity in the wireless communication system without additional power and bandwidth. MRC reception was employed at the receiver in the coherent SSD system model to reduce the errors in the detection as the system requires the full knowledge of CSI at the receiver. The SEP performance of the coherent SSD system was analyzed using UB, MDLB and NN approximation in a closed form. Numerical and analytical results for both 16-QAM and 64-QAM signal constellations when $N_r = 2$ and $N_r = 4$ were presented. It was observed that the for both 16-QAM and 64-QAM signal constellations, the performance of the UB, MDLB and NN approximation lowers from that of coherent SSD MLD as the number of receivers increase.

CHAPTER 4

CONVENTIONAL DIFFERENTIAL MODULATION AND GENERALIZED DIFFERENTIAL MODULATION

This chapter presents two differential modulation (DM) schemes, the conventional differential modulation (CDM) and generalized differential modulation (GDM). Both CDM and GDM schemes are employed in wireless communication systems to simplify the complexity of the coherent detection by using differential detection.

4.1 Introduction

This section presents the background of the CDM and GDM schemes which are non-coherent detections to improve the error performance of wireless communication systems. These schemes are presented in separate sections below.

4.1.1 Conventional differential modulation

Conventional differential modulation is used to improve wireless communication systems error performance by performing detection without the knowledge of channel state information (CSI) at the receiver. Though CDM has been proven in [24] to perform detection without the knowledge of CSI through differential detection, it suffers a 3dB performance loss compared to the coherent detection. As indicated in Section 2.3, information symbols are differential encoded at the source before being transmitted. In CDM, information symbols are encoded using a symbol-by-symbol encoder in a way that the previous symbol encodes the next symbol.

After differential encoding is performed, there are $(N + 1)$ differentially encoded symbols in each frame to be transmitted from the source to the destination. The first encoded symbol is referred to as the reference symbol (RS) and the remaining symbols are referred to as normal symbols (NSs).

4.1.2 Generalized differential modulation

Generalized differential modulation is a differential modulation scheme employed in wireless communication system to reduce non-coherent CDM error performance loss to its coherent counterpart. In [18, 11], GDM schemes are proposed where the concept of power allocation is employed between the reference block (RB) and normal blocks (NBs) to reduce the error performance gap between non-coherent CDM detection and coherent detection. In [11, 18], information symbols are differential encoded at the source before transmission using a block-by-block differential encoder in a way that the NBs in a frame are differentially encoded based on the previous and current RB. It is observed that the

non-coherent CDM error performance is improved by allocating more transmit power to the RB as compared to the NBs in order to maximize the average output signal-to-noise ratio (SNR) of the respective systems. This results in an improved channel estimation. Similarly to [19], the GDM presented in [18] uses the frame structure and applies the block-by-block differential encoder. In [18], the RB and NBs convey information except for the first RB.

The GDM scheme presented in [11], also uses the frame structure consisting of the RB and NBs however, only normal blocks convey information. Normal blocks in a frame are differentially encoded based on the reference block in the same frame. The reference symbol remains constant throughout transmission to allow the information carrying symbols in the normal-block to be drawn from *M*-ary quadrature amplitude modulation (*M*-QAM) constellation.

Following [18, 19], the GDM scheme presented in this dissertation is based on the concept of power allocation between the reference symbol and normal symbols where more power is allocated to the reference symbol as compared to the normal symbols. Assume each frame length is $(N + 1)$ symbols, the symbols are divided into several blocks where each block consists of n symbols. The first symbol in each block is referred to as the RS, and the remaining $n - 1$ symbols are referred to as NSs. Thus, information is transmitted via symbols in blocks. Using a block-by-block differential encoder, information symbols are differential encoded at the source before transmission in a way that the NSs in a frame are differentially encoded based on the RS. Assume that the RS in each frame remains constant throughout the transmission across all blocks.

4.2 System model

This section presents the system models for CDM and GDM schemes. In both these non-coherent systems, information symbols are differentially encoded before transmission. Also, it is assumed that fading channels experienced by the symbols during transmission remain constant thus, quasi-static fading channel (QSFC).

4.2.1 Conventional differential modulation system model

Consider a non-coherent CDM $N_t \times N_r$ single-input-multiple-output (SIMO) system where $N_t = 1$ is the number of transmit antennas and $N_r \geq N_t$ is the number of receive antennas as illustrated in Figure 4.1 below. We assume that the receive antennas must be spaced far enough apart from each other so that there is no correlation among the respective received signals.

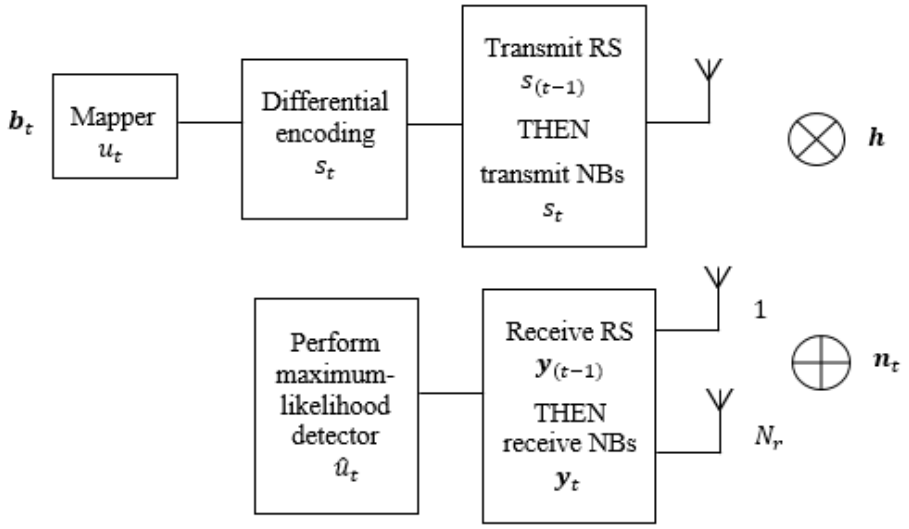

Figure 4.1: Block diagram of conversation differential modulation system model.

Information bits $\boldsymbol{b}_t = [b_{t,1}\ b_{t,2}\ b_{t,3}\ \cdots b_{t,k}]$ are grouped in sequences of $k = log_2 M$ bits in size where M is the modulation order and subscript t, $t \in [1:T]$ determines the index to be transmitted at the time slot T.

The grouped information bits are directly mapped onto M-ary phase shift keying (M-PSK) signal set $\boldsymbol{\Psi}$, and yields symbol $u_t = u_t^I + ju_t^Q$, assuming $E[|u_t|^2] = 1$. Differential encoding is then performed on the information symbol (u_t) before transmission using the differential transmission matrix on Eq (4.1):

$$s_t = s_{(t-1)}\, u_t, \tag{4.1}$$

where $s_0 = 1$ and has normalized energy $E[|s_0|^2]$ known at the receiver. s_t is the differentially encoded symbol to be transmitted at time t, $t \in [1:T]$, $s_{(t-1)}$ is the reference symbol, and u_t is the information symbol. This means information is conveyed in two symbols u_t and $s_{(t-1)}$.

During transmission each symbol experiences QSFC and additive white Gaussian noise (AWGN) giving the received symbol $\boldsymbol{y}_t$:

$$\boldsymbol{y}_t = \sqrt{E_s}\boldsymbol{h}s_t + \boldsymbol{n}_t, \tag{4.2}$$

where $\boldsymbol{y}_t \in \mathbb{C}^{N_r \times 1}$ is the received symbol vector, E_s is the transmitted power, $\boldsymbol{h}$ is an independent quasi-static fading coefficient vector whose entries are independent and identically distributed (i.i.d.) complex Gaussian random variables (RVs) with distribution $CN(0,1)$ and, $\boldsymbol{n}_t$ is the AWGN vector with entries n_{tk} modeled as i.i.d. complex Gaussian RVs with distribution $n_{tk} \sim CN(0,1)$. The subscript k, $k \in [1:N_r]$ is the receive antenna index.

A. Detection

Assuming that $\boldsymbol{y}_t$ and $\boldsymbol{y}_{(t-1)}$ are known at the receiver. Where $\boldsymbol{y}_{(t-1)}$ is the previous received symbol defined as:

$$\boldsymbol{y}_{(t-1)} = \sqrt{E_s}\boldsymbol{h}\boldsymbol{s}_{(t-1)} + \boldsymbol{n}_{(t-1)}. \tag{4.3}$$

Therefore,

$$\sqrt{E_s}\boldsymbol{h}\boldsymbol{s}_{(t-1)} = \boldsymbol{y}_{(t-1)} - \boldsymbol{n}_{(t-1)}. \tag{4.4}$$

The received symbol vector in Eq (4.2) may be rewritten as:

$$\begin{aligned} \boldsymbol{y}_t &= \sqrt{\frac{E_s}{E_\omega}}\boldsymbol{h}\boldsymbol{s}_t + \boldsymbol{n}_t, \\ &= \sqrt{\frac{E_s}{E_\omega}}\boldsymbol{h}\boldsymbol{s}_{(t-1)}u_t + \boldsymbol{n}_t. \end{aligned} \tag{4.5}$$

Substituting Eq (4.4) into Eq (4.5) gives:

$$\begin{aligned} \boldsymbol{y}_t &= \sqrt{\frac{E_s}{E_\omega}}\left(\boldsymbol{y}_{(t-1)} - \boldsymbol{n}_{(t-1)}\right)u_t + \boldsymbol{n}_t, \\ &= \sqrt{\frac{E_s}{E_\omega}}\boldsymbol{y}_{(t-1)}u_t - \sqrt{\frac{E_s}{E_\omega}}\boldsymbol{n}_{(t-1)}u_t + \boldsymbol{n}_t. \end{aligned} \tag{4.6}$$

The receiver then performs maximum-likelihood detection (MLD) for a non-coherent CDM system denoted as:

$$\hat{u}_t = \min_{u_t \in \boldsymbol{\Psi}} \left\| \boldsymbol{y}_t - \sqrt{\frac{E_s}{E_\omega}}\ \boldsymbol{y}_{(t-1)}u_t \right\|^2, \tag{4.7}$$

where $\hat{u}_t$ is the detected symbol and $\boldsymbol{\Psi}$ is the *M*-PSK signal set.

$\boldsymbol{y}_{(t-1)}$ is used to estimate the channel so to recover information conveyed in $\boldsymbol{y}_t$.

4.2.2 Generalized differential modulation system model

Consider a non-coherent GDM $N_t \times N_r$ SIMO system where $N_t = 1$ is the number of transmit antennas and $N_r \geq N_t$ is the number of receive antennas as illustrated in Figure 4.2 below. We assume that the receive antennas must be spaced far enough apart from each other so that there is no correlation among the respective received signals.

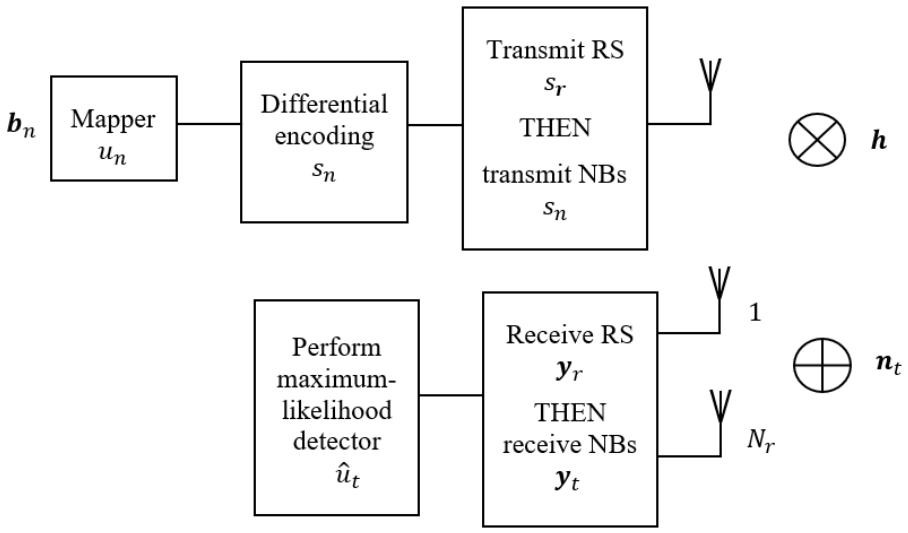

Figure 4.2: Block diagram of generalized differential modulation system model.

Information bits $\boldsymbol{b}_n = [b_{n,1}\, b_{n,2}\, b_{n,3} \cdots b_{n,k}]$ are grouped in sequences of $k = log_2 M$ bits in size where M is the modulation order and n is the signal index.

The grouped information bits are directly mapped onto M-QAM signal $\boldsymbol{\Omega}$ and yields symbol u_n, assuming $E[|u_n|^2] = 1$. Differentially encoding is then performed on the information symbol (u_n) before transmission using the differential transmission matrix on Eq (4.8):

$$s_n = s_r u_n\,, \tag{4.8}$$

where s_n denotes differentially encoded symbol in a block to be transmitted, s_r is the reference symbol and u_n is information symbol.

A. Reference symbol

The reference symbol s_r, is the first transmitted symbol across all frames through the source denoted as:

$$s_r = 1. \tag{4.9}$$

s_r remains constant for each frame throughout the transmission and does not convey information. This allows for the information carrying symbols in NSs to be drawn from M-QAM constellation. During transmission, the transmitted symbol experience QSFC and AWGN as it arrives at the destination, giving received reference symbol vector $\boldsymbol{y}_r$:

$$\boldsymbol{y}_r = \sqrt{E_{RS}}\,\boldsymbol{h}s_r + \boldsymbol{n}_r, \tag{4.10}$$

where $\boldsymbol{y}_r \in \mathbb{C}^{N_r \times 1}$ is the received reference symbol vector, E_{RS} is the RS transmitted power, $\boldsymbol{h}$ is an independent quasi-static fading coefficient vector whose entries are i.i.d. complex Gaussian RVs with distribution $CN(0,1)$ and, $\boldsymbol{n}_r$ is the AWGN vector with entries n_{rk} modeled as i.i.d. complex Gaussian RVs with distribution $n_{rk} \sim CN(0,1)$. The subscript k, $k \in [1: N_r]$ is the receive antenna index.

B. Normal symbols

Normal symbols are the remaining encoded symbols in the transmission frame. NSs are encoded based on the RS of the same block as in Eq (4.11):

$$s_n = s_r u_n, \tag{4.11}$$

where the subscript n, denotes the symbol index in a block, s_n is the differentially encoded normal symbol, s_r is the reference symbol and u_n is the information symbol.

Normal symbols are transmitted after the transmission of the reference symbol in different time slots. Similarly to the RS, during transmission each symbol experiences QSFC and AWGN giving the received normal symbol $\boldsymbol{y}_t$:

$$\boldsymbol{y}_t = \sqrt{E_{NS}}\,\boldsymbol{h}s_t + \boldsymbol{n}_t, \tag{4.12}$$

where $\boldsymbol{y}_t \in \mathbb{C}^{N_r \times 1}$, $t, t \in [1:T]$ is the received normal symbol vector at time t, E_{NS} is the NSs transmitted power, $\boldsymbol{h}$ is an independent quasi-static fading coefficient vector whose entries are i.i.d. complex Gaussian RVs with distribution $CN(0,1)$ and, $\boldsymbol{n}_t$ is the AWGN vector with entries n_{tk} modeled as i.i.d. complex Gaussian RVs with distribution $n_{tk} \sim CN(0,1)$. The subscript k, $k \in [1: N_r]$ is the receive antenna index.

C. Detection

Assuming that $\boldsymbol{y}_r$ and $\boldsymbol{y}_t$ are known at the receiver. As in Eq (4.10), $\boldsymbol{y}_r$ is defined as:

$$\boldsymbol{y}_r = \sqrt{E_{RS}}\,\boldsymbol{h}s_r + \boldsymbol{n}_r.$$

Therefore,

$$\sqrt{E_{RS}}\,\boldsymbol{h}s_r = \boldsymbol{y}_r - \boldsymbol{n}_r. \tag{4.13}$$

The received symbol vector in Eq (4.12) may be rewritten as:

$$\boldsymbol{y}_t = \sqrt{\frac{E_{NS}}{E_{RS}}}\boldsymbol{h}s_t + \boldsymbol{n}_t = \sqrt{\frac{E_{NS}}{E_{RS}}}\boldsymbol{h}s_r u_n + \boldsymbol{n}_t. \quad (4.14)$$

Substituting Eq (4.13) on to Eq (4.14) gives:

$$\begin{aligned}\boldsymbol{y}_t &= \sqrt{\frac{E_{NS}}{E_{RS}}}(\boldsymbol{y}_r - \boldsymbol{n}_r)u_n + \boldsymbol{n}_t, \\ &= \sqrt{\frac{E_{NS}}{E_{RS}}}(\boldsymbol{y}_r u_n - \boldsymbol{n}_r u_n) + \boldsymbol{n}_t, \end{aligned} \quad (4.15)$$

where $\frac{E_{NS}}{E_{RS}}$ is the average transmitted power.

The receiver then performs MLD for a non-coherent GDM system denoted as:

$$\hat{u}_t = \min_{s_t \in \boldsymbol{\Omega}} \left\| \boldsymbol{y}_t - \sqrt{\frac{E_{NS}}{E_{RS}}}\boldsymbol{y}_r u_t \right\|^2, \quad (4.16)$$

where $\hat{u}_t$ is the detected symbol, $\boldsymbol{\Omega}$ is the *M*-QAM signal set.

$\boldsymbol{y}_r$ is used to estimate the channels so to recover information conveyed in $\boldsymbol{y}_t$. Symbols transmission powers are independently allocated amongst the RS and NSs where more power is allocated to the RS compared to NSs. Allocating more power to the RS results to a better estimation of the channel.

4.2.3 Power allocation

This section presents power allocation literature based on the symbol's signal-to-noise ratio (SNR) since the receiver detection of the GDM system model in Section 4.2.2 is based on the transmitted symbols in a block. Assuming that each frame length is $(N + 1)$ encoded symbols. Employing optimal power allocation from [19] obtained using Lagrange multiplier method, let the average power at the transmit antenna be denoted as E_s and, the SNR for RS and NSs be E_{RS} and E_{NS}, respectively. The total transmit power of the system is then denoted as:

$$(N + 1)E_S = E_{RS} + NE_{NS}. \quad (4.17)$$

In order to improve the channel estimation, let a portion of power from each normal symbol be removed and re-allocated to the reference symbol. Doing so reduces the errors. Therefore, the average signal-to-noise ratios (SNRs) for the RS and NSs can be denoted as:

$$E_{RS} = (1 + \rho N)E_S, \quad (4.18a)$$

$$E_{NS} = (1 - \rho)E_S, \quad (4.18b)$$

where ρ is the portion of power from the normal symbols.

From Eq (4.18a) and Eq (4.18b), it can be evident that the RS has more power that NSs.

4.3 Error performance analysis

This section presents the symbol error probability (SEP) analysis of non-coherent CDM and GDM system models presented in Section 4.2.1 and Section 4.2.2. The SEP analysis is performed with *M*-ary differential phase-shift keying (*M*-DPSK) for CDM and differential *M*-ary quadrature amplitude modulation for GDM based on the error probability of the system considering that u_i is the transmitted symbol and $\hat{u}_i$ is the chosen detected symbol.

4.3.1 Conventional differential modulation error performance analysis

The error performance of CDM is performed with *M*-DPSK as it eliminates the coherent referral signal at the receiver. This is performed by combining the differential encoding of the input signal and phase shift keying at the receiver [25]. The symbol error probability for *M*-DPSK is given as in Eq (4.19):

$$P_{M-DPSK}(e) = \int_0^{\infty} P_{M-DPSK}(e|\gamma)\, f_{\gamma}(\gamma) d\gamma, \tag{4.19}$$

where $\gamma = \sum_{i=1}^{N_r} \gamma_i$ for $i \in [1:2]$ is the average instantaneous SNR with $\gamma_i = \frac{E_s}{N_o}$ as an instantaneous SNR, E_S is the average power, $N_o = 1$ is the power spectrum density, $P_{M-DPSK}(e|\gamma)$ is the conditional SEP over instantaneous SNR and, $f_{\gamma}(\gamma)$ is the probability density function (PDF) denoted as $f_{\gamma}(\gamma) = \frac{1}{(N_r-1)!\bar{\gamma}^{N_r}} \gamma^{N_r-1} exp\left(-\frac{\gamma}{\bar{\gamma}}\right)$ with $\bar{\gamma} = E\{\gamma_t\}$, t, $t \in [1:T]$ as the average SNR at time t.

The conditional SEP in Eq (4.19) is defined as:

$$P_{M-DPSK}(e|\gamma) = \frac{1}{\pi} \int_0^{\eta\pi} exp\left(-\frac{\kappa\gamma}{1+cos\frac{\pi}{M}\, cos\,\theta}\right) d\theta, \tag{4.20}$$

where $\eta = \left(\frac{M-1}{M}\right)$, $\kappa = \sin^2\left(\frac{\pi}{M}\right)$ and *M* is the modulation order.

The conditional SEP is simplified by applying a trapezoidal approximation using the uniform distribution $\int_a^b f(x)dx = \frac{b-a}{n}\left[\frac{f(a)+f(b)}{2} + \sum_{k=1}^{n-1} f(a + k\,\frac{b-a}{n})\right]$ where n is the total number of iterations such that $n > 10$ [9].

Therefore the conditional SEP is computed as:

$$P_{M-DPSK}(e|\gamma) = \left(\frac{1}{\pi} \times \frac{\eta\pi - 0}{n} \left[\frac{exp\left(- \frac{\kappa\gamma}{1+cos\frac{\pi}{M} \times cos\, \eta\pi} \right) - exp\left(- \frac{\kappa\gamma}{1+cos\frac{\pi}{M} \times cos\, 0} \right)}{2} + \right. \right.$$

$$\left. \left. \sum_{k=1}^{n-1} exp\left(- \frac{\kappa\gamma}{\left(1+\cos\frac{\pi}{M}\, cos\left(0+\frac{k\eta\pi}{n}\right)\right)} \right) \right] \right),$$

$$P_{M-DPSK}(e|\gamma) = \frac{\eta}{n}\left[\frac{\exp\left(-\frac{\kappa\gamma}{p}\right) - \exp\left(-\frac{\kappa\gamma}{L}\right)}{2} + \sum_{k=1}^{n-1} exp\left(-\frac{\kappa\gamma}{R}\right) \right], \tag{4.21}$$

where $p = 1 + \cos\left(\frac{\pi}{M}\right) cos\,(\eta\pi)$, $L = 1 + \cos\frac{\pi}{M}$, $R = \left(1 + \cos\frac{\pi}{M}\, cos\left(\frac{k\eta\pi}{n}\right)\right)$.

Refer to Appendix D for an effective computation of Eq (4.21). Substituting Eq (4.21) into Eq (4.19) gives the unconditional error probability for *M*-DPSK as:

$$P_{M-DPSK}(e) = \int_0^\infty \frac{\eta}{n}\left[\frac{\exp\left(-\frac{\kappa\gamma}{p}\right) - \exp\left(-\frac{\kappa\gamma}{L}\right)}{2} + \sum_{k=1}^{n-1} exp\left(-\frac{\kappa\gamma}{R}\right) \right] f_\gamma(\gamma) d\gamma, \tag{4.22}$$

To simplify Eq (4.22), the moment generating function (MGF) of random variables $M(s) = \int_0^\infty \exp(-s\gamma)\, f_\gamma(\gamma) d\gamma = (1 + s\bar{\gamma})^{-N_r}$ defined in [13], is applied giving the new unconditional error probability for *M*-DPSK as:

$$P_{M-DPSK}(e) = \frac{\eta}{n}\left[\frac{1}{2}\left(\left(\frac{p}{p+k\bar{\gamma}} \right)^{N_r} - \left(\frac{L}{L+k\bar{\gamma}} \right)^{N_r} \right) + \sum_{k=1}^{n-1} \left(\frac{R}{R+k\bar{\gamma}} \right)^{N_r} \right], \tag{4.23}$$

Refer to Appendix D for an effective computation of Eq (4.23).

4.3.2 Generalized differential modulation error performance analysis

The error performance of the generalized differential modulation is performed with differential *M*-QAM [19] as the average SEP for *M*-QAM is given as:

$$P_{M-QAM}(e) = \int_0^\infty P_{M-QAM}(e|\gamma)\, f_\gamma(\gamma), \tag{4.24}$$

where $P_{M-QAM}(e|\gamma)$ is the conditional SEP over instantaneous SNR, γ is the SNR for multiple receive antennas given by $\gamma = \sum_{i=1}^{N_r} \gamma_i$ for $i \in [1{:}\,2]$, where γ_i is an instantaneous SNR given by $\gamma_i = \frac{E_s}{N_o}$ and $f_\gamma(\gamma)$ is the PDF for N_r receive antennas.

The conditional SEP is defined as:

$$P_{M-QAM}(e|\gamma) = 4\left(1 - \frac{1}{\sqrt{M}}\right) Q\left(\sqrt{\frac{3\gamma}{(M-1)}}\right) - 4\left(1 - \frac{1}{\sqrt{M}}\right)^2 Q^2\left(\sqrt{\frac{3\gamma}{(M-1)}}\right), \tag{4.25}$$

where M is the modulation order and Q is the Gaussian Q-function.

The relationship between the error probability and the Q-function is defined in Appendix A.

Letting $\left(1-\frac{1}{\sqrt{M}}\right)=a$ and $\left(\frac{3}{M-1}\right)=b$, Eq (4.25) can be written as:

$$P_{M-QAM}(e|\gamma)=4aQ\left(\sqrt{b\gamma}\right)-4a^2Q^2(b\gamma). \tag{4.26}$$

The expressions for the Q-functions $Q\left(\sqrt{b\gamma}\right)$ and $Q^2\left(\sqrt{b\gamma}\right)$ are defined in Appendix E. To simplify the conditional SEP the trapezoidal approximation is applied on $Q\left(\sqrt{b\gamma}\right)$ and $Q^2\left(\sqrt{b\gamma}\right)$ using the uniform distribution $\int_a^b f(x)dx=\frac{b-a}{n}\left[\frac{f(a)+f(b)}{2}+\sum_{k=1}^{n-1}f(a+k\,\frac{b-a}{n})\right]$ where n is the total number of iterations such that $n>10$ [9], refer to Appendix E for the derivation of the Q-functions. The new expression for the conditional SEP is denoted as:

$$P_{M-QAM}(e|\gamma)=4a\times\left[{}^{1}\!/_{2n}\left(\left(\frac{1}{2}exp^{\,{}^{-b\gamma}\!/_{2}}\right)+\sum_{i=1}^{n-1}exp^{\,{}^{-b\gamma}\!/_{S_i}}\right)\right]-4a^2\times \left[{}^{1}\!/_{4n}\left(\frac{1}{2}exp^{-b\gamma}+\sum_{i=n}^{2n-1}exp^{\,{}^{-b\gamma}\!/_{S_{iB}}}\right)\right],$$

$$=\frac{a}{n}\left[\frac{1}{2}exp\left(-\frac{b\gamma}{2}\right)-\frac{a}{2}exp(-b\gamma)+(1-a)\left(\sum_{i=1}^{n-1}e^{\,{}^{-b\gamma}\!/_{S_i}}+\sum_{i=n}^{2n-1}exp\left(-\frac{b\gamma}{s_i}\right)\right)\right], \tag{4.27}$$

where $S_i=2\,sin^2\,\theta_k$, $\theta_k=\frac{i\pi}{4n}$, $S_{iB}=2\,sin^2\,\beta_k$, and $\beta_k=\frac{i\pi}{4n}$.

Refer to Appendix E for an effective computation of Eq (4.27). Substituting Eq (4.27) onto Eq (4.24) give the new average SEP as:

$$P_{M-QAM}(e)\;=\int_0^\infty\frac{a}{n}\left\{\frac{1}{2}e^{-\frac{b\gamma}{2}}-\frac{1}{2}ae^{-b\gamma}+(1-a)\left(\sum_{i=1}^{n-1}e^{\frac{-b\gamma}{S_i}}+\sum_{i=n}^{2n-1}e^{\frac{-b\gamma}{S_{iB}}}\right)\right\}f_\gamma(\gamma)d\gamma \tag{4.28}$$

Applying the MGF of random variables $M(s)=\int_0^\infty\exp(-s\gamma)\,f_\gamma(\gamma)d\gamma=(1+s\bar{\gamma})^{-N_r}$ onto Eq (4.28) gives the new unconditional error probability for differential M-QAM as:

$$P_{M-QAM}(e)\;=\int_0^\infty\frac{a}{n}\left\{\frac{1}{2}e^{-\frac{b\gamma}{2}}-\frac{1}{2}ae^{-b\gamma}+(1-a)\left(\sum_{i=1}^{n-1}e^{\frac{-b\gamma}{S_i}}+\sum_{i=n}^{2n-1}e^{\frac{-b\gamma}{S_{iB}}}\right)\right\}f_\gamma(\gamma)d\gamma,$$

$$=\frac{a}{n}\left\{\frac{1}{2}\times\left(\frac{2}{2+b\bar{\gamma}}\right)^{N_r}-\frac{a}{2}\left(\frac{1}{1+b\,\bar{\gamma}}\right)^{N_r}+(1-a)\left(\sum_{i=1}^{n-1}\left(\frac{S_i}{S_i+b\bar{\gamma}}\right)^{N_r}+\sum_{i=n}^{2n-1}\left(\frac{S_{iB}}{S_{iB}+b\bar{\gamma}}\right)^{N_r}\right)\right\}, \tag{4.29}$$

where $\bar{\gamma}=E\{\gamma_t\}$, t, $t\in[1{:}T]$ is the average SNR at time t for $\bar{\gamma}_1=\frac{E_{RS}}{N_0}$ and $\bar{\gamma}_2=\frac{E_{NS}}{N_0}$, for the fading channels that are identical we let $\bar{\gamma}=\bar{\gamma}_t$.

Refer to Appendix E for an effective computation of Eq (4.29).

4.4 Numerical and analytical results

In this section, Monte Carlo simulation results for CDM using M-PSK and GDM using M-QAM constellations are compared. Additionally, employing M-QAM and M-PSK constellations, we illustrate how GDM outperforms CDM in terms of error performance with systems of same spectral efficiency. Results were simulated for frame lengths of $N = 100$ and $N = 400$, we assume that $N_r = 2$ since N_r has no effect on the power allocation of the system. The SEP analysis for the systems in Section 4.2 is performed with M-DPSK for CDM and differential M-QAM for GDM as discussed in Section 4.3, is plotted against the average SNR (dB) for the systems.

4.4.1 CDM numerical and analytical results

Numerical and analytical results of non-coherent CDM system over quasi-static fading channel compared with that of coherent detection system over Rayleigh fading channel for 16-PSK and 64-PSK constellation with $N = 100$ and $N = 400$ are as follows:

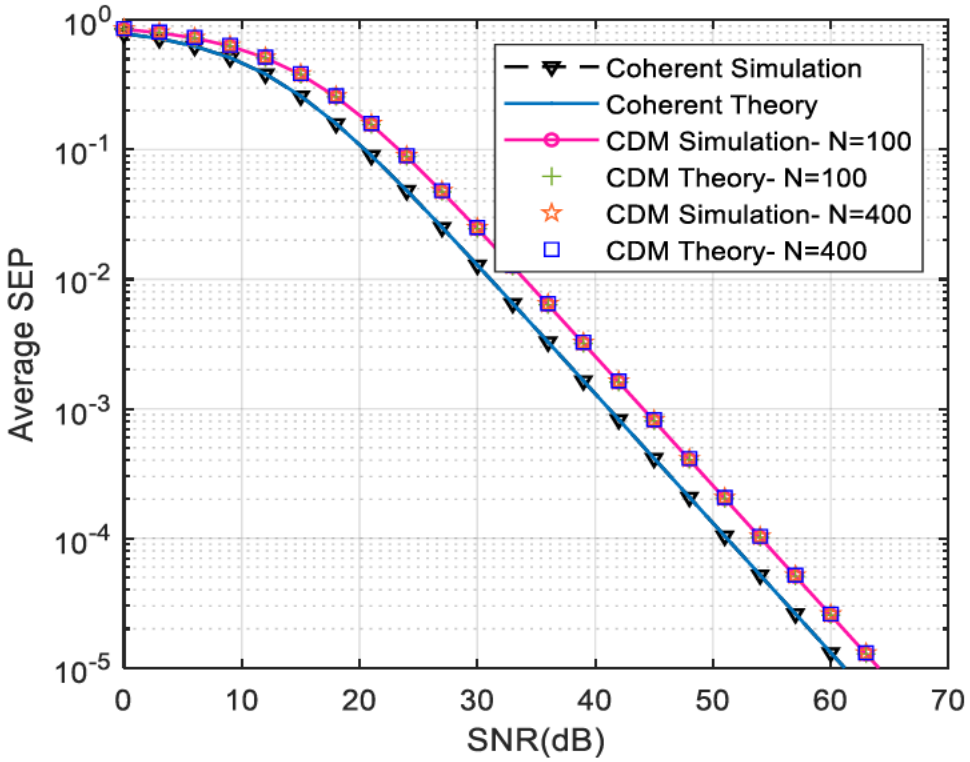

Figure 4.3: Non-coherent CDM and SEP performance analytical results for 16-PSK compared with that of coherent 16-PSK.

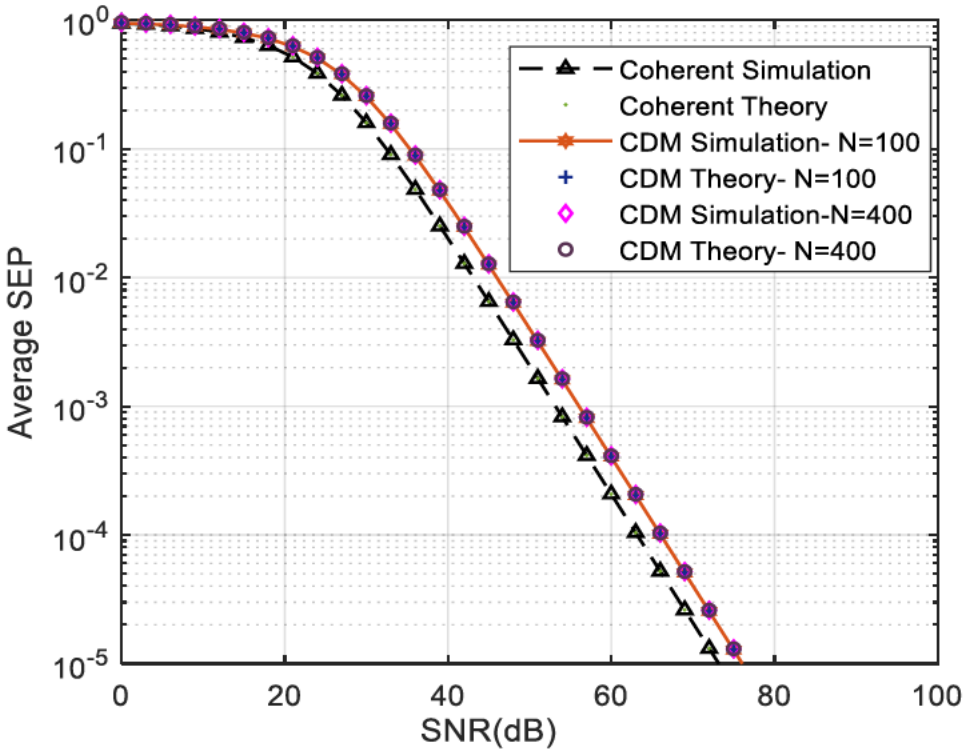

Figure 4.4: Non-coherent CDM and SEP performance analytical results for 64-PSK compared with that of coherent 64-PSK.

It is observed from Figure 4.3 and Figure 4.4, that for both 16-PSK and 64-PSK, the SEP performance of non-coherent CDM is about 3dB higher than that of the coherent detection, which results to a performance loss compared to the coherent detection. The SEP performance of non-coherent CDM barely lowers as N increase. Therefore, it is evident that coherent detection gains about 3dB SEP performance to non-coherent CDM detection.

4.4.2 GDM numerical and analytical results

Numerical and analytical results of non-coherent GDM system over quasi-static fading channel compared with that of coherent detection system over Rayleigh fading channel for the 16-QAM and 64-QAM with $N = 100$ and $N = 400$ transmitted signals.

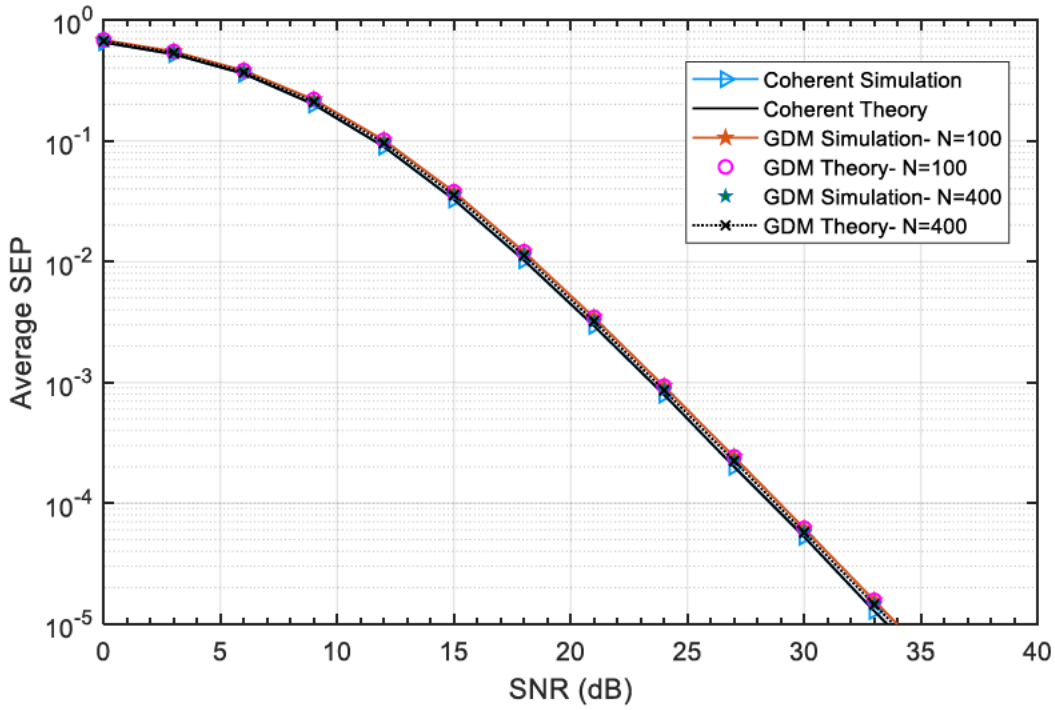

Figure 4.5: Non-coherent GDM and SEP performance analytical results compared with that of coherent system for 16-QAM.

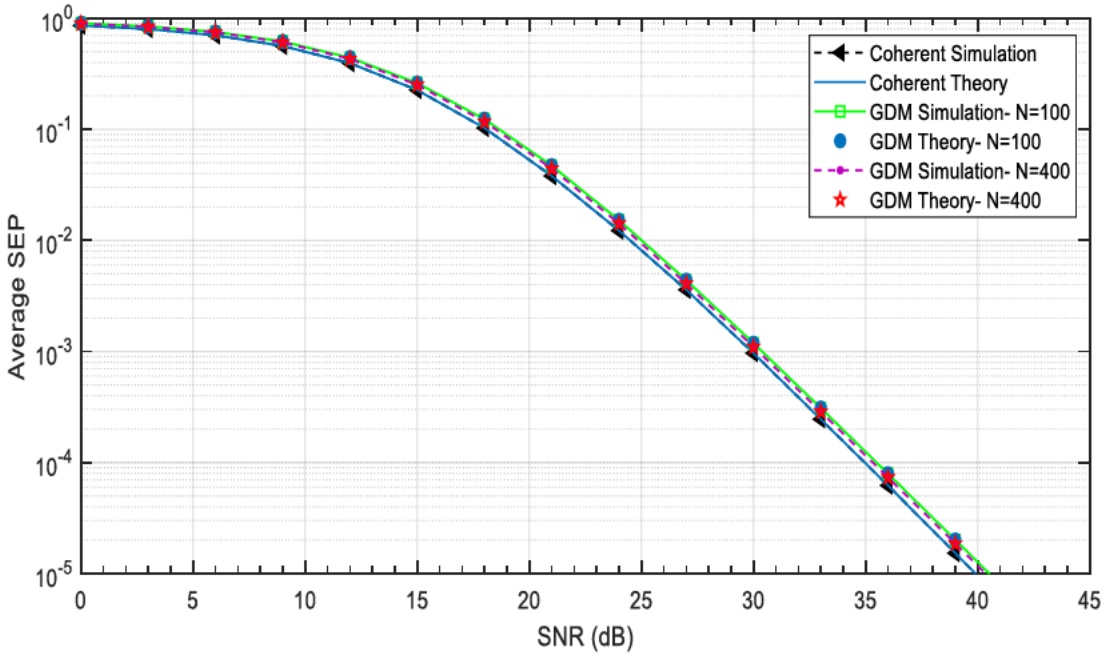

Figure 4.6: Non-coherent GDM and SEP performance analytical results compared with that of coherent system for 64-QAM.

Figure 4.5 and Figure 4.6 shows non-coherent GDM and SEP performance analytical results compared with that of coherent system for 16-QAM and 64-QAM. It is observed that the gap between the SEP performance of non-coherent GDM and its coherent counterpart is about 1dB, better that of non-coherent

CDM. Furthermore, it is observed that when N increases, the SEP performance of GDM is slightly approaching that of the coherent detection. This means as the number of symbols increase the SEP performs of non-coherent GDM improves.

4.5 Chapter summary

In this chapter, two differential detections over quasi-static fading channel were presented to improve the complexity of the coherent system. Non-coherent CDM detection losses about 3dB to coherent detection. Non-coherent GDM which uses power allocation between RS and NSs to bridge the error performance gap between non-coherent CDM and coherent detection was presented. Numeric results show that the gap between the non-coherent CDM and the coherent system is reduced by non-coherent GDM scheme with about 2dB performance gap gain.

CHAPTER 5

GENERALIZED DIFFERENTIAL MODULATION WITH SIGNAL SPACE DIVERSITY FOR *M*-QAM

This chapter presents a new proposed scheme generalized differential modulation with signal space diversity (GDM-SSD) for *M*-ary quadrature amplitude modulation (*M*-QAM).

5.1 Introduction

Signal space diversity (SSD) also known as modulation diversity as presented in [9], was proposed to emphases on equalization techniques for frequency selective channels. The basic premise of SSD is that multidimensional signal constellations are used and the components (also known as in-phase (I) and quadrature phase (Q)) of each signal constellation point are transmitted over independent fading channels [2, 10, 9]. SSD obtain the diversity order across fading channels using two concepts: constellation rotation and components interleaving [9, 10]. Signal constellation rotation is applied in such a way that any two points obtain the maximum number of distinct components to increase diversity [9]. Although, signal constellation rotation is important, the independence of the fading channels can be accomplished by component interleaving to obtain diversity gain [9]. Moreover, SSD is capable to achieve diversity without an additional bandwidth and transmission power.

In [9], a signal space diversity scheme is presented where it is combined with receive maximal ratio combining (MRC) reception to achieve more diversity gain in fading channels. A theoretical analysis for the symbol error probability (SEP) for SSD systems paired with MRC over Rayleigh fading channels was derived for 4-QAM and 16-QAM. Additionally, the numerical results indicated that the angle of rotation affects the error performance, resulting in low complexity of the scheme. SSD was investigated in [9], in a Single-Input-Multi-Output (SIMO) coherent system with *M*-ary quadrature amplitude modulation symbol to improve the error performance of the system however, at the cost of increased detection complexity. The increase in detection complexity of the coherent systems is due to the requirement of the knowledge of the channel state information (CSI) at the receiver. Thus, the receiver in coherent wireless communication system has complete knowledge of the fading coefficients, and the parameter of the fading channel is a random number known to both the receiver and the transmitter. Due to the detection complexity of coherent systems, a non-coherent system has been used in wireless communication to reduce the detection complexity of coherent systems [24]. In contrast to coherent systems, non-coherent systems do not require CSI at the receiver [26]. Thus, in non-coherent wireless communications systems, neither the receiver nor the transmitter is aware of the knowledge of the channel coefficients. Coefficient statistics should be used to perform encoding and decoding in a non-coherent system [26].

Generalized differential modulation (GDM) was introduced in [18], as a non-coherent detection which uses power allocation to reduce the error performance loss incurred by non-coherent conventional differential modulation (CDM) detection to its coherent counterpart. The non-coherent GDM system enhances the error performance and reliability of the wireless communication system. This modulation highlights the potential of the power allocation strategy to provide a more stable communication system without requiring channel state information at the receiver. The concept of power allocation is to maximise the average output signal-to-noise ratio (SNR) of the respective non-coherent system [18]. The transmission power is allocated between the reference block (RB) and normal blocks (NBs) where, more power is allocated to the RB. It was discovered that allocating more power to the RB results to an improved error performance when the frame length is increased [11]. However, the channel must remain unchanged for the duration of the frame. Thus, quasi-static fading channel (QSFC).

In [19, 27], GDM was presented for spatial modulation (SM) schemes that implements the concept of power allocation amongst the RB and NBs. Similarly to [18, 11], the transmission power is allocation between the reference block and normal blocks where more power is allocated to the reference block. However, in [19] only normal blocks convey information. The RB remains constant throughout the transmission, while NBs are differentially encoded based on the RB. This means the RB remains constant across all frames, provided the channel remains constant for each transmission frame. It was shown that generalized differential spatial modulation (GD-SM) incurred about 0.5 dB performance loss as compared to coherent SM when the frame length is 400 [19].

Motivated by the work in [9] of SSD in a coherent system and, the work presented in [19, 27], of GDM based on the concept of power allocation, a generalized differential modulation with signal space diversity for *M*-ary quadrature amplitude modulation is proposed in this chapter. The purpose of the proposed system is to investigate diversity gain based on SSD in a non-coherent system to improve the error performance of wireless communication systems. The concept of applying signal space diversity in generalized differential modulation scheme is encouraged by its ability to obtain diversity in wireless systems without the addition of bandwidth and transmission power as in [4], since GDM uses power allocation to improve the error performance of a non-coherent detection.

5.2 System model

Consider a non-coherent GDM-SSD $N_t \times N_r$ Single-Input-Multi-Output system where $N_t = 1$ is the number of transmit antennas and $N_r \geq N_t$ is the number of receive antennas as illustrated in Figure 5.1 below, assuming that the receive antennas are spaced far enough apart from each other so that there is no correlation among the respective received signals.

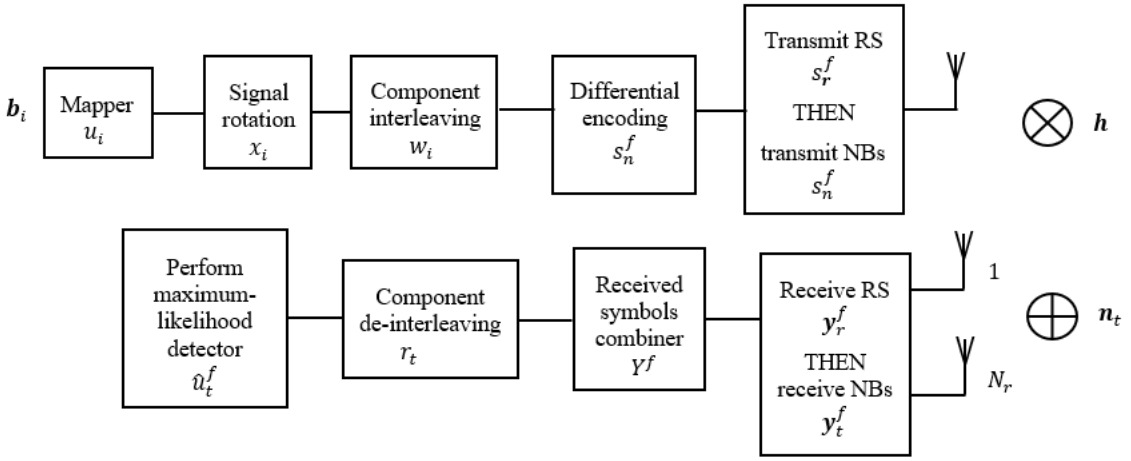

Figure 5.1: Block diagram of generalized differential modulation with signal space diversity system model.

Information bits $\boldsymbol{b}_i = \left[b_{i,1}\ b_{i,2}\ b_{i,3}\ \cdots b_{i,k}\right]$ are grouped in sequences of $k = log_2 M$ bits in size where M is the modulation order and i, $i \in [1:2]$ is the symbol index.

The grouped information bits are then directly mapped onto conventional M-QAM signal set $\boldsymbol{\Omega}$, and yields symbol $u_i = u_i^I + ju_i^Q$, assuming $E[|u_i|^2] = 1$. $(\cdot)^I$ and $(\cdot)^Q$ refer to the in-phase (real) and quadrature (imaginary) components of a signal, respectively. The symbols (u_i) are rotated at a certain angle to maximize the minimum number of distinct components between any two points in the constellation while retaining the same average energy.

The rotation of the symbols is obtained by applying a rotation matrix $\boldsymbol{R}^\theta$ for a rotation angle θ to each element of the symbols u_i to form a pair of rotated symbols expressed as in Eq (5.1) [9]:

$$\left[x_i^I \quad x_i^Q\right] = [u_i^I \ \ u_i^Q\ ] \times \boldsymbol{R}^\theta, \tag{5.1}$$

where $\mathbf{R}^\theta = \begin{bmatrix} cos\,\theta & sin\,\theta \\ -\,sin\,\theta & cos\,\theta \end{bmatrix}$ is the rotation matrix with rotational angle $\theta = 31.7°$. The angle $31.7°$ is used as an angle of rotation in order to achieve SSD in two dimensions.

The rotation of symbols is effectively computed as follows:

$$\begin{aligned} \left[x_i^I \quad x_i^Q\right] &= [u_i^I \ \ u_i^Q\ ] \begin{bmatrix} cos\,\theta & sin\,\theta \\ -\,sin\,\theta & cos\,\theta \end{bmatrix}, \\ &= \left[u_i^I\, cos\,\theta - u_i^Q sin\theta \quad u_i^I\, sin\,\theta + u_i^Q\, cos\,\theta\right], \end{aligned} \tag{5.2}$$

where $x_i^I = u_i^I\, cos\,\theta - u_i^Q\, sin\,\theta$ and $x_i^Q = u_i^I\, sin\,\theta + u_i^Q\, cos\,\theta$.

The rotated symbol pair x_i are applied to a component interleaver giving a typical pair of interleaved symbols w_i, $i \in [1:2]$ denoted as:

$$w_1 = x_1^I + jx_2^Q, \tag{5.3a}$$

$$w_2 = x_2^I + jx_1^Q. \tag{5.3b}$$

Differential encoding is performed on the interleaved symbols prior to transmission in different frames using differential matrix giving a symbol pair of differentially encoded symbol defined as $s_n^f = s_r^f\, w_n$:

$$s_1^1 = s_0^1\, w_1, \tag{5.4a}$$

$$s_1^2 = s_0^2\, w_2, \tag{5.4b}$$

where s_n^f denotes the differentially encoded symbol in a block to be transmitted, the subscript n denotes the symbol index in a block, superscript $f \in [1:2]$ is the frame index, s_r^f is the reference symbol and w_n is the interleaved symbol now to be referred as the information symbol.

A. Reference symbol

The reference symbol (RS) s_r^f, is the first transmitted symbol across all frames through the source and it is defined as:

$$s_r^f = 1, \tag{5.5}$$

where the superscript f, $f \in [1:2]$ is the frame index.

s_r^f remains constant for each frame throughout the transmission and does not convey information. This allows for the information carrying symbols in normal symbols to be drawn from *M*-QAM constellation. The encoded reference symbol is then transmitted individually in different time slots on separate frames respectively, giving the received reference symbol vector $\boldsymbol{y}_r^f$:

$$\boldsymbol{y}_r^f = \sqrt{E_{RS}}\, \boldsymbol{h}^f s_r^f + \boldsymbol{n}_r^f, \tag{5.6}$$

where $\boldsymbol{y}_r^f \in \mathbb{C}^{N_r \times 1}$ is the received reference symbol vector, the superscript f, $f \in [1:2]$ is the frame index, E_{RS} is the RS transmitted power, $\boldsymbol{h}^f$ is the quasi-static fading coefficient vector for each transmission frame f whose entries are independent and identically distributed (i.i.d.) complex Gaussian random variables (RVs) with distribution $CN(0,1)$ and, $\boldsymbol{n}_r^f$ is the additive white Gaussian

noise (AWGN) vector with entries n_{rk}^{f} modelled as i.i.d. complex Gaussian RVs with distribution $n_{rk}^{f} \sim CN(0,1)$. The subscript $k, k \in [1:N_r]$ is the receive antenna index.

B. Normal symbols

Normal symbols (NSs) are the remaining encoded symbols in the transmission frame. Normal symbols are encoded based on the reference symbol and are defined using differential matrix in Eq (5.4) as:

$$s_n^f = s_r^f \, w_n, \tag{5.7}$$

where the subscript n is the symbol index in a block, s_n^f is the differentially encoded symbol in a frame, s_r^f is the reference symbol in a frame and w_n is the information symbol.

Similar to the reference symbol, the transmitted symbol experience QSFC and AWGN as they arrive at the destination in different time slots on separate frames respectively, giving the received normal symbol $\boldsymbol{y}_t^f$ vector:

$$\boldsymbol{y}_t^f = \sqrt{E_{NS}}\, \boldsymbol{h}^f s_t^f + \boldsymbol{n}_t^f, \tag{5.8}$$

where $\boldsymbol{y}_t^f \in \mathbb{C}^{N_r \times 1}$ $t \in [1:T]$ is the received normal symbol vector at time t, E_{NS} is the NSs transmitted power, $\boldsymbol{h}^f$ is an independent quasi-static fading coefficient vector for each transmission frame whose entries are i.i.d. complex Gaussian RVs with distribution $CN(0,1)$ and, $\boldsymbol{n}_t^f$ is the AWGN vector with entries n_{tk}^f modelled as i.i.d. complex Gaussian RVs with distribution $n_{tk}^f \sim CN(0,1)$. The superscript $f, f \in [1:2]$ is the frame index and the subscript $k, k \in [1:N_r]$ is the receive antenna index.

The received symbols order is presented in the table below:

Table 5.1: GDM-SSD received symbols,

Frame 1	Frame 2
$\boldsymbol{y}_0^1 = \sqrt{E_{RS}}\, \boldsymbol{h}^1 s_0^1 + \boldsymbol{n}_0^1$	$\boldsymbol{y}_0^2 = \sqrt{E_{RS}}\, \boldsymbol{h}^2 s_0^2 + \boldsymbol{n}_0^2$
$\boldsymbol{y}_1^1 = \sqrt{E_{NS}}\, \boldsymbol{h}^1 s_1^1 + \boldsymbol{n}_1^1$	$\boldsymbol{y}_1^2 = \sqrt{E_{NS}}\, \boldsymbol{h}^2 s_1^2 + \boldsymbol{n}_1^2$
$\boldsymbol{y}_2^1 = \sqrt{E_{NS}}\, \boldsymbol{h}^1 s_2^1 + \boldsymbol{n}_2^1$	$\boldsymbol{y}_2^2 = \sqrt{E_{NS}}\, \boldsymbol{h}^2 s_2^2 + \boldsymbol{n}_2^2$
$\vdots$	$\vdots$
$\boldsymbol{y}_t^1 = \sqrt{E_{NS}}\, \boldsymbol{h}^1 s_t^1 + \boldsymbol{n}_t^1$	$\boldsymbol{y}_t^2 = \sqrt{E_{NS}}\, \boldsymbol{h}^2 s_t^2 + \boldsymbol{n}_t^2$

where $\boldsymbol{y}_0^f = \boldsymbol{y}_r^f$ and $s_0^f = 1$ for $f \in [1:2]$.

More transmission power is allocated to the RS as compared to NSs to improve the error performance of the system since the reference symbol provides the combine channel estimation for normal symbols. The transmission power of the RS is represented as E_{RS} and it is denoted as $(1 + N\rho)E_s$ and, the transmission power of NSs is represented as E_{NS} and it is denoted as $(1 - \rho)E_s$. E_s is the average transmission power of the system. Refer to Section 4.2.3 for power allocation.

C. Detection

Substituting Eq (5.4a) and Eq (5.4b) into the received symbol pair vector, the received symbol pair vector may be rewritten as in Eq (5.9a) and Eq (5.9b):

$$\begin{aligned} \boldsymbol{y}_1^1 &= \sqrt{E_{NS}}\,\boldsymbol{h}^1 s_1^1 + \boldsymbol{n}_1^1, \\ &= \sqrt{E_{NS}}\,\boldsymbol{h}^1 (s_0^1 w_1) + \boldsymbol{n}_1^1, \\ \boldsymbol{y}_1^1 &= \sqrt{E_{NS}}\,\boldsymbol{h}^1 w_1 + \boldsymbol{n}_1^1, \end{aligned} \tag{5.9a}$$

$$\begin{aligned} \boldsymbol{y}_1^2 &= \sqrt{E_{NS}}\,\boldsymbol{h}^2 s_1^2 + \boldsymbol{n}_1^2, \\ &= \sqrt{E_{NS}}\,\boldsymbol{h}^2 (s_0^2 w_2) + \boldsymbol{n}_1^2, \\ \boldsymbol{y}_1^2 &= \sqrt{E_{NS}}\,\boldsymbol{h}^2 w_2 + \boldsymbol{n}_1^2. \end{aligned} \tag{5.9b}$$

Due to quasi-static fading channel, $\boldsymbol{y}_0^f$ and $\boldsymbol{y}_t^f$ are known at the receiver. Similar to Eq (4.9), $\boldsymbol{y}_0^f$ is defined as:

$$\boldsymbol{y}_0^f = \sqrt{E_{RS}}\,\boldsymbol{h}^f s_0^f + \boldsymbol{n}_0^f.$$

Therefore,

$$\begin{aligned} \sqrt{E_{RS}}\,\boldsymbol{h}^f &= \boldsymbol{y}_0^f - \boldsymbol{n}_0^f, \\ \boldsymbol{h}^f &= \frac{\boldsymbol{y}_0^f - \boldsymbol{n}_0^f}{\sqrt{E_{RS}}}. \end{aligned} \tag{5.10}$$

Substituting Eq (5.10) into Eq (5.9a) and Eq (5.9b) gives:

$$\begin{aligned} \boldsymbol{y}_1^1 &= \sqrt{E_{NS}}\left(\frac{\boldsymbol{y}_0^1 - \boldsymbol{n}_0^1}{\sqrt{E_{RS}}}\right) w_1 + \boldsymbol{n}_1^1, \\ &= \sqrt{\frac{E_{NS}}{E_{RS}}}\,[\boldsymbol{y}_0^1 w_1 - \boldsymbol{n}_0^1 w_1] + \boldsymbol{n}_1^1, \end{aligned} \tag{5.11a}$$

$$\begin{aligned} \boldsymbol{y}_1^2 &= \sqrt{E_{NS}}\left(\frac{\boldsymbol{y}_0^2 - \boldsymbol{n}_0^2}{\sqrt{E_{RS}}}\right) w_2 + \boldsymbol{n}_1^2, \\ &= \sqrt{\frac{E_{NS}}{E_{RS}}}\,[\boldsymbol{y}_0^2 w_2 - \boldsymbol{n}_0^2 w_2] + \boldsymbol{n}_1^2, \end{aligned} \tag{5.11b}$$

where $\boldsymbol{y}_1^1$ and $\boldsymbol{y}_1^2$ are the received normal symbol vectors for each transmission frame and, $\boldsymbol{y}_0^1$ and $\boldsymbol{y}_0^2$ are the received reference symbol vectors for each transmission frame, respectively. $\frac{E_{NS}}{E_{RS}}$ is the average transmitted power.

The received symbols are combined as they are received at the receiver using maximum ratio combining (MRC) reception on a symbol-by-symbol basis. The combined received symbols are defined as $Y^f = \left(\boldsymbol{y}_0^f\right)^H \boldsymbol{y}_t^f$ where the superscript f, $f \in [1:2]$ is the frame index, the subscript t, $t \in [1:2]$ is the time slot index and superscript H is the Hermitian transpose. The combined received symbol pair is denoted as in Eq (5.12a) and Eq (5.12b):

$$
\begin{aligned}
Y^1 &= (\boldsymbol{y}_0^1)^H \boldsymbol{y}_1^1, \\
&= (\boldsymbol{y}_0^1)^H \left[\sqrt{\frac{E_{NS}}{E_{RS}}}(\boldsymbol{y}_0^1 w_1 - \boldsymbol{n}_0^1 w_1) + \boldsymbol{n}_1^1\right], \\
&= \sqrt{\frac{E_{NS}}{E_{RS}}}\left[\left\|\boldsymbol{y}_0^1\right\|^2 w_1 - (\boldsymbol{y}_0^1)^H \boldsymbol{n}_0^1 w_1\right] + (\boldsymbol{y}_0^1)^H \boldsymbol{n}_1^1, \\
Y^1 &= \sqrt{\frac{E_{NS}}{E_{RS}}}\left[\left\|\boldsymbol{y}_0^1\right\|^2 \left(x_1^I + j x_2^Q\right) - \tilde{n}_0^1\right] + \tilde{n}_1^1, \qquad (5.12a)
\end{aligned}
$$

$$
\begin{aligned}
Y^2 &= (\boldsymbol{y}_0^2)^H \boldsymbol{y}_1^2, \\
&= (\boldsymbol{y}_0^2)^H \left[\sqrt{\frac{E_{NS}}{E_{RS}}}(\boldsymbol{y}_0^2 w_2 - \boldsymbol{n}_0^2 w_2) + \boldsymbol{n}_1^2\right], \\
&= \sqrt{\frac{E_{NS}}{E_{RS}}}\left[\left\|\boldsymbol{y}_0^2\right\|^2 w_2 - (\boldsymbol{y}_0^2)^H \boldsymbol{n}_0^2 w_2\right] + (\boldsymbol{y}_0^2)^H \boldsymbol{n}_1^2, \\
Y^2 &= \sqrt{\frac{E_{NS}}{E_{RS}}}\left[\left\|\boldsymbol{y}_0^2\right\|^2 \left(x_2^I + j x_1^Q\right) - \tilde{n}_0^2\right] + \tilde{n}_1^2, \qquad (5.12b)
\end{aligned}
$$

where $\left\|\boldsymbol{y}_0^f\right\|^2$ is the received reference signal power, $f \in [1:2]$ and $\tilde{n}_0^f = \sqrt{\frac{E_{NS}}{E_{RS}}}\left(\boldsymbol{y}_0^f\right)^H \boldsymbol{n}_0^f w_t$ and $\tilde{n}_t^f = \left(\boldsymbol{y}_0^f\right)^H \boldsymbol{n}_t^f$ are a noise term.

De-interleaving is then performed on the combined received symbol pair in Eq (5.12a) and Eq (5.12b) to ensure that the in-phase and quadrature components of the original symbols are reassembled before detection is performed. De-interleaving is performed by swapping the in-phase and quadrature components of the combined received symbols where a typical pair of de-interleaved symbols is given as $r_t,\ t \in [1:2]$:

$$
r_1 = Re\left\{\sqrt{\frac{E_{NS}}{E_{RS}}}\left[\left\|\boldsymbol{y}_0^1\right\|^2 \left(x_1^I + j x_2^Q\right) - \tilde{n}_0^1\right] + \tilde{n}_1^1\right\} + jIm\left\{\sqrt{\frac{E_{NS}}{E_{RS}}}\left[\left\|\boldsymbol{y}_0^2\right\|^2 \left(x_2^I + j x_1^Q\right) - \tilde{n}_0^2\right] + \tilde{n}_1^2\right\},
$$

$$= \sqrt{\frac{E_{NS}}{E_{RS}}} \left\| \boldsymbol{y}_0^1 \right\|^2 x_1^I + j\sqrt{\frac{E_{NS}}{E_{RS}}} \left\| \boldsymbol{y}_0^2 \right\|^2 x_1^Q - \tilde{\tilde{n}}_0^1 + \tilde{\tilde{n}}_1^1, \tag{5.13a}$$

$$r_2 = Re\left\{\sqrt{\frac{E_{NS}}{E_{RS}}}\left[\left\| \boldsymbol{y}_0^2 \right\|^2 \left(x_2^I + jx_1^Q\right) - \tilde{n}_0^2\right] + \tilde{n}_1^2\right\} + jIm\left\{\sqrt{\frac{E_{NS}}{E_{RS}}}\left[\left\| \boldsymbol{y}_0^1 \right\|^2 \left(x_1^I + jx_2^Q\right) - \tilde{n}_0^1\right] + \tilde{n}_1^1\right\},$$

$$= \sqrt{\frac{E_{NS}}{E_{RS}}} \left\| \boldsymbol{y}_0^2 \right\|^2 x_2^I + j\sqrt{\frac{E_{NS}}{E_{RS}}} \left\| \boldsymbol{y}_0^1 \right\|^2 x_2^Q - \tilde{\tilde{n}}_0^2 + \tilde{\tilde{n}}_1^2, \tag{5.13b}$$

where the resultant noise term $\tilde{\tilde{n}}_0^f$ and $\tilde{\tilde{n}}_t^f$ is a random variable which can be approximated as Gaussian distribution $\tilde{\tilde{n}}_t^f \sim CN(0,1)$ and $j = \sqrt{-1}$.

The receiver then performs maximum-likelihood detection (MLD) for a non-coherent GDM-SSD system denoted as:

$$\hat{u}_1^1 = \underset{u_1^1 \in \boldsymbol{\Omega}}{argmin}\left\{P_2 \left| r_1^I - \sqrt{\frac{E_{NS}}{E_{RS}}} \left\| \boldsymbol{y}_0^1 \right\|^2 \left(u_1^I \cos\theta - u_1^Q \sin\theta\right)\right|^2 + P_1 \left| r_1^Q - \mathrm{j}\sqrt{\frac{E_{NS}}{E_{RS}}} \left\| \boldsymbol{y}_0^2 \right\|^2 \left(u_1^I \sin\theta + u_1^Q \cos\theta\right)\right|^2\right\}, \tag{5.14a}$$

$$\hat{u}_1^2 = \underset{u_1^2 \in \boldsymbol{\Omega}}{argmin}\left\{P^1 \left| r_2^I - \sqrt{\frac{E_{NS}}{E_{RS}}} \left\| \boldsymbol{y}_0^2 \right\|^2 \left(u_2^I \cos\theta - u_2^Q \sin\theta\right)\right|^2 + P^2 \left| r_2^Q - \mathrm{j}\sqrt{\frac{E_{NS}}{E_{RS}}} \left\| \boldsymbol{y}_0^1 \right\|^2 \left(u_2^I \sin\theta + u_2^Q \cos\theta\right)\right|^2\right\}, \tag{5.14b}$$

where $\hat{u}_1^1$ and $\hat{u}_1^2$ are the detected symbols, $\boldsymbol{\Omega}$ is the *M*-QAM signal set, $u_1^I \cos\theta - u_1^Q \sin\theta = x_1^I$, $u_2^I \cos\theta - u_2^Q \sin\theta = x_2^I$ are the real and $u_1^I \sin\theta + u_1^Q \cos\theta = x_1^Q$, $u_2^I \sin\theta + u_2^Q \cos\theta = x_2^Q$ are the imaginary component of the rotated symbols u_1^1 and u_1^2, respectively. P^1 and $P^2$are the received reference signal power denoted as $P^f = \left\| \boldsymbol{y}_0^f \right\|^2$, $f \in [1{:}\,2]$.

$\boldsymbol{y}_0^1$ and $\boldsymbol{y}_0^2$ are used to estimate the channels of the system so to recover information in $\boldsymbol{y}_1^1$ and $\boldsymbol{y}_1^2$.

5.3 Error performance analysis

This section presents the symbol error probability (SEP) analysis of the proposed non-coherent GDM-SSD system. The SEP analysis is performed with differential *M*-QAM based on the error probability of the system in a closed form using minimum distance lower bound of the transmitted symbol u_i for each rotated constellation point and $\hat{u}_i$ as the chosen detected symbol.

In the high SNR region one symbol u_2 can be assumed to always be detected correct and u_1 can be considered to be a transmitted symbol and $\hat{u}_1$ as the detected symbol.

5.3.1 Minimum distance lower bound

Minimum distance lower bound (MDLB) as presented in [9], is the analysis method used to derive a lower bound on the SEP using the minimum Euclidean distance of the rotated constellation considering the independent fading on the in-phase (real) and quadrature (imaginary) components of the signal due to component interleaving/de-interleaving. Therefore, the MDLB on the SEP conditioned on independent fading is given as:

$$P_{M-QAM}^{MDLB}((e|\boldsymbol{h}) \geq 4aQ\left(\sqrt{\frac{d^2}{2N_0}}\right) - 4a^2Q^2\left(\sqrt{\frac{d^2}{2N_0}}\right), \tag{5.15}$$

where $\boldsymbol{h}$ is the quasi-static fading coefficient vector whose entries are independent and i.i.d. complex RVs with distribution $CN(0,1)$ and it is constant over a frame and independently changes from one frame to the next, $N_0 = 1$ is the power spectrum density and, d is the minimum distance between constellations given as in [9]:

$$d_{min} = \min_{x_1, x_2 \in \boldsymbol{\Omega}} \left\{\sqrt{|x_1 - x_2|^2}\right\}, \tag{5.16}$$

where $\boldsymbol{\Omega}$ is the M-QAM signal set, x_1 and x_2 are the rotated symbol corresponding to u_1 and u_2, respectively.

Following the approach from [9], the minimum distance in Eq (5.16) is modified to account for the independent fading on the in-phase and quadrature components of the signal as in Eq (5.17):

$$d_{min} = \min_{x_1, x_2 \in \boldsymbol{\Omega}} \left\{\sqrt{\boldsymbol{h}^2|x_1^I - x_2^I|^2 + \boldsymbol{h}^2\left|x_1^Q - x_2^Q\right|^2}\right\}, \tag{5.17}$$

where x_1^I,x_2^I are the real and x_1^Q,x_2^Q are the imaginary component of the rotated symbols corresponding to u_1 and u_2, respectively.

Taking into consideration the rotation angel θ of the rotated two dimensional constellations, the minimum distance in Eq (5.16) can be written as:

$$d_{min}^x = \sqrt{4\|\boldsymbol{h}\|^2\, Cos^2\theta + 4\,\|\boldsymbol{h}\|^2 Sin^2\theta}, \tag{5.18}$$

where $\left|x_1^I - x_2^I\right| = 4\, Cos^2\theta$ and $\left|x_1^Q - x_2^Q\right| = 4\, sin^2\,\theta$.

Due to independent fading and rotation angel, the conditional MDLB on the SEP in Eq (5.15) can be conditioned over instantaneous signal-to-noise ratio (SNR) and denoted as:

$$P_{M-QAM}^{MDLB}(e|\gamma_1,\gamma_2) \geq 4aQ\left(\sqrt{b\zeta}\right) - 4a^2Q^2\left(\sqrt{b\zeta}\right), \tag{5.19}$$

where γ_1 and γ_2 are the RS and NBs instantaneous signal-to-noise ratios defined as $\gamma_1 = \frac{E_{RS}}{N_o}$ and $\gamma_2 = \frac{E_{NS}}{N_o}$, E_{RS} is the reference symbol transmitted power, E_{NS} is the normal symbols transmitted power, respectively, $N_o = 1$ as defined in Eq (5.15), $a = \left(1 - \frac{1}{\sqrt{M}}\right)$, $b = \left(\frac{3}{M-1}\right)$ and $\zeta = \gamma_t \cos^2\theta + \gamma_t \sin^2\theta$ for $t \in [1:T]$ is the time index with the reference symbol being the first transmitted symbol across all frames.

Integrating Eq (5.19) gives the MDLB on the SEP as:

$$P_{M-QAM}^{MDLB}(e) = \int_0^\infty \int_0^\infty P_{M-QAM}^{MDLB}(e|\gamma_1\gamma_2)\, f_{\gamma_1}(\gamma_1)d\gamma_2\, f_{\gamma_2}(\gamma_2)d\gamma_2, \tag{5.20}$$

where $f_{\gamma_1}(\gamma_1)$ and $f_{\gamma_2}(\gamma_2)$ are the probability density function (PDF) for N_r receive antennas.

Substituting Eq (5.19) onto Eq (5.20) gives the new MDLB on the SEP as:

$$\begin{aligned} P_{M-QAM}^{MDLB}(e) &= \int_0^\infty \int_0^\infty 4aQ\left(\sqrt{b\zeta}\right) - 4a^2Q^2\left(\sqrt{b\zeta}\right) f_{\gamma_1}(\gamma_1)d\gamma_1\, f_{\gamma_2}(\gamma_2)d\gamma_2 \\ &= \frac{a}{n}\left\{\frac{1}{2} \times \left(\frac{2}{2+\alpha b\bar{\gamma}_1}\right)^{N_r}\left(\frac{2}{2+\delta b\bar{\gamma}_1}\right)^{N_r} - \frac{a}{2}\left(\frac{1}{1+\alpha b\bar{\gamma}_2}\right)^{N_r}\left(\frac{1}{1+\delta b\bar{\gamma}_2}\right)^{N_r} + (1-a)\right. \\ &\left.\left(\sum_{i=1}^{n-1}\left(\frac{S_i}{S_i+\alpha b\bar{\gamma}_1}\right)^{N_r}\left(\frac{S_i}{S_i+\delta b\bar{\gamma}_1}\right)^{N_r} + \sum_{i=n}^{2n-1}\left(\frac{S_{iB}}{S_{iB}+\alpha b\bar{\gamma}_2}\right)^{N_r}\left(\frac{S_{iB}}{S_{iB}+\delta b\bar{\gamma}_2}\right)^{N_r}\right)\right\}, \\ &= \frac{a}{n}\left\{\frac{1}{2} \times F - \frac{a}{2} \times A + (1-a)\left(\sum_{i=1}^{n-1} \mathrm{C} + \sum_{i=n}^{2n-1} O\right)\right\}, \end{aligned} \tag{5.21}$$

where $\alpha = \cos^2\theta$, $\delta = \sin^2\theta$, $F = \left(\frac{2}{2+\alpha b\bar{\gamma}_1}\right)^{N_r}\left(\frac{2}{2+\delta b\bar{\gamma}_1}\right)^{N_r}$, $A = \left(\frac{1}{1+\alpha b\bar{\gamma}_2}\right)^{N_r}\left(\frac{1}{1+\delta b\bar{\gamma}_2}\right)^{N_r}$, $C = \left(\frac{S_i}{S_i+\alpha b\bar{\gamma}_1}\right)^{N_r}\left(\frac{S_i}{S_i+\delta b\bar{\gamma}_1}\right)^{N_r}$ and $O = \left(\frac{S_{iB}}{S_{iB}+\alpha b\bar{\gamma}_2}\right)^{N_r}\left(\frac{S_{iB}}{S_{iB}+\delta b\bar{\gamma}_1}\right)^{N_r}$. $\bar{\gamma} = E\{\gamma_t\}, t, t \in [1:T]$ is the average SNR at time t, $\bar{\gamma}_1 = \frac{E_{RS}}{N_0}$ and $\bar{\gamma}_2 = \frac{E_{NS}}{N_0}$ are the average SNR as defined in Eq (5.19).

Noting that the transmission powers for the symbols are independently allocated amongst the RS and NSs where more power is allocated to the RS compared to NSs for a better estimation of the channel.

Refer to Appendix C for an effectively computation of the final expression of the MDLB on the SEP in Eq (5.21).

5.4 Numerical and analytical results

This section presents numerical and analytical results of the proposed non-coherent GDM-SSD for *M*-QAM maximum-likelihood detection and the SEP performance analyses of the system model presented on the previous section. The presented results are for 16-QAM and 64-QAM constellation with $N = 100$ and $N = 400$ transmitted symbols with the number of receive antennas $N_r = 2$. The results are compared with that of coherent SSD combined with MRC detections.

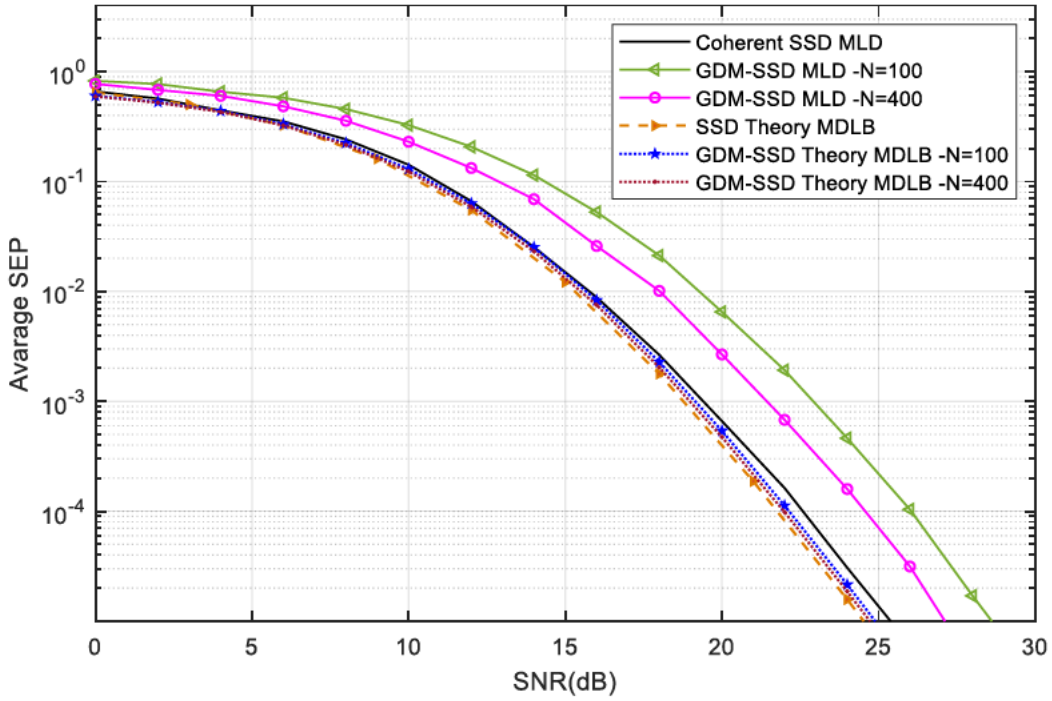

Figure 5.2: Non-coherent GDM-SSD MLD and SEP performance analytical results compared with that of coherent SSD for 16-QAM.

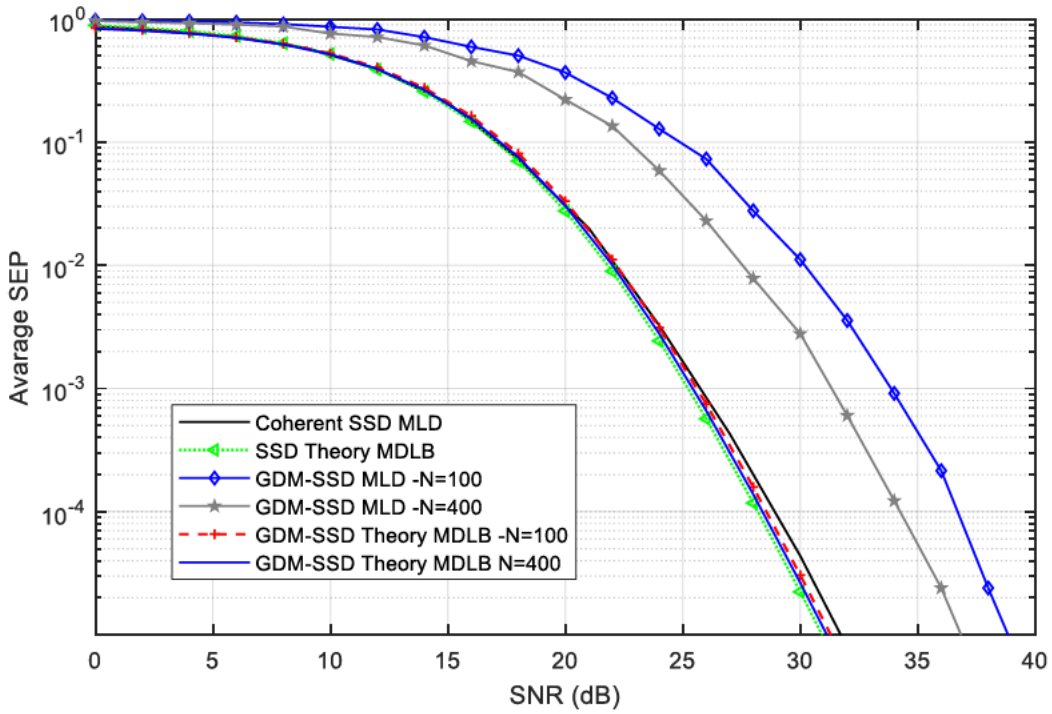

Figure 5.3: Non-coherent GDM-SSD MLD and SEP performance analytical results compared with that of coherent SSD for 64-QAM.

It is observed that for both16-QAM and 64-QAM, the SEP performance of the proposed GDM-SD system is closely approaching that of coherent SSD MLD as the number of symbols increases. When $N = 100$, the SEP performance of the proposed GDM-SSD scheme is about 5dB higher than that of the coherent detection. When $N = 400$ the SEP performance is about 4dB higher than that of the coherent detection, resulting to a performance loss compared to the coherent detection.

It is further observed that for a large number of transmitted symbols, the error performance of GDM-SSD approach that of coherent detection.

5.5 Chapter summary

In this chapter, the proposed GDM-SSD scheme including the system model was presented. SSD was applied to the non-coherent GDM system to improve the SEP performance of non-coherent detection. Numerical and analytical results of the SEP performance of the proposed scheme GDM-SSD compared to that of the coherent SSD MLD for 16-QAM and 64-QAM was presented using MATLAB. The results show performance loss of the proposed scheme of about 5dB compared to the coherent detection.

CHAPTER 6

CONCLUSION

This chapter summarizes the research concluding remarks on the presented schemes and the future research. The fundamental idea of the proposed generalized differential modulation with signal space diversity (GDM-SSD) scheme is to employ diversity in a non-coherent system.

6.1 Conclusion remarks

A literature survey of wireless communication techniques involved in the investigation of the proposed scheme is presented in chapter 2.

In chapter 3, a coherent signal space diversity (SSD) system over Rayleigh fading and additive white Gaussian noise (AWGN) channel was presented. Maximum ratio combining (MRC) reception was employed at the receiver to reduce errors that cause an increase in the signal-to-noise ratio (SNR) of the coherent SSD detection. This is due to the system requirement of the full knowledge of channel state information (CSI) at the receiver. The symbol error probability (SEP) performance of the coherent SSD was analyzed using the union bound (UB), minimum distance lower bound (MDLB) and nearest neighbour (NN) approximation models in a closed form. Numerical results show that as the number of receive antennas increase, the SEP performance of the UB, MDLB and NN approximation approaches 0 SNR and away from that of coherent SSD. Therefore, the coherent SSD SEP performance is significant as diversity is achieved.

Non-coherent detections conventional differential modulation (CDM) and generalized differential modulation (GDM) are presented in chapter 4 to simplify the complexity of the coherent detection. These schemes are presented over quasi-static fading channel (QSFC), where GDM uses power allocation to bridge the performance gab between non-coherent CDM and coherent detection. Numerical results show non-coherent CDM 3dB performance loss to coherent detection. And, that the gap between non-coherent CDM and its coherent counterpart is reduced by non-coherent GDM detection with about 1dB performance gap gain. This signifies GDM as an alternative non-coherent detection to non-coherent CDM.

The proposed GDM-SSD scheme was presented in chapter 5 which employs diversity in a non-coherent system to improve the error performance of wireless communication systems by applying SSD in GDM. Numeric results show that the SEP performance of the proposed GDM-SSD scheme losses about 5dB performance gap over coherent SSD scheme. It is observed that the performance of GDM-SSD detection gets better as the number of transmitted symbols in a frame increase.

Therefore, diversity was successfully applied to a non-coherent GDM system. The proposed GDM-SSD scheme is significant in enhancing the performance of wireless communication systems.

6.2 Future research

This presents an opportunity to investigate the performance the following schemes:

1. Non-coherent conventional differential modulation with signal space diversity (CDM-SSD) detection schemes.

2. The employment of other diversity techniques to bridge the SEP performance gap between the non-coherent GDM-SSD and coherent detection.

APPENDIX A

This section presents the derivation of UB conditional PEP in Eq (3.11) of the performance analysis of the coherent SSD with N_r-branches MRC reception system in Section 3.

DERIVATION OF UNION BOUND CONDITIONAL PEP

The UB conditional PEP is effectively computed using the received symbol in Eq (3.4) $\boldsymbol{y}_t = \sqrt{\frac{Es}{E\omega}}\boldsymbol{h}_t w_t \ + \ \boldsymbol{n}_t \ , \ t \in [1\colon 2]$. A typical received symbol pair is denoted as:

$$\boldsymbol{y}_1 = \sqrt{\frac{Es}{E\omega}}\boldsymbol{h}_1\left(x_1^I + jx_2^Q\right) \ + \ \boldsymbol{n}_1, \tag{A.1a}$$

$$\boldsymbol{y}_2 = \sqrt{\frac{Es}{E\omega}}\boldsymbol{h}_2\left(x_2^I + \ jx_1^Q\right) \ + \ \boldsymbol{n}_2. \tag{A.1b}$$

The received symbols vectors $\boldsymbol{y}_t$ with entries y_{tk}, $t \in [1\colon 2]$ and $k \in [1\colon N_r]$ are combined using MRC reception on a symbol-by-symbol basis as they are received and are denoted as $\boldsymbol{z}_t, \ t \in [1\colon 2]$ with entries z_{kt}, $t \in [1\colon 2]$ and $k \in [1\colon N_r]$. $\boldsymbol{h}_t$ is the independent Rayleigh fading coefficient vector with entries h_{kt} and $k \in [1\colon N_r]$ where h_{kt} is defined in Eq (3.10) in the dissertation. For each receiver the symbol pair is denoted as:

$$\begin{aligned}
z_{1k} &= e^{-jQ_{1k}}y_{1k}, \\
&= e^{-jQ_{1k}}\left(\sqrt{\frac{Es}{E\omega}}h_{1k}\left(x_1^I + jx_2^Q\right) \ + \ n_{1k}\right), \\
&= e^{-jQ_{1k}}\left(\sqrt{\frac{Es}{E\omega}}\alpha_{1k}e^{jQ_{1k}}\left(x_1^I + \ jx_2^Q\right) + \ n_{1k}\right), \\
&= \sqrt{\frac{Es}{E\omega}}\left(e^{-jQ_{1k}}\alpha_{1k}e^{jQ_{1k}}\left(x_1^I + \ jx_2^Q\right)\right) \ + \ e^{-jQ_{1k}}n_{1k}, \\
&= \sqrt{\frac{Es}{E\omega}}\left(\alpha_{1k}e^{j(Q_{1k}-Q_{1k})}\left(x_1^I + \ jx_2^Q\right)\right) \ + \ e^{-jQ_{1k}}n_{1k}, \\
z_{1k} &= \sqrt{\frac{Es}{E\omega}}\left(\alpha_{1k}\left(x_1^I + \ jx_2^Q\right)\right) \ + \ \tilde{n}_{1k},
\end{aligned} \tag{A.2a}$$

$$\begin{aligned}
z_{2k} &= e^{-jQ_{2k}}y_{2k}, \\
&= e^{-jQ_{2k}}\left(\sqrt{\frac{Es}{E\omega}}h_{2k}\left(x_2^I + \ jx_1^Q\right) \ + \ n_{2k}\right), \\
&= e^{-jQ_{2k}}\left(\sqrt{\frac{Es}{E\omega}}\alpha_{2k}e^{jQ_{2k}}\left(x_2^I + \ jx_1^Q\right) + \ n_{2k}\right), \\
&= \sqrt{\frac{Es}{E\omega}}\left(e^{-jQ_{2k}}\alpha_{2k}e^{jQ_{2k}}\left(x_2^I + \ jx_1^Q\right)\right) \ + \ e^{-jQ_{2k}}n_{2k},
\end{aligned}$$

$$= \sqrt{\frac{Es}{E\omega}}\left(\alpha_{2k} e^{j(Q_{2k}-Q_{2k})}\left(x_2^I + jx_1^Q\right)\right) + e^{-jQ_{2k}} n_{2k},$$

$$z_{2k} = \sqrt{\frac{Es}{E\omega}}\left(\alpha_{2k}\left(x_2^I + jx_1^Q\right)\right) + \tilde{n}_{2k}, \tag{A.2b}$$

where $\tilde{n}_{tk} = e^{-jQ_{tk}} n_{tk}$, $t \in [1:2]$ and $k \in [1:N_r]$ is a complex random variable with distribution $\tilde{n}_{tk} \sim (0,1)$.

Performing de-interleaving on Eq (A.2a) and Eq (A.2b) gives:

$$r_{1k} = Re\left\{\sqrt{\frac{Es}{E\omega}}\alpha_{1k}\left(x_1^I + jx_2^Q\right) + \tilde{n}_{1k}\right\} + jIm\left\{\sqrt{\frac{Es}{E\omega}}\left(\alpha_{2k}\left(x_2^I + jx_1^Q\right)\right) + \tilde{n}_{2k}\right\},$$

$$= \sqrt{\frac{E_s}{E_\omega}}\alpha_{1k}\, x_1^I + j\sqrt{\frac{E_s}{E_\omega}}\alpha_{2k}\, x_1^Q + \tilde{\tilde{n}}_{1k}, \tag{A.3a}$$

$$r_{2k} = Re\left\{\sqrt{\frac{Es}{E\omega}}\left(\alpha_{2k}\left(x_2^I + jx_1^Q\right)\right) + \tilde{n}_{2k}\right\} + jIm\left\{\sqrt{\frac{Es}{E\omega}}\alpha_{1k}\left(x_1^I + jx_2^Q\right) + \tilde{n}_{1k}\right\},$$

$$= \sqrt{\frac{E_s}{E_\omega}}\alpha_{2k}\, x_2^I + j\sqrt{\frac{E_s}{E_\omega}}\alpha_{1k}\, x_2^Q + \tilde{\tilde{n}}_{2k}, \tag{A.3b}$$

where similar to Eq (A.2a) and Eq (A.2b), the resultant noise term $\tilde{\tilde{n}}_{tk}$, $t \in [1:2]$and $k \in [1:N_r]$ is a complex random variable with distribution $\tilde{\tilde{n}}_{tk} \sim (0,1)$ and $j = \sqrt{-1}$.

The UB conditional PEP is then computed as below:

$$P(u_1 \to \hat{u}_1 | \boldsymbol{h}_1, \boldsymbol{h}_2) = P\left(\sum_{k=1}^{N_r}\left|r_{1k} - \sqrt{\frac{E_s}{E_\omega}}\alpha_{1k}\, x_1^I - j\sqrt{\frac{E_s}{E_\omega}}\alpha_{2k}\, x_1^Q\right|^2 > \sum_{k=1}^{N_r}\left|r_{1k} - \sqrt{\frac{E_s}{E_\omega}}\alpha_{1k}\, \hat{x}_1^I - j\sqrt{\frac{E_s}{E_\omega}}\alpha_{2k}\, \hat{x}_1^Q\right|^2\right),$$

$$= P\left(\sum_{k=1}^{N_r}\left|\left(\sqrt{\frac{E_s}{E_\omega}}\left(\alpha_{1k}\, x_1^I + j\alpha_{2k}\, x_1^Q\right) + \tilde{\tilde{n}}_{1k}\right) - \sqrt{\frac{E_s}{E_\omega}}\alpha_{1k}\, x_1^I - j\sqrt{\frac{E_s}{E_\omega}}\alpha_{2k}\, x_1^Q\right|^2 > \sum_{k=1}^{N_r}\left|\left(\sqrt{\frac{E_s}{E_\omega}}\left(\alpha_{1k}\, x_1^I + j\alpha_{2k}\, x_1^Q\right) + \tilde{\tilde{n}}_{1k}\right) - \sqrt{\frac{E_s}{E_\omega}}\alpha_{1k}\, \hat{x}_1^I - j\sqrt{\frac{E_s}{E_\omega}}\alpha_{2k}\, \hat{x}_1^Q\right|^2\right),$$

$$= P\left(\sum_{k=1}^{N_r}\left|\sqrt{\frac{E_s}{E_\omega}}\alpha_{1k}\, x_1^I + j\sqrt{\frac{E_s}{E_\omega}}\alpha_{2k}\, x_1^Q + \tilde{\tilde{n}}_{1k} - \sqrt{\frac{E_s}{E_\omega}}\alpha_{1k}\, x_1^I - j\sqrt{\frac{E_s}{E_\omega}}\alpha_{2k}\, x_1^Q\right|^2 > \sum_{k=1}^{N_r}\left|\sqrt{\frac{E_s}{E_\omega}}\alpha_{1k}\, x_1^I + j\sqrt{\frac{E_s}{E_\omega}}\alpha_{2k}\, x_1^Q + \tilde{\tilde{n}}_{1k} - \sqrt{\frac{E_s}{E_\omega}}\alpha_{1k}\, \hat{x}_1^I - j\sqrt{\frac{E_s}{E_\omega}}\alpha_{2k}\, \hat{x}_1^Q\right|^2\right),$$

$$= P\left(\sum_{k=1}^{N_r}\left|\sqrt{\frac{E_s}{E_\omega}}\alpha_{1k}\, x_1^I - \sqrt{\frac{E_s}{E_\omega}}\alpha_{1k}\, x_1^I + j\sqrt{\frac{E_s}{E_\omega}}\alpha_{2k}\, x_1^Q - j\sqrt{\frac{E_s}{E_\omega}}\alpha_{2k}\, x_1^Q + \tilde{\tilde{n}}_{1k}\right|^2 > \sum_{k=1}^{N_r}\left|\sqrt{\frac{E_s}{E_\omega}}\alpha_{1k}\, x_1^I - \sqrt{\frac{E_s}{E_\omega}}\alpha_{1k}\, \hat{x}_1^I + j\sqrt{\frac{E_s}{E_\omega}}\alpha_{2k}\, x_1^Q - j\sqrt{\frac{E_s}{E_\omega}}\alpha_{2k}\, \hat{x}_1^Q + \quad \tilde{\tilde{n}}_{1k}\right|^2\right),$$

$$= P\left(\sum_{k=1}^{N_r}\left|\tilde{\tilde{n}}_{1k}\right|^2 > \sum_{k=1}^{N_r}\left|\sqrt{\frac{E_S}{E_\omega}}\left(\alpha_{1k}(x_1^I - \hat{x}_1^I) + j\alpha_{2k}(x_1^Q - \hat{x}_1^Q)\right) + \tilde{\tilde{n}}_{1k}\right|^2\right). \quad \text{(A.4)}$$

Let $(x_1^I - \hat{x}_1^I) = d_1$ and $(x_1^Q - \hat{x}_1^Q) = d_2$ where x_1^I,x_2^I and x_1^Q, x_2^Q are defined in Eq (3.11).

$$P(u_1 \to \hat{u}_1|\boldsymbol{h}_1, \boldsymbol{h}_2) = P\left(\sum_{k=1}^{N_r}\left|\tilde{\tilde{n}}_{1k}\right|^2 > \sum_{k=1}^{N_r}\left|\sqrt{\frac{E_S}{E_\omega}}(\alpha_{1k}\, d_1 + j\alpha_{2k}\, d_2) + \tilde{\tilde{n}}_{1k}\right|^2\right). \quad \text{(A.5)}$$

Apply $|A + B|^2 = |A|^2 + |B|^2 + 2\mathrm{Re}\{AB^*\}$ onto Eq (A.5):

$$P(u_1 \to \hat{u}_1|\boldsymbol{h}_1, \boldsymbol{h}_2) = P\left(\sum_{k=1}^{N_r}\left|\tilde{\tilde{n}}_{1k}\right|^2 > \sum_{k=1}^{N_r}\left|\sqrt{\frac{E_S}{E_\omega}}(\alpha_{1k}\, d_1 + j\alpha_{2k}\, d_2)\right|^2 + \sum_{k=1}^{N_r}\left|\tilde{\tilde{n}}_{1k}\right|^2 + \sum_{k=1}^{N_r} 2Re\left\{\left(\sqrt{\frac{E_S}{E_\omega}}(\alpha_{1k}\, d_1 + j\alpha_{2k}\, d_2)\right)\tilde{\tilde{n}}_{1k}^{\,*}\right\}\right),$$

$$= P\left(\sum_{k=1}^{N_r}\left|\tilde{\tilde{n}}_{1k}\right|^2 - \sum_{k=1}^{N_r}\left|\tilde{\tilde{n}}_{1k}\right|^2 > \sum_{k=1}^{N_r}\left|\sqrt{\frac{E_S}{E_\omega}}(\alpha_{1k}\, d_1 + j\alpha_{2k}\, d_2)\right|^2 + \sum_{k=1}^{N_r} 2Re\left\{\left(\sqrt{\frac{E_S}{E_\omega}}(\alpha_{1k}\, d_1 + j\alpha_{2k}\, d_2)\right)\tilde{\tilde{n}}_{1k}^{\,*}\right\}\right),$$

$$= P\left(0 > \sum_{k=1}^{N_r}\left|\sqrt{\frac{E_S}{E_\omega}}(\alpha_{1k}\, d_1 + j\alpha_{2k}\, d_2)\right|^2 + \sum_{k=1}^{N_r} 2Re\left\{\left(\sqrt{\frac{E_S}{E_\omega}}(\alpha_{1k}\, d_1 + j\alpha_{2k}\, d_2)\right)\tilde{\tilde{n}}_{1k}^{\,*}\right\}\right),$$

$$= P\left(\sum_{k=1}^{N_r} 2Re\left\{\left(\sqrt{\frac{E_S}{E_\omega}}(\alpha_{1k}\, d_1 + j\alpha_{2k}\, d_2)\right)\tilde{\tilde{n}}_{1k}^{\,*}\right\} > \sum_{k=1}^{N_r}\left|\sqrt{\frac{E_S}{E_\omega}}(\alpha_{1k}\, d_1 + j\alpha_{2k}\, d_2)\right|^2\right),$$

$$= P\left(\sum_{k=1}^{N_r} Re\left\{\left(\sqrt{\frac{E_S}{E_\omega}}(\alpha_{1k}\, d_1 + j\alpha_{2k}\, d_2)\right)\tilde{\tilde{n}}_{1k}^{\,*}\right\} > \sum_{k=1}^{N_r}\frac{\left|\sqrt{\frac{E_S}{E_\omega}}(\alpha_{1k}\, d_1 + j\alpha_{2k}\, d_2)\right|^2}{2}\right),$$

$$= P\left(\sum_{k=1}^{N_r} Re\left\{\left(\sqrt{\frac{E_S}{E_\omega}}(\alpha_{1k}\, d_1 + j\alpha_{2k}\, d_2)\right)\tilde{\tilde{n}}_{1k}^{\,*}\right\} > \sum_{k=1}^{N_r}\frac{E_S}{2E_\omega}(\alpha_{1k}{}^2\, d_1^2 + \alpha_{2k}{}^2\, d_2^2)\right). \quad \text{(A.6)}$$

Let $n = \dfrac{\sum_{k=1}^{N_r} Re\left\{\left(\sqrt{\frac{E_S}{E_\omega}}(\alpha_{1k}\, d_1 + j\alpha_{2k}\, d_2)\right)\tilde{\tilde{n}}_{1k}^{\,*}\right\}}{\sqrt{\sum_{k=1}^{N_r}\frac{E_S}{2E_\omega}(\alpha_{1k}{}^2\, d_1^2 + \alpha_{2k}{}^2\, d_2^2)}}$ be a Gaussian random variable distributed as $n \sim N(0,1)$ considering that:

$$\sum_{k=1}^{N_r} Re\left\{\left(\sqrt{\frac{E_S}{E_\omega}}(\alpha_{1k}\, d_1 + j\alpha_{2k}\, d_2)\right)\tilde{\tilde{n}}_{1k}^{\,*}\right\} \sim N\left(0, \sum_{k=1}^{N_r}\frac{E_S}{2E_\omega}(\alpha_{1k}{}^2\, d_1^2 + \alpha_{2k}{}^2\, d_2^2)\right) \quad \text{(A.7)}$$

Substituting accordingly in Eq (A.6) gives:

$$P(u_1 \to \hat{u}_1|\boldsymbol{h}_1, \boldsymbol{h}_2) = P\left(\frac{\sum_{k=1}^{N_r} Re\left\{\left(\sqrt{\frac{E_S}{E_\omega}}(\alpha_{1k}\, d_1 + j\alpha_{2k}\, d_2)\right)\tilde{\tilde{n}}_{1k}^{\,*}\right\}}{\sqrt{\sum_{k=1}^{N_r}\frac{E_S}{2E_\omega}(\alpha_{1k}{}^2\, d_1^2 + \alpha_{2k}{}^2\, d_2^2)}} > \frac{\sum_{k=1}^{N_r}\frac{E_S}{2E_\omega}(\alpha_{1k}{}^2\, d_1^2 + \alpha_{2k}{}^2\, d_2^2)}{\sqrt{\sum_{k=1}^{N_r}\frac{E_S}{2E_\omega}(\alpha_{1k}{}^2\, d_1^2 + \alpha_{2k}{}^2\, d_2^2)}}\right).$$

$$= P\left(n > \frac{\sum_{k=1}^{N_r} \frac{E_S}{2E_\omega}\left({\alpha_{1k}}^2\, d_1^2 + j{\alpha_{2k}}^2\, d_2^2\right)}{\sqrt{\sum_{k=1}^{N_r} \frac{E_S}{2E_\omega}\left({\alpha_{1k}}^2\, d_1^2 + {\alpha_{2k}}^2\, d_2^2\right)}}\right),$$

$$= P\left(n > \sqrt{\sum_{k=1}^{N_r} \frac{E_S}{2E_\omega}\left({\alpha_{1k}}^2\, d_1^2 + {\alpha_{2k}}^2\, d_2^2\right)}\right). \quad \text{(A.8)}$$

Let $\gamma_{tk} = {\alpha_{tk}}^2(E_s), t \in [1:2]$and $k \in [1:N_r]$ be the combined instantaneous SNR in the time slot t.

The probability that $n > \sqrt{\sum_{k=1}^{N_r} \frac{1}{2E_\omega}\left(\gamma_{1k}\, d_1^2 + \gamma_{2k}\, d_2^2\right)}$ can be written in tearms of the Q-Function as:

$$P\left(n > \sqrt{\sum_{k=1}^{N_r} \frac{1}{2E_\omega}\left(\gamma_{1k}\, d_1^2 + \gamma_{2k}\, d_2^2\right)}\right) = Q\left(\sqrt{\sum_{k=1}^{N_r} \frac{1}{2E_\omega}\left(\gamma_{1k}\, d_1^2 + \gamma_{2k}\, d_2^2\right)}\right). \quad \text{(A.9)}$$

Therefore, Eq (A.8) can be written as:

$$P(u_1 \to \hat{u}_1 | \boldsymbol{h}_1, \boldsymbol{h}_2) = P\left(n > \sqrt{\sum_{k=1}^{N_r} \frac{1}{2E_\omega}\left(\gamma_{1k}\, d_1^2 + \gamma_{2k}\, d_2^2\right)}\right),$$

$$= Q\left(\sqrt{\sum_{k=1}^{N_r} \frac{1}{2E_\omega}\left(\gamma_{1k}\, d_1^2 + \gamma_{2k}\, d_2^2\right)}\right),$$

$$= Q\left(\sqrt{\frac{1}{2E_\omega}\left(\gamma_1 d_1^2 + \gamma_2 d_2^2\right)}\right), \quad \text{(A.10)}$$

where $\gamma_t = \sum_{k=1}^{N_r} \gamma_{tk}$ for $t \in [1:2]$, and $k \in [1:N_r]$.

APPENDIX B

This section presents the derivation of the UB unconditional PEP in Eq (3.13) of the performance analysis of the coherent SSD with N_r-branches MRC reception system in Section 3.

DERIVATION OF UNION BOUND UNCONDITIONAL PEP

The UB unconditional PEP is effectively computed by applying the trapezoidal approximation to the $Q(x)$ function as shown below:

$$P(u_1 \to \hat{u}_1) = \int_0^\infty \int_0^\infty Q\left(\sqrt{\frac{1}{2E_\omega}(\gamma_1 d_1^2 + \gamma_2 d_2^2)}\right) f_{\gamma_1}(\gamma_1)\, f_{\gamma_2}(\gamma_2)\, d\gamma_1\, d\gamma_2, \tag{B.1}$$

where $f_{\gamma_1}(\gamma_1)$ and $f_{\gamma_2}(\gamma_2)$ are defined in Eq (3.10).

Given that:

$$Q(x) = \frac{1}{2n}\left[\frac{1}{2}e^{\frac{-x^2}{2}} + \sum_{i=1}^{n-1} e^{\frac{-x^2}{s_i}}\right], \tag{B.2}$$

where $i \in [1{:}\,2]$, $s_i = 2\,sin^2\,\theta_j$ and $\theta_j = \frac{t\pi}{2n}$.

Substituting Eq (B.2) onto Eq (B.1) where $x = \sqrt{\frac{1}{2E_\omega}(\gamma_1 d_1^2 + \gamma_2 d_2^2)}$ yields:

$$P(u_1 \to \hat{u}_1) = \int_0^\infty \int_0^\infty \frac{1}{2n}\left[\frac{1}{2}exp\left\{\frac{-\left(\sqrt{\frac{1}{2E_\omega}(\gamma_1 d_1^2+\gamma_2 d_2^2)}\right)^2}{2}\right\} + \sum_{i=1}^{n-1} exp\left\{\frac{-\left(\sqrt{\frac{1}{2E_\omega}(\gamma_1 d_1^2+\gamma_2 d_2^2)}\right)^2}{S_i}\right\}\right] f_{\gamma_1}(\gamma_1)\, f_{\gamma_2}(\gamma_2)\, d\gamma_1\, d\gamma_2,$$

$$= \frac{1}{2n}\int_0^\infty \int_0^\infty \left[\frac{1}{2}exp\left\{\frac{-\left(\sqrt{\frac{1}{2E_\omega}(\gamma_1 d_1^2+\gamma_2 d_2^2)}\right)^2}{2}\right\} + \sum_{i=1}^{n-1} exp\left\{\frac{-\left(\sqrt{\frac{1}{2E_\omega}(\gamma_1 d_1^2+\gamma_2 d_2^2)}\right)^2}{S_i}\right\}\right] f_{\gamma_1}(\gamma_1)\, f_{\gamma_2}(\gamma_2)\, d\gamma_1\, d\gamma_2,$$

$$= \frac{1}{2n}\left[\frac{1}{2}\int_0^\infty \int_0^\infty exp\left\{\frac{-\left(\sqrt{\frac{1}{2E_\omega}(\gamma_1 d_1^2+\gamma_2 d_2^2)}\right)^2}{2}\right\} f_{\gamma_1}(\gamma_1)\, f_{\gamma_2}(\gamma_2)\, d\gamma_1\, d\gamma_2 + \right.$$

$$\left.\sum_{i=1}^{n-1}\int_0^\infty \int_0^\infty exp\left\{\frac{-\left(\sqrt{\frac{1}{2E_\omega}(\gamma_1 d_1^2+\gamma_2 d_2^2)}\right)^2}{S_i}\right\} f_{\gamma_1}(\gamma_1)\, f_{\gamma_2}(\gamma_2) d\gamma_1\, d\gamma_2\right]. \quad \text{(B.3)}$$

For simplicity of Eq (B.3), let $\int_0^\infty \int_0^\infty exp\left\{\frac{-\left(\sqrt{\frac{1}{2E_\omega}(\gamma_1 d_1^2+\gamma_2 d_2^2)}\right)^2}{2}\right\} f_{\gamma_1}(\gamma_1)\, f_{\gamma_2}(\gamma_2)\, d\gamma_1\, d\gamma_2 = G$ and can be computed as:

$$G = \int_0^\infty \int_0^\infty \left(exp\left\{\frac{-\left(\frac{1}{2E_\omega}(\gamma_1 d_1^2)\right)}{2}\right\} \times exp\left\{\frac{-\left(\frac{1}{2E_\omega}(\gamma_1 d_1^2)\right)}{2}\right\}\right) f_{\gamma_1}(\gamma_1)\, f_{\gamma_2}(\gamma_2)\, d\gamma_1\, d\gamma_2,$$

$$= \left(\int_0^\infty exp\left\{\frac{-\left(\frac{1}{2E_\omega}(\gamma_1 d_1^2)\right)}{2}\right\} f_{\gamma_1}(\gamma_1)\, d\gamma_1 \times \int_0^\infty exp\left\{\frac{-\left(\frac{1}{2E_\omega}(\gamma_1 d_1^2)\right)}{2}\right\} f_{\gamma_2}(\gamma_2)\, d\gamma_2\right). \quad \text{(B.4)}$$

Let $\frac{d_1^2}{2E_\omega} = P_1$ therefore, $\int_0^\infty exp\left\{\frac{-\left(\frac{1}{2E_\omega}(\gamma_1 d_1^2)\right)}{2}\right\} f_{\gamma_1}(\gamma_1)\, d\gamma_1 = \int_0^\infty exp\left\{\frac{-(P_1\gamma_1)}{2}\right\} f_{\gamma_1}(\gamma_1)\, d\gamma_1$. Perform integration by applying the MGF expression $\int_0^\infty e^{-s\gamma_t} f(\gamma_t)\, d(\gamma_t) = (1+s\bar{\gamma})^{-N_r}, t \in [1{:}\,2]$ as shown below:

$$\int_0^\infty e^{\frac{-(P_1\gamma_1)}{2}} f_{\gamma_1}(\gamma_1)\, d\gamma_1 = \left[1+\left(\frac{P_1}{2}\right)\bar{\gamma}\right]^{-N_r},$$

$$= \left(\frac{2+P_1\bar{\gamma}}{2}\right)^{-N_r},$$

$$= \left(\frac{2}{2+P_1\bar{\gamma}}\right)^{N_r}. \quad \text{(B.5)}$$

The same can be done for $\int_0^\infty exp\left\{\frac{-\left(\frac{1}{2E_\omega}(\gamma_2 d_2^2)\right)}{2}\right\} f_{\gamma_2}(\gamma_2)\, d\gamma_2$ giving:

$$\int_0^\infty exp\left\{\frac{-\left(\frac{1}{2E_\omega}(\gamma_2 d_2^2)\right)}{2}\right\} f_{\gamma_2}(\gamma_2)\, d\gamma_2 = \left(\frac{2}{2+P_2\bar{\gamma}}\right)^{N_r}. \quad \text{(B.6)}$$

Therefore:

$$\int_0^\infty \int_0^\infty exp\left\{\frac{-\left(\sqrt{\frac{1}{2E_\omega}(\gamma_1 d_1^2+\gamma_2 d_2^2)}\right)^2}{2}\right\} f_{\gamma_1}(\gamma_1)\, f_{\gamma_2}(\gamma_2)\, d\gamma_1\, d\gamma_2 = \left(\frac{2}{2+P_1\bar{\gamma}}\right)^{N_r}\left(\frac{2}{2+P_2\bar{\gamma}}\right)^{N_r}. \quad \text{(B.7)}$$

The same can be done for $\int_0^\infty \int_0^\infty exp\left\{\frac{-\left(\sqrt{\frac{1}{2E_\omega}\left(\gamma_1 d_1^2+\gamma_2 d_2^2\right)}\right)^2}{S_i}\right\} f_{\gamma_1}(\gamma_1)\, f_{\gamma_2}(\gamma_2) d\gamma_1\, d\gamma_2$ giving:

$$\int_0^\infty \int_0^\infty exp\left\{\frac{-\left(\sqrt{\frac{1}{2E_\omega}\left(\gamma_1 d_1^2+\gamma_2 d_2^2\right)}\right)^2}{S_i}\right\} f_{\gamma_1}(\gamma_1)\, f_{\gamma_2}(\gamma_2) d\gamma_1\, d\gamma_2 = \left(\frac{S_i}{S_i+P_1\overline{\gamma}}\right)^{N_r}\left(\frac{S_i}{S_i+P_2\overline{\gamma}}\right)^{N_r},$$

Therefore:

$$\begin{aligned} P(u_1 \to \hat{u}_1) &= \frac{1}{2n}\left[\frac{1}{2}\left(\left(\frac{2}{2+P_1\overline{\gamma}}\right)^{N_r}\left(\frac{2}{2+P_2\overline{\gamma}}\right)^{N_r}\right)+\sum_{i=1}^{n-1}\left(\frac{S_i}{S_i+P_1\overline{\gamma}}\right)^{N_r}\left(\frac{S_i}{S_i+P_2\overline{\gamma}}\right)^{N_r}\right], \\ &= \frac{1}{4n}\left(\left(\frac{2}{2+P_1\overline{\gamma}}\right)^{N_r}\left(\frac{2}{2+P_2\overline{\gamma}}\right)^{N_r}\right)+\frac{1}{2n}\sum_{i=1}^{n-1}\left(\frac{S_i}{S_i+P_1\overline{\gamma}}\right)^{N_r}\left(\frac{S_i}{S_i+P_2\overline{\gamma}}\right)^{N_r}. \end{aligned} \quad \text{(B.8)}$$

APPENDIX C

This section presents the derivation of the MDLB unconditional PEP in Eq (3.24) of the performance analysis of the coherent SSD with N_r- branches MRC reception system in Section 3.

DERIVATION OF MINIMUM DISTANCE LOWER BOUND UNCONDITIONAL PEP

The unconditional SEP for *M*-QAM is effectively computed as:

$$P_{M-QAM}^{MDLB}(e) = \int_0^\infty \int_0^\infty 4aQ\left(\sqrt{b\zeta}\right) - 4a^2Q^2\left(\sqrt{b\zeta}\right) f_{\gamma_1}(\gamma_1)d\gamma_1\, f_{\gamma_2}(\gamma_2)d\gamma_2. \tag{C.1}$$

Let $a = \left(1 - \frac{1}{\sqrt{M}}\right)$ and $b = \left(\frac{3}{M-1}\right)$, $\zeta = \gamma_1\, cos^2\,\theta + \gamma_2\, sin^2\,\theta$, where γ_t for $t\,[1{:}\,2]$ defined in Eq (3.22) and $f_{\gamma_t}(\gamma_t)$ is defined in Eq (3.23).

The relationship between the error probability and the Q-function is defined in Appendix A. Apply the trapezoidal approximation on $Q\left(\sqrt{b\zeta}\right)$ and $Q^2\left(\sqrt{b\zeta}\right)$ using the uniform distribution $\int_a^b f(x)dx = \frac{b-a}{n}\left[\frac{f(a)+f(b)}{2} + \sum_{k=1}^{n-1} f(a + k\,\frac{b-a}{n})\right]$ as presented below:

$$Q\left(\sqrt{b\zeta}\right) = \frac{1}{\pi} \times \frac{b-a}{n}\left[\frac{\exp\left(-\frac{\sqrt{b\zeta}^2}{2sin^2\,a}\right)+\exp\left(-\frac{\sqrt{b\zeta}^2}{2sin^2\,b}\right)}{2} + \sum_{k=1}^{n-1} exp\left(-\frac{\sqrt{b\zeta}^2}{2sin^2\left(a+k\left(\frac{b-a}{n}\right)\right)}\right)\right], \tag{C.2}$$

where $f(a) = exp\left(-\frac{\sqrt{b\zeta}^2}{2sin^2\,0}\right)$, $f(b) = exp\left(-\frac{\sqrt{b\zeta}^2}{2sin^2\frac{\pi}{2}}\right)$ and where n is the number of iterations such that $n > 10$ [9].

The Q-function $Q\left(\sqrt{b\zeta}\right)$ is then computed as:

$$Q\left(\sqrt{b\zeta}\right) = \frac{1}{\pi} \times \frac{\frac{\pi}{2}-0}{n}\left[\frac{exp\left(-\frac{\sqrt{b\zeta}^2}{2sin^2\,0}\right)+exp\left(-\frac{\sqrt{b\zeta}^2}{2sin^2\frac{\pi}{2}}\right)}{2} + \sum_{k=1}^{n-1} exp\left(-\frac{\sqrt{b\zeta}^2}{2sin^2\left(0+k\left(\frac{\frac{\pi}{2}-0}{n}\right)\right)}\right)\right],$$

$$= \frac{1}{2n}\left[\frac{0+exp\left(-\frac{\sqrt{b\zeta}^2}{2sin^2\frac{\pi}{2}}\right)}{2} + \sum_{k=1}^{n-1} exp\left(-\frac{\sqrt{b\zeta}^2}{2sin^2\left(k\left(\frac{\pi}{2n}\right)\right)}\right)\right],$$

$$= \frac{1}{2n}\left[\frac{exp\left(-\frac{\sqrt{b\zeta}^2}{2sin^2\frac{\pi}{2}}\right)}{2} + \sum_{k=1}^{n-1} exp\left(-\frac{\sqrt{b\zeta}^2}{2sin^2\left(k\left(\frac{\pi}{2n}\right)\right)}\right)\right],$$

$$= \frac{1}{2n}\left[\frac{1}{2}exp\left(-\frac{\sqrt{b\zeta}^2}{2}\right) + \sum_{k=1}^{n-1} exp\left(-\frac{\sqrt{b\zeta}^2}{2sin^2\left(k\left(\frac{\pi}{2n}\right)\right)}\right)\right]. \quad \text{(C.3)}$$

The same can be done for $Q^2\left(\sqrt{b\zeta}\right)$ giving:

$$Q^2\left(\sqrt{b\zeta}\right) = \frac{1}{2n}\left[\frac{1}{2}exp\left(-\sqrt{b\zeta}^2\right) + \sum_{k=1}^{n-1} exp\left(-\frac{\sqrt{b\zeta}^2}{2sin^2\left(k\left(\frac{\pi}{4n}\right)\right)}\right)\right]. \quad \text{(C.4)}$$

The Q-functions $Q\left(\sqrt{b\zeta}\right)$ and $Q^2\left(\sqrt{b\zeta}\right)$ may be written as:

$$Q\left(\sqrt{b}\zeta\right) = {}^{1}/_{2n}\left[\frac{1}{2}e^{\frac{-\left(\sqrt{b\zeta}\right)^2}{2}} + \sum_{i=1}^{n-1} e^{\frac{-\left(\sqrt{b\zeta}\right)^2}{S_i}}\right], \quad \text{(C.5a)}$$

$$Q^2\left(\sqrt{b}\zeta\right) = \left({}^{1}/_{4n}\right)\left[\frac{1}{2}e^{-\left(\sqrt{b\zeta}\right)^2} + \sum_{i=n}^{2n-1} e^{\frac{-\left(\sqrt{b\zeta}\right)^2}{S_i}}\right], \quad \text{(C.5b)}$$

where $S_i = 2\,sin^2\,\theta_k$, $\theta_k = \frac{i\pi}{4n}$, $S_{iB} = 2\,sin^2\,\beta_k$, and $\beta_k = \frac{i\pi}{4n}$.

Substitute Eq (C.5a) and Eq (C.5b) onto Eq (C.1) gives:

$$P_{M-DQAM}^{MDLB}(e) = \int_0^\infty \int_0^\infty 4a \times \left[{}^{1}/_{2n}\left(\left(\frac{1}{2}e^{-b\zeta/2}\right) + \sum_{i=1}^{n-1} e^{-b\zeta/S_i}\right)\right] - 4a^2 \times \left[{}^{1}/_{4n}\left(\frac{1}{2}e^{-b\zeta} + \sum_{i=n}^{2n-1} e^{-b\zeta/S_{iB}}\right)\right] f_{\gamma_1}(\gamma_1)d\gamma_1\, f_{\gamma_2}(\gamma_2)d\gamma_2,$$

$$= \int_0^\infty \int_0^\infty a \times \left[{}^{1}/_{n}\left(\frac{1}{2}e^{-b\zeta/2}\right) + \sum_{i=1}^{n-1} e^{\frac{-b\zeta}{S_i}}\right] - a^2 \times \left[{}^{1}/_{n}\left(\frac{1}{2}e^{-b\zeta} + \sum_{i=n}^{2n-1} e^{-b\zeta/S_{iB}}\right)\right] f_{\gamma_1}(\gamma_1)d\gamma_1\, f_{\gamma_2}(\gamma_2)d\gamma_2\,,$$

$$= \int_0^\infty \int_0^\infty {}^{a}/_{n}\left(\left(\frac{1}{2}e^{-b\zeta/2}\right) + \sum_{i=1}^{n-1} e^{-b\zeta/S_i}\right) - {}^{a^2}/_{n}\left(\left(\frac{1}{2}e^{-b\zeta}\right) + \sum_{i=n}^{2n-1} e^{-b\zeta/S_{iB}}\right) f_{\gamma_1}(\gamma_1)d\gamma_1\, f_{\gamma_2}(\gamma_2)d\gamma_2,$$

$$= \int_0^\infty \int_0^\infty {}^{a}/_{n}\left[\left(\frac{1}{2}e^{-b\zeta/2}\right) + \sum_{i=1}^{n-1} e^{-b\zeta/S_i} - a\left(\frac{1}{2}e^{-b\zeta}\right) - a\sum_{i=n}^{2n-1} e^{-b\zeta/S_{iB}}\right] f_{\gamma_1}(\gamma_1)d\gamma_1\, f_{\gamma_2}(\gamma_2)d\gamma_2,$$

$$= \int_0^\infty \int_0^\infty {}^{a}/_{n}\left[\left(\frac{1}{2}e^{-b\zeta/2}\right) - a\left(\frac{1}{2}e^{-b\zeta}\right) + \sum_{i=1}^{n-1} e^{-b\zeta/S_i} - a\sum_{i=n}^{2n-1} e^{-b\zeta/S_{iB}}\right] f_{\gamma_1}(\gamma_1)d\gamma_1\, f_{\gamma_2}(\gamma_2)d\gamma_2,$$

$$= \int_0^{\infty} \int_0^{\infty} \frac{a}{n} \left\{ \frac{1}{2} e^{-b\zeta/2} - \frac{a}{2} e^{-b\zeta} + (1-a) \left(\sum_{i=1}^{n-1} e^{-b\zeta/s_i} + \sum_{i=n}^{2n-1} e^{-b\zeta/s_{iB}} \right) \right\} f_{\gamma_1}(\gamma_1) d\gamma_1 \, f_{\gamma_2}(\gamma_2) d\gamma_2. \quad \text{(C.6)}$$

Considering that $\zeta = \gamma_t \cos^2\theta + \gamma_t \sin^2\theta$ for $t\,[1{:}2]$, let $\alpha = \cos^2\theta$; $\delta = \sin^2\theta$. Eq (C.6) can be written as:

$$P_{M-DQAM}^{SER}(e) = \int_0^{\infty} \int_0^{\infty} \frac{a}{n} \left\{ \left(\frac{1}{2} e^{-\frac{\alpha b \gamma_t}{2}} \right) \left(\frac{1}{2} e^{-\frac{\delta b \gamma_t}{2}} \right) - \left(\frac{1}{2} a e^{-\alpha b \gamma_t} \right) \left(\frac{1}{2} a e^{-\delta b \gamma_t} \right) + (1 - a) \left(\sum_{i=1}^{n-1} \left(e^{\frac{-\alpha b \gamma_t}{S_i}} \right) \left(e^{\frac{-\delta b \gamma_t}{S_i}} \right) + \sum_{i=n}^{2n-1} \left(e^{\frac{-\alpha b \gamma_t}{S_{iB}}} \right) \left(e^{\frac{-\delta b \gamma_t}{S_{iB}}} \right) \right) \right\} f_{\gamma_1}(\gamma_1) d\gamma_1 \, f_{\gamma_2}(\gamma_2) d\gamma_2. \quad \text{(C.7)}$$

Apply the MGF $\int e^{-s\gamma} f(\gamma)\, d(\gamma) = (1 + s\bar{\gamma})^{-N_r}$ on Eq (C.7) as follows:

$$P_{M-DQAM}^{SER}(e) = \int_0^{\infty} \int_0^{\infty} \frac{a}{n} \left\{ \left(\frac{1}{2} e^{-\frac{\alpha b \gamma}{2}} \right) \left(\frac{1}{2} e^{-\frac{\delta b \gamma}{2}} \right) - \left(\frac{1}{2} a e^{-\alpha b \gamma} \right) \left(\frac{1}{2} a e^{-\delta b \gamma} \right) + (1 - a) \left(\sum_{i=1}^{n-1} \left(e^{\frac{-\alpha b \gamma}{S_i}} \right) \left(e^{\frac{-\delta b \gamma}{S_i}} \right) + \sum_{i=n}^{2n-1} \left(e^{\frac{-\alpha b \gamma}{S_{iB}}} \right) \left(e^{\frac{-\delta b \gamma}{S_{iB}}} \right) \right) \right\} f_{\gamma_1}(\gamma_1) d\gamma_1 \, f_{\gamma_2}(\gamma_2) d\gamma_2,$$

$$= \frac{a}{n} \left\{ \frac{1}{2} \left(1 + \left(\frac{\alpha b \bar{\gamma}}{2} \right) \right)^{-N_r} \left(1 + \left(\frac{\delta b \bar{\gamma}}{2} \right) \right)^{-N_r} - \frac{a}{2} (1 + \alpha b \bar{\gamma})^{-N_r} (1 + \delta b \bar{\gamma})^{-N_r} + (1 - a) \left(\sum_{i=1}^{n-1} \left(1 + \left(\frac{\alpha b \bar{\gamma}}{S_i} \right) \right)^{-N_r} \left(1 + \left(\frac{\delta b \bar{\gamma}}{S_i} \right) \right)^{-N_r} + \sum_{i=n}^{2n-1} \left(1 + \left(\frac{\alpha b \bar{\gamma}}{S_{iB}} \right) \right)^{-N_r} \left(1 + \left(\frac{\delta b \bar{\gamma}}{S_{iB}} \right) \right)^{-N_r} \right) \right\},$$

$$= \frac{a}{n} \left\{ \frac{1}{2} \left(\frac{2 + \alpha b \bar{\gamma}}{2} \right)^{-N_r} \left(\frac{2 + \delta b \bar{\gamma}}{2} \right)^{-N_r} - \frac{a}{2} (1 + \alpha b \bar{\gamma})^{-N_r} (1 + \delta b \bar{\gamma})^{-N_r} + (1 - a) \left(\sum_{i=1}^{n-1} \left(\frac{S_i + \alpha b \bar{\gamma}}{S_i} \right)^{-N_r} \left(\frac{S_i + \delta b \bar{\gamma}}{S_i} \right)^{-N_r} + \sum_{i=n}^{2n-1} \left(\frac{S_{iB} + \alpha b \bar{\gamma}}{S_{iB}} \right)^{-N_r} \left(\frac{S_{iB} + \delta b \bar{\gamma}}{S_{iB}} \right)^{-N_r} \right) \right\},$$

$$= \frac{a}{n} \left\{ \frac{1}{2} \times \left(\frac{2}{2 + \alpha b \bar{\gamma}} \right)^{N_r} \left(\frac{2}{2 + \delta b \bar{\gamma}} \right)^{N_r} - \frac{a}{2} \left(\frac{1}{1 + \alpha b \bar{\gamma}} \right)^{N_r} \left(\frac{1}{1 + \delta b \bar{\gamma}} \right)^{N_r} + (1 - a) \left(\sum_{i=1}^{n-1} \left(\frac{S_i}{S_i + \alpha b \bar{\gamma}} \right)^{N_r} \left(\frac{S_i}{S_i + \delta b \bar{\gamma}} \right)^{N_r} + \sum_{i=n}^{2n-1} \left(\frac{S_{iB}}{S_{iB} + \alpha b \bar{\gamma}} \right)^{N_r} \left(\frac{S_{iB}}{S_{iB} + \delta b \bar{\gamma}} \right)^{N_r} \right) \right\}, \quad \text{(C.8)}$$

APPENDIX D

This section presents the derivation of the unconditional SEP for *M*-DPSK in Eq (4.21) of the performance analysis of the non-coherent CDM system in Section 4.2.1.

DERIVATION OF UNCONDITIONAL SEP FOR *M*-DPSK

The unconditional SEP for *M*-DPSK is effectively computed as:

$$P_{M-DPSK}(e) = \int_0^{\infty} \left(\frac{1}{\pi} \int_0^{\eta\pi} exp\left(- \frac{\kappa\gamma}{1+cos\frac{\pi}{M}\, cos\,\theta} \right) d\theta \right) f_{\gamma}(\gamma) d\gamma, \tag{D.1}$$

where $\frac{1}{\pi} \int_0^{\eta\pi} exp\left(- \frac{\kappa\gamma}{1+cos\frac{\pi}{M}\, cos\,\theta} \right) d\theta = P_{M-DPSK}(e|\gamma)$, η and κ are defined in Eq (4.20).

Apply the trapezoidal approximation on Eq (D.1) using the uniform distribution $\int_a^b f(x)dx = \frac{b-a}{n}\left[\frac{f(a)+f(b)}{2} + \sum_{k=1}^{n-1} f(a + k\ \frac{b-a}{n})\right]$ as presented below:

$$P_{M-DPSK}(e) = \int_0^{\infty} \left(\frac{1}{\pi} \times \frac{\eta\pi - 0}{n} \left[\frac{exp\left(- \frac{\kappa\gamma}{1+cos\frac{\pi}{M} \times cos\,\eta\pi} \right) - exp\left(- \frac{\kappa\gamma}{1+cos\frac{\pi}{M} \times cos\,0} \right)}{2} + \right.\right.$$
$$\left.\left. \sum_{k=1}^{n-1} exp\left(- \frac{\kappa\gamma}{\left(1+\cos\frac{\pi}{M}\, cos\left(0+\frac{k\eta\pi}{n}\right)\right)} \right) \right] \right) f_{\gamma}(\gamma) d\gamma,$$

$$= \int_0^{\infty} \left(\frac{\eta}{n} \left[\frac{exp\left(- \frac{\kappa\gamma}{1+cos\left(\frac{\pi}{M}\right) cos\,(\eta\pi)} \right) - exp\left(- \frac{\kappa\gamma}{1+cos\frac{\pi}{M} \times 1} \right)}{2} + \right.\right.$$
$$\left.\left. \sum_{k=1}^{n-1} exp\left(- \frac{\kappa\gamma}{\left(1+cos\frac{\pi}{M}\, cos\left(\frac{k\eta\pi}{n}\right)\right)} \right) \right] \right) f_{\gamma}(\gamma) d\gamma, \tag{D.2}$$

where $f(a) = exp\left(- \frac{\kappa\gamma}{1+cos\left(\frac{\pi}{M}\right) cos\,(\eta\pi)} \right)$ and $f(b) = -exp\left(- \frac{\kappa\gamma}{1+cos\frac{\pi}{M} \times 1} \right)$.

Let $1 + \cos\left(\frac{\pi}{M}\right) cos\,(\eta\pi) = p$, $1 + \cos\frac{\pi}{M} = L$, $\left(1 + \cos\frac{\pi}{M}\, cos\left(\frac{k\eta\pi}{n}\right)\right) = R$. The unconditional SEP is then denoted as:

$$P_{M-DPSK}(e) = \int_0^{\infty} \left(\frac{\eta}{n} \left[\frac{\exp\left(-\frac{\kappa\gamma}{p}\right) - \exp\left(-\frac{\kappa\gamma}{L}\right)}{2} + \sum_{k=1}^{n-1} exp\left(- \frac{\kappa\gamma}{R} \right) \right] \right) f_{\gamma}(\gamma) d\gamma. \tag{D.3}$$

Apply the MGF $\int e^{-s\gamma} f(\gamma)\, d(\gamma) = (1 + s\bar{\gamma})^{-N_r}$ on Eq (D.3) as follows:

$$P_{M-DPSK}(e) = \int_0^{\infty} \left(\frac{\eta}{n} \left[\frac{\exp\left(-\frac{\kappa\gamma}{p}\right) - \exp\left(-\frac{\kappa\gamma}{L}\right)}{2} + \sum_{k=1}^{n-1} exp\left(- \frac{\kappa\gamma}{R} \right) \right] \right) f_{\gamma}(\gamma) d\gamma,$$

$$= \frac{\eta}{n}\left[\frac{\left(1+\left(\frac{k}{p}\right)\bar{\gamma}\right)^{-N_r}-\left(1+\left(\frac{k}{L}\right)\bar{\gamma}\right)^{-N_r}}{2}+\sum_{k=1}^{n-1}\left(1+\left(\frac{k}{R}\right)\bar{\gamma}\right)^{-N_r}\right],$$

$$= \frac{\eta}{n}\left[\frac{1}{2}\left(\left(\frac{1+k\bar{\gamma}}{p}\right)^{-N_r}-\left(\frac{1+k\bar{\gamma}}{L}\right)^{-N_r}\right)+\sum_{k=1}^{n-1}\left(\frac{1+k\bar{\gamma}}{R}\right)^{-N_r}\right],$$

$$= \frac{\eta}{n}\left[\frac{1}{2}\left(\left(\frac{p}{1+k\bar{\gamma}}\right)^{N_r}-\left(\frac{L}{1+k\bar{\gamma}}\right)^{N_r}\right)+\sum_{k=1}^{n-1}\left(\frac{R}{1+k\bar{\gamma}}\right)^{N_r}\right]. \quad \text{(D.4)}$$

APPENDIX E

This section presents the derivation of the unconditional SEP for differential *M*-QAM in Eq (4.29) of the performance analysis of the non-coherent GDM system in Section 4.2.2.

DERIVATION OF UNCONDITIONAL SEP FOR DIFFERENTIAL *M*-QAM

The unconditional SEP for differential *M*-QAM is effectively computed as:

$$P_{M-DQAM}(e) = \int_0^{\infty} 4\left(1-\frac{1}{\sqrt{M}}\right) Q\left(\sqrt{\frac{3\gamma}{(M-1)}}\right) - 4\left(1-\frac{1}{\sqrt{M}}\right)^2 Q^2\left(\sqrt{\frac{3\gamma}{(M-1)}}\right) f_\gamma(\gamma)d\gamma. \quad \text{(E.1)}$$

Let $\left(1-\frac{1}{\sqrt{M}}\right) = a$ and $\left(\frac{3}{M-1}\right) = b$. As in Eq (4.19) , $\gamma = \frac{E_S}{N_O}$. The unconditional SEP of differential *M*-QAM can then be denoted as:

$$P_{M-DQAM}(e) = \int_0^{\infty} 4aQ\left(\sqrt{b\gamma}\right) - 4a^2Q^2\left(\sqrt{b\gamma}\right) f_\gamma(\gamma)d\gamma, \quad \text{(E.2)}$$

where γ and $f_\gamma(\gamma)$ are defined in Eq (4.19).

The Q-functions are given as:

$$Q(x) = \frac{1}{\pi}\int_0^{\frac{\pi}{2}} exp\left(-\frac{x^2}{2sin^2\theta}\right) d\theta, \quad \text{(E.3a)}$$

$$Q^2(x) = \frac{1}{\pi}\int_0^{\frac{\pi}{4}} \exp\left(-\frac{\sqrt{b\gamma}^2}{2\sin^2\theta}\right) d\theta, \quad \text{(E.3b)}$$

where $x = \sqrt{b\gamma}$.

The relationship between the error probability and the Q-function is defined in Appendix A. Apply the trapezoidal approximation on $Q\left(\sqrt{b\gamma}\right)$ and $Q^2\left(\sqrt{b\gamma}\right)$ using the uniform distribution $\int_a^b f(x)dx = \frac{b-a}{n}\left[\frac{f(a)+f(b)}{2} + \sum_{k=1}^{n-1} f(a+k\ \frac{b-a}{n})\right]$ as presented below:

$$Q\left(\sqrt{b\gamma}\right) = \frac{1}{\pi} \times \frac{b-a}{n}\left[\frac{\exp\left(-\frac{\sqrt{b\gamma}^2}{2\sin^2 a}\right)+\exp\left(-\frac{\sqrt{b\gamma}^2}{2\sin^2 b}\right)}{2} + \sum_{k=1}^{n-1} exp\left(-\frac{\sqrt{b\gamma}^2}{2\sin^2\left(a+k\left(\frac{b-a}{n}\right)\right)}\right)\right], \quad \text{(E.4)}$$

where $f(a) = exp\left(-\frac{\sqrt{b\gamma}^2}{2sin^2 0}\right)$ and $f(b) = exp\left(-\frac{\sqrt{b\gamma}^2}{2sin^2\frac{\pi}{2}}\right)$.

The Q-function $Q\left(\sqrt{b\gamma}\right)$ is then computed as:

$$Q\left(\sqrt{b\gamma}\right) = \frac{1}{\pi} \times \frac{\frac{\pi}{2}-0}{n}\left[\frac{\exp\left(-\frac{\sqrt{b\gamma}^2}{2\sin^2 0}\right)+\exp\left(-\frac{\sqrt{b\gamma}^2}{2\sin^2\frac{\pi}{2}}\right)}{2} + \sum_{k=1}^{n-1} exp\left(-\frac{\sqrt{b\gamma}^2}{2\sin^2\left(0+k\left(\frac{\frac{\pi}{2}-0}{n}\right)\right)}\right)\right],$$

$$= \frac{1}{2n}\left[\frac{0+\exp\left(-\frac{\sqrt{b\gamma}^2}{2\sin^2\frac{\pi}{2}}\right)}{2} + \sum_{k=1}^{n-1} exp\left(-\frac{\sqrt{b\gamma}^2}{2\sin^2\left(k\left(\frac{\pi}{2n}\right)\right)}\right)\right],$$

$$= \frac{1}{2n}\left[\frac{\exp\left(-\frac{\sqrt{b\gamma}^2}{2\sin^2\frac{\pi}{2}}\right)}{2} + \sum_{k=1}^{n-1} exp\left(-\frac{\sqrt{b\gamma}^2}{2\sin^2\left(k\left(\frac{\pi}{2n}\right)\right)}\right)\right],$$

$$= \frac{1}{2n}\left[\frac{1}{2}\exp\left(-\frac{\sqrt{b\gamma}^2}{2}\right) + \sum_{k=1}^{n-1} exp\left(-\frac{\sqrt{b\gamma}^2}{2\sin^2\left(k\left(\frac{\pi}{2n}\right)\right)}\right)\right]. \quad \text{(E.5)}$$

The same can be done for $Q^2\left(\sqrt{b\gamma}\right)$ giving:

$$Q^2\left(\sqrt{b\gamma}\right) = \frac{1}{2n}\left[\frac{1}{2}\exp\left(-\sqrt{b\gamma}^2\right) + \sum_{k=1}^{n-1} exp\left(-\frac{\sqrt{b\gamma}^2}{2\sin^2\left(k\left(\frac{\pi}{4n}\right)\right)}\right)\right], \quad \text{(E.6)}$$

The Q-functions $Q\left(\sqrt{b\gamma}\right)$ and $Q^2\left(\sqrt{b\gamma}\right)$ may be written as:

$$Q\left(\sqrt{b\gamma}\right) = {}^1\!/_{2n}\left[\frac{1}{2}e^{\frac{-\left(\sqrt{b\gamma}\right)^2}{2}} + \sum_{i=1}^{n-1} e^{\frac{-\left(\sqrt{b\gamma}\right)^2}{S_i}}\right], \quad \text{(E.7a)}$$

$$Q^2\left(\sqrt{b\gamma}\right) = \left({}^1\!/_{4n}\right)\left[\frac{1}{2}e^{-\left(\sqrt{b\gamma}\right)^2} + \sum_{i=n}^{2n-1} e^{\frac{-\left(\sqrt{b\gamma}\right)^2}{S_i}}\right], \quad \text{(E.7b)}$$

where $S_i = 2\,sin^2\,\theta_k$, $\theta_k = \frac{i\pi}{4n}$, $S_{iB} = 2\,sin^2\,\beta_k$, and $\beta_k = \frac{i\pi}{4n}$.

Substitute Eq (E.7a) and Eq (E.7b) onto Eq (E.2) gives:

$$P_{M-DQAM}(e) = \int_0^\infty 4a \times \left[{}^1\!/_{2n}\left(\left(\frac{1}{2}e^{-b\gamma/2}\right) + \sum_{i=1}^{n-1} e^{-b\gamma/S_i}\right)\right] - 4a^2 \times \left[{}^1\!/_{4n}\left(\frac{1}{2}e^{-b\gamma} + \sum_{i=n}^{2n-1} e^{-b\gamma/S_{iB}}\right)\right] f_\gamma(\gamma)d\gamma,$$

$$= \int_0^\infty a \times \left[{}^1\!/_{n}\left(\frac{1}{2}e^{-b\gamma/2}\right) + \sum_{i=1}^{n-1} e^{\frac{-b\gamma}{S_i}}\right] - a^2 \times \left[{}^1\!/_{n}\left(\frac{1}{2}e^{-b\gamma} + \sum_{i=n}^{2n-1} e^{-b\gamma/S_{iB}}\right)\right] f_\gamma(\gamma)d\gamma,$$

$$= \int_0^\infty {}^a\!/_{n}\left(\left(\frac{1}{2}e^{-b\gamma/2}\right) + \sum_{i=1}^{n-1} e^{-b\gamma/S_i}\right) - {}^{a^2}\!/_{n}\left(\left(\frac{1}{2}e^{-b\gamma}\right) + \sum_{i=n}^{2n-1} e^{-b\gamma/S_{iB}}\right) f_\gamma(\gamma)d\gamma,$$

$$= \int_0^\infty {}^a\!/_{n}\left[\left(\frac{1}{2}e^{-b\gamma/2}\right) + \sum_{i=1}^{n-1} e^{-b\gamma/S_i} - a\left(\frac{1}{2}e^{-b\gamma}\right) - a\sum_{i=n}^{2n-1} e^{-b\gamma/S_{iB}}\right] f_\gamma(\gamma)d\gamma,$$

$$= \int_0^{\infty} {}^{a}/_{n} \left[\left(\frac{1}{2} e^{{}^{-b\gamma}/_{2}} \right) - a \left(\frac{1}{2} e^{-b\gamma} \right) + \sum_{i=1}^{n-1} e^{{}^{-b\gamma}/_{S_i}} - a \sum_{i=n}^{2n-1} e^{{}^{-b\gamma}/_{S_{iB}}} \right] f_{\gamma}(\gamma) d\gamma,$$

$$= \int_0^{\infty} \frac{a}{n} \left\{ \frac{1}{2} e^{{}^{-b\gamma}/_{2}} - \frac{a}{2} e^{-b\gamma} + (1-a) \left(\sum_{i=1}^{n-1} e^{{}^{-b\gamma}/_{s_i}} + \sum_{i=n}^{2n-1} e^{{}^{-b\gamma}/_{s_{iB}}} \right) \right\} f_{\gamma}(\gamma) d\gamma. \quad \text{(E.8)}$$

Apply the MGF $\int e^{-s\gamma} f(\gamma)\, d(\gamma) = (1 + s\bar{\gamma})^{-N_r}$ on Eq (E.8) as follows:

$$P_{M-DQAM}(e) = \int_0^{\infty} \frac{a}{n} \left\{ \frac{1}{2} e^{-\frac{b\gamma}{2}} - \frac{1}{2} a e^{-b\gamma} + (1-a) \left(\sum_{i=1}^{n-1} e^{\frac{-b\gamma}{S_i}} + \sum_{i=n}^{2n-1} e^{\frac{-b\gamma}{S_{iB}}} \right) \right\} f_{\gamma}(\gamma) d\gamma,$$

$$= \frac{a}{n} \left\{ \frac{1}{2} \left(1 + \left(\frac{b}{2} \right) \bar{\gamma} \right)^{-N_r} - \frac{a}{2} (1 + b\,\bar{\gamma})^{-N_r} + (1-a) \left(\sum_{i=1}^{n-1} \left(1 + \left(\frac{b}{S_i} \right) \bar{\gamma} \right)^{-N_r} + \sum_{i=n}^{2n-1} \left(1 + \left(\frac{b}{S_{iB}} \right) \bar{\gamma} \right)^{-N_r} \right) \right\},$$

$$= \frac{a}{n} \left\{ \frac{1}{2} \left(\frac{2 + b\bar{\gamma}}{2} \right)^{-N_r} - \frac{a}{2} (1 + b\,\bar{\gamma})^{-N_r} + (1-a) \left(\sum_{i=1}^{n-1} \left(\frac{S_i + b\bar{\gamma}}{S_i} \right)^{-N_r} + \sum_{i=n}^{2n-1} \left(\frac{S_{iB} + b\bar{\gamma}}{S_{iB}} \right)^{-N_r} \right) \right\},$$

$$= \frac{a}{n} \left\{ \frac{1}{2} \times \left(\frac{2}{2 + b\bar{\gamma}} \right)^{N_r} - \frac{a}{2} \left(\frac{1}{1 + b\,\bar{\gamma}} \right)^{N_r} + (1-a) \left(\sum_{i=1}^{n-1} \left(\frac{S_i}{S_i + b\bar{\gamma}} \right)^{N_r} + \sum_{i=n}^{2n-1} \left(\frac{S_{iB}}{S_{iB} + b\bar{\gamma}} \right)^{N_r} \right) \right\}, \quad \text{(E.9)}$$

REFERENCES

[1] A. Grami, Introduction to Wireless Communications, Boston: Academic Press, 2016, pp. 493-527.

[2] Z. Naseem, I. Nausheen and Z. Mirza, "Propagation Models for Wireless Communication System," *International Journal of Science, Engineering and Technology Research (IJSETR),* vol. 5, no. 1, pp. 237-242, 2018.

[3] S. K. Rout, R. N. Panda, A. Meda, K. N. Panda and P. K. Mohapatra, "Performance Analysis of Fading Channels in a Wireless Communication," Cham, 2022.

[4] A. M. Hamed and R. K. Rao, "Bandwidth and Power Efficiency Analysis of Fading Communication Link," in *International Symposium on Performance Evaluation of Computer and Telecommunication Systems (SPECTS),* Montreal, QC, Canada, 2016.

[5] D. Mitić, A. Lebl, B. Trenkić and Ž. Markov, "An Overview and Analysis of BER for Three Diversity Techniques in Wireless Communications Systems," *Yugoslav Journal of Operations Research,* vol. 25, no. 2, pp. 7-7, 2015.

[6] W. L. Ramasila and H. Xu, "Improved Error Performance of a 3/4-Sezginer Space-Time Block Codes," *Internationl Journal of Communication Systems,* vol. 32, 2019.

[7] H. Xu and N. Pillay, "Multiple Complex Symbol Golden Code," *IEEE Access,* vol. 8, pp. 103576-103584, 2020.

[8] S. Sharma and P. Chowdhary, "Diversity Techniques in Wireless Communication," *Iconic Research and Engineering Journals,* vol. 1, no. 10, 2018.

[9] Z. Paruk and H. Xu, "Performance Analysis and Simplified Detection for Two-Dimensional Signal Space Diversity with MRC Reception," *SAIEE Africa Research Journal,* vol. 104, no. 3, pp. 97-106, 2013.

[10] A. Essop and H. Xu, Signal Space Diversity with and without Alamouti Transmit Diversity using Generalised Selection Combining, Durban: University of KwaZulu-Natal, 2015.

[11] G. O. Otieno, Generalised Differential Golden Code Modulation: Error Performance Analysis and Bandwidth Efficiency, Durban: University of KwaZulu-Natal, Howard College, 2022.

[12] M. G. Sadeque, S. C. Mohonta and M. A. Firoj, "Modeling and Characterization of Different Types of Fading Channel," *International Journal of Science, Engineering and technology Research (IJSETR),* vol. 4, no. 5, pp. 2278-7798, 2015.

[13] B. Dlolo, Trellis Code-Aided High-Rate Differential Space-Time Block Code and Enhanced Uncoded Space-Time Labling Diversity, Durban: University of KwaZulu-Natal, 2017.

[14] S. Shinya, "Secrecy Performance of Eigendecomposition-Based FTN Signaling and NOFDM in Quasi-Static Fading Channels," *IEEE Transactions on Wireless Communications,* vol. 20, no. 9, pp. 5872-5882, 2021.

[15] P. Ferrand, J.-M. Gorce and C. Goursaud, "Approximations of the packet error rate under quasi-static fading in direct and relayed links," *EURASIP Journal on Wireless Communications and Networking*, 2015.

[16] V. Vasiljevic, H. Stefanovic, S. Obradovic and A. Savic, "Some Advantages of Multi-Beam Transmit Diversity Scheme in Wireless Communication System," in *International Scientific Conference*, Gabrovo, 2019.

[17] G. K. Ijemaru, O. Akinsanmi and O. G. Daniel, "A Space-Diversity Technique for Mitigating Signal Fading in Radio Transmission," in *International Conference On Computing Research And Innovations (CORI 2016)*, Ibadan-Nigeria, 2016.

[18] D. Jose and S. Sameer, "Differential Transmission Schemes for Generalized Spatial Modulation," *IEEE Transactions on Vehicular Technology*, vol. 70, no. 12, pp. 12640-12650, 2021.

[19] K. Kadathlal, H. Xu and N. Pillay, "Generalised Differential Scheme for Spatial Modulation Systems," *IET Communications*, vol. 11, no. 13, pp. 2020-2026, 2017.

[20] S. P. Jadhav and V. S. Hendre, "Performance of Maximum Ratio Combining (MRC) MIMO Systems for Rayleigh Fading Channel," *International Journal of Scientific and Research Publications*, vol. 3, no. 2, 2013.

[21] M. K. Patel, S. M. Berber and K. W. Sowerby, "Maximal Ratio Combining Using Channel Estimation in Chaos Based Pilot-Added DS-CDMA System with Antenna Diversity," *Wireless Communications and Mobile Computing*, vol. 2017, p. 11, 2017.

[22] T. Song, C. Lim, A. Nirmalathas and K. Wang, "Optical Wireless Communications Using Signal Space Diversity with Spatial Modulation," *Photonics*, vol. 8, no. 11, p. 468, 2021.

[23] N. Sibanda, Error Performance of N-ray Alamouti Scheme with Signal Space Diversity, Durban: University of KwaZulu -Natal, 2018.

[24] M. Avendi, Differential Modulation and Non-Coherent Detection in Wireless Relay Networks, Canada: University of Saskatchewan, 2014.

[25] A. Farzamnia, M. Mariappan, E. Moung and R. Thangasalvam, "BER Performance Evaluation of M-PSK and M-QAM Schemes in AWGN, Rayleigh and Rician Fading Channels," in *Control Engineering in Robotics and Industrial Automation: Malaysian Society for Automatic*, vol. 371, M. Mariappan, M. R. Arshad, R. Akmeliawati and C. S. Chong, Eds., Cham, Springer International, 2021, pp. 257-266.

[26] S. Bucher and C. Waldschmidt, "Advanced Noncoherent Detection in Massive MIMO Systems via Digital Beamspace Preprocessing," *Telecom*, vol. 1, no. 3, pp. 211-227, 2020.

[27] M. Wen, X. Cheng, Y. Bian and H. V. Poor, "A Low-Complexity Near-ML Differential Spatial Modulation Detector," *IEEE Signal Processing Letters*, vol. 22, no. 11, pp. 1834-1838, 2015.